SUBSTITUTED [10]CYCLOPARAPHENYLENES

SYNTHESIS AND THEIR SUPRAMOLECULAR BEHAVIOR

Inauguraldissertation zur Erlangung des Doktorgrades (Dr. rer. nat.)
der Naturwissenschaftlichen Fachbereiche im Fachgebiet Chemie
der Justus-Liebig-Universität Gießen

vorgelegt von

Jannis Volkmann

aus Gießen

Betreuer: Prof. Dr. Hermann A. Wegner

Gießen 2023

NACH §17 DER PROMOTIONSORDNUNG

Ich erkläre: Ich habe die vorgelegte Dissertation selbstständig und ohne unerlaubte fremde Hilfe und nur mit den Hilfen angefertigt, die ich in der Dissertation angegeben habe. Alle Textstellen, die wörtlich oder sinngemäß aus veröffentlichten Schriften entnommen sind, und alle Angaben, die auf mündlichen Auskünften beruhen, sind als solche kenntlich gemacht. Ich stimme einer evtl. Überprüfung meiner Dissertation durch eine Antiplagiat-Software zu. Bei den von mir durchgeführten und in der Dissertation erwähnten Untersuchungen habe ich die Grundsätze guter wissenschaftlicher Praxis, wie sie in der „Satzung der Justus-Liebig-Universität Gießen zur Sicherung guter wissenschaftlicher Praxis“ niedergelegt sind, eingehalten.

Jannis Volkmann

Ort, Datum

Dekan:	Prof. Dr. Thomas Wilke
Erstgutachter:	Prof. Dr. Hermann A. Wegner
Zweitgutachter:	Prof. Dr. Peter R. Schreiner, PhD

Curiosity has its own reason for existence.

— Albert Einstein —

TABLE OF CONTENT

ABSTRACT

Cycloparaphenylenes (CPPs), the shortest section of armchair carbon nanotubes, are a class of organic compounds with exceptional structural characteristics and potential applications across various scientific and technological domains. Their potential application in carbon-based functional materials derives from the radially oriented π-system and the inherent strain of these nanohoops. The former not only confers unusual optoelectronic properties of CPPs, but also makes them excellent hosts for fullerenes.

In this thesis, a new strategy for the synthesis of a substituted [10]CPP derivative was developed. The [2+2+2] cycloaddition reaction was used as key step to introduce substituents in this synthesis to obtain a diethyl phthalane-containing [10]CPP in seven steps and with 8% overall yield.

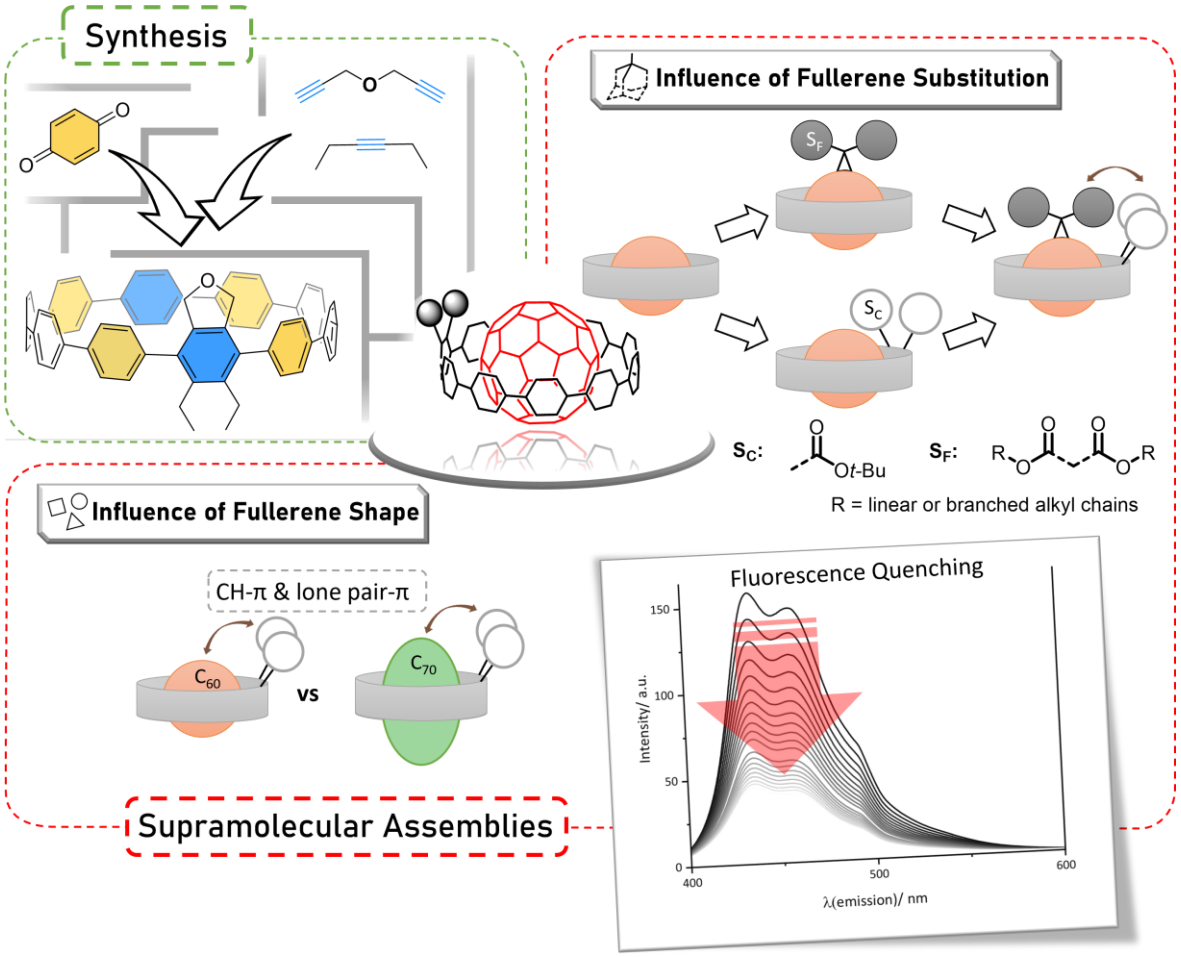

This efficient synthesis allowed additional studies on the behavior of these nanohoop in supramolecular assemblies. The diethyl phthalane-containing CPP was used together with di- and tetra-*tert*-butyl ester-substituted [10]CPP to investigate the substitution effect in supramolecular fullerene (C_{60} and C_{70}) architectures. Experimental analysis, supported by theoretical investigations,

revealed that in complexes of the ellipsoidal C_{70} the attractive substituent-fullerene interactions are enhanced with respect to C_{60}.

Furthermore, a systematic study of the substituent-substituent interactions in such supramolecular motifs was conducted with di-*tert*-butyl ester-substituted [10]CPP and a series of methano-fullerenes. These Bingel adducts of fullerene C_{60} were functionalized with different linear or branched alkyl esters and the interaction between these and the *tert*-butyl ester substituted CPP was evaluated. While all alkyl ester derivatives showed a stabilizing effect – based on a double mutant cycle – these effects were enhanced with longer chain length, while the steric demand plays a significant role in the branched alkyl derivatives. As an exception, the adamantyl substitution on the fullerene shows an increased stabilizing effect being rationalized with the increased London dispersion ability.

ZUSAMMENFASSUNG

Cycloparaphenylene (CPPs) repräsentieren den kleinstmöglichen Ausschnitt von „armchair“ Kohlenstoff-Nanoröhren und sind eine Klasse organischer Verbindungen mit besonderen strukturellen Merkmalen und potenziellen Anwendungen in verschiedensten wissenschaftlichen und technischen Bereichen. Ihre potenzielle Anwendung in kohlenstoffbasierten funktionellen Materialien ergibt sich aus dem radialen π-System und ihrer inhärenten Spannung. Ersteres verleiht CPPs nicht nur ungewöhnliche optoelektronische Eigenschaften, sondern macht sie auch zu hervorragenden Wirten für Fullerene.

In dieser Thesis wurde eine neue Strategie für die Synthese eines substituierten [10]CPP-Derivats entwickelt. Als Schlüsselschritt wurde eine [2+2+2]-Cycloadditionsreaktion verwendet, um Substituenten einzuführen. Dies ermöglichte, in einer siebenschrittigen Synthese und mit 8 % Gesamtausbeute, ein [10]CPP Diethylphthalan-Derivat zu erhalten.

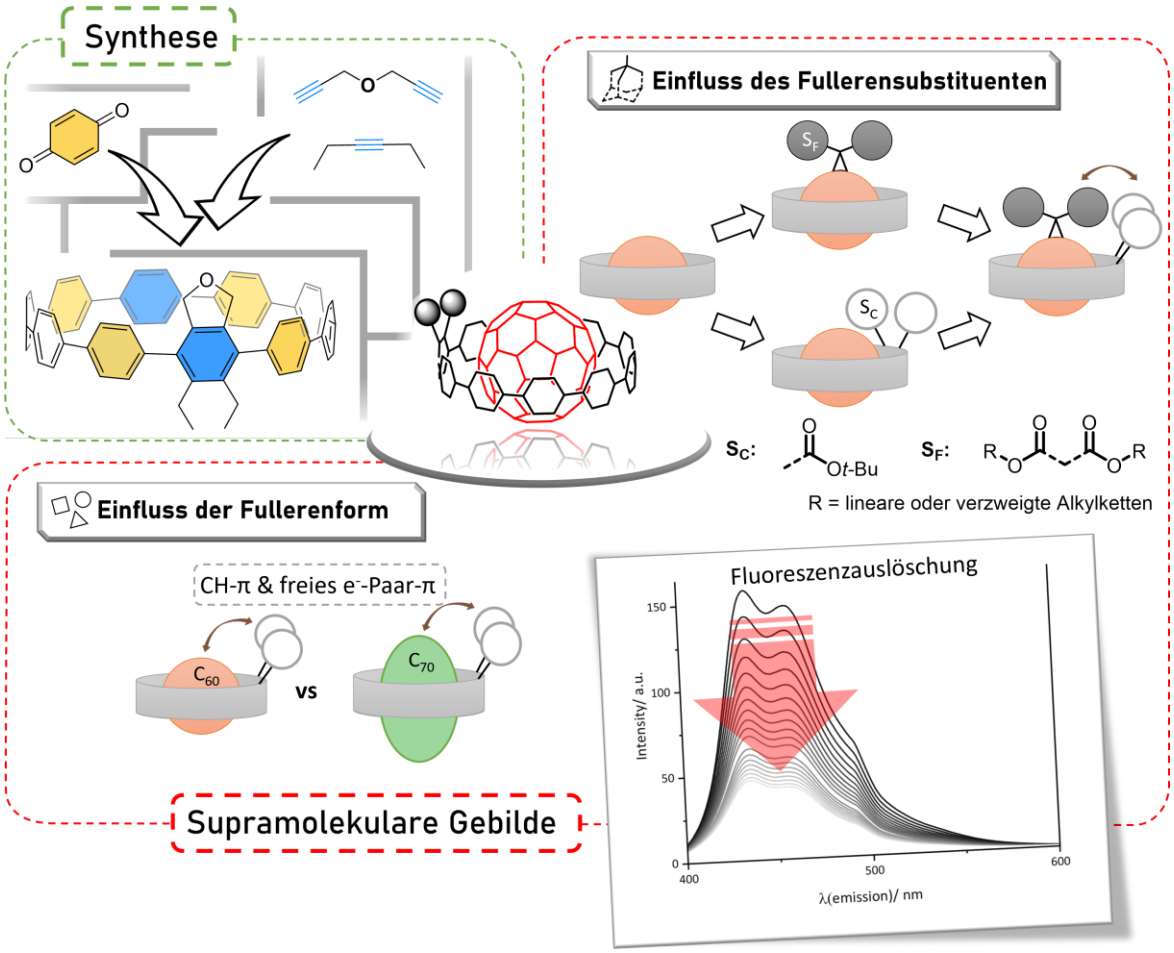

Die erfolgreiche Synthese des Diethylphthalan-Derivats ermöglichte zusätzliche Studien über das Verhalten dieser Verbindungsklasse in supramolekularen Architekturen. Zusammen mit di- und

tetra-*tert*-Butylester-substituiertem [10]CPP wurde der Einfluss der Substituenten auf das Bindungsverhalten in Komplexen mit den Fullerenen C_{60} und C_{70} untersucht. Experimentell wurde eine verstärkte attraktive Wechselwirkung in den Komplexen des elliptischen C_{70} mit substituiertem CPP entdeckt und durch theoretische Untersuchungen unterstützt.

Darüber hinaus wurde eine systematische Studie der Substituent-Substituent-Wechselwirkungen zwischen di-*tert*-Butylester-substituiertem [10]CPP und einer Reihe von Methanofullerenen durchgeführt. Diese Bingel-Addukte des Fulleren C_{60} wurden mit verschiedenen linearen oder verzweigten Alkylestern funktionalisiert und die Wechselwirkung zwischen den Substituenten beider Komplexpartner untersucht. Während alle Alkylester-Derivate eine stabilisierende Wirkung zeigten - basierend auf einem doppelten Mutationszyklus (*engl.* double mutant cycle) - wurden diese Effekte mit zunehmender Kettenlänge verstärkt. Im Gegensatz hierzu schien bei verzweigten Alkylderivaten der sterische Anspruch eine wichtigere Rolle zu spielen. Eine Ausnahme bildete die Adamantyl-Substitution am Fulleren, welche einen erhöhten Stabilisierungseffekt zeigte und mit der erhöhten Fähigkeit zu London‘schen Dispersion erklärt wurde.

1 Introduction

The favorable arrangement of an uncharged carbon center bonded to three neighboring atoms is planar. With respect to graphite this circumstance was interpreted by Pauling in 1931 laying the foundation for hybridization.[1] Distortion of this geometry results in an energetic penalty, however, bending the formal sp^2 hybridized carbons accesses novel classes of compounds with unique properties.[2] Such an example, the carbon nanotubes (CNTs, Figure 1), were first reported in the early 1950s by Radushkevich and Lukyanovich[3] and gained further attention after Iijima's discovery of CNTs in the crude soot as a side product of fullerenes.[4] These wrapped up graphene sheets[5] are solely build from carbon atoms, and thus, display an allotrope of carbon. CNTs have exceptional physical stability with a tensile strength two orders of magnitude higher than that of stainless steel,[6] a high surface area and intriguing electronic properties, making CNTs excellent candidates for organic functional materials and molecular electronics.[7,8]

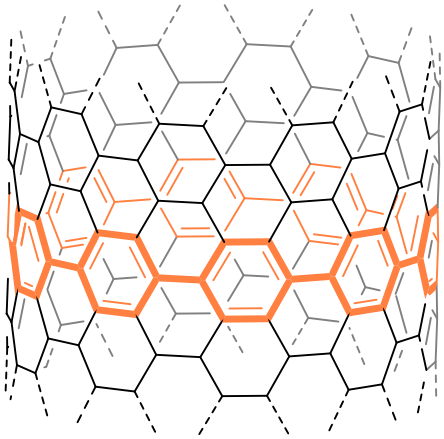

Figure 1: *(10,10) armchair CNT with the inherent [10]cycloparaphenylene (CPP) highlighted in orange. The double bonds of the nanotube were omitted for clarity.*

The selective preparation of those nanotubes is an ongoing challenge.[8] An attempt in this regard is to apply the shortest repeatable unit of CNTs, the cycloparaphenylene (CPP).[9] While their application for the growth of CNTs is still limited,[10] the nanohoops itself raised attention due to their appealing structure and outstanding properties.[11]

1.1 Cycloparaphenylenes

From the Beginning to Current State and Application

[*n*]CPPs are cyclic *para*-connected phenylenes, where *n* is equal to the number of phenyl units in the macrocyclic ring. These strained nanohoops bear a radial π-system, with an electron enriched concave and an electron reduced convex surface (Figure 2).[12]

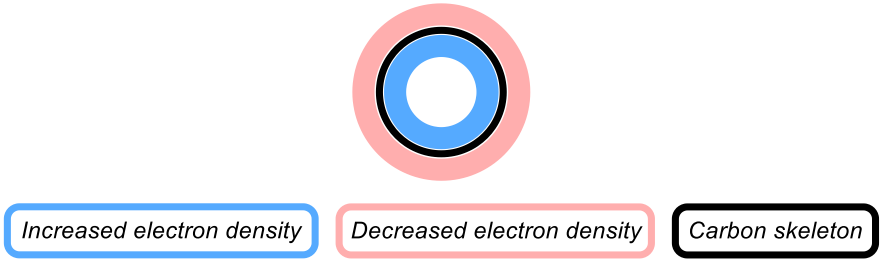

***Figure 2**: Schematic representation of the electron density originating from the radially orientated π-orbitals.*

The first reported synthetic attempt dates back to 1934, when Parekh and Guha subjected *para*-benzene dithiol to oxidative conditions resulting in oligomeric cyclic benzene disulfides.[13] Amongst others, the dimeric disulfide **1** was obtained, which was further desulfurized with elemental copper leading to sulfide **2** (Scheme 1). Further desulfurization was unsuccessful, which is from today's perspective perspicuous. However, 60 years later the group of Vögtle picked up this synthetic strategy.[14]

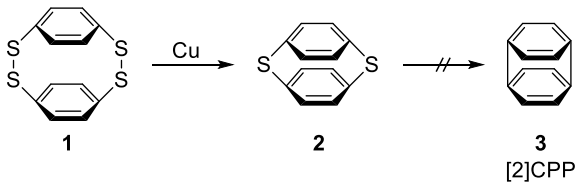

***Scheme 1:** Synthetic attempt by Parekh and Guha for the synthesis of [2]CPP via desulfurization.[13]*

In a landmark paper they published a desulfurization attempt – besides others – striving the synthesis of larger CPPs. The increased size has the advantage of a reduced ring strain, due to less distortion of the sp^2 centers. Introduction of sulfides in the backbone of the *para*-phenylene has the advantage of naturally bent units, which allow the formation of strain reduced macrocyclic CPP precursors. In addition to sulfides, the Vögtle group applied *syn*-cyclohexanediols, as well as

aliphatic and olefinic spacers for this purpose. In the end, none of their strategies liberated the targeted CPPs. Nevertheless, the general idea of strain reduced macrocyclic precursors is omnipresent in nowadays syntheses.[15]

The first successful synthesis disclosing the compound class of CPPs was realized by Jasti and Bertozzi in 2008 (Scheme 2).[16] In this study, 1,4-diiodobenzene (**4**) was monolithiated and added to *para*-benzoquinone to yield an angled three-membered building block **5**. This building block was borylated (**6**) and exposed to Suzuki cross-coupling conditions together with diiodide **5**. In this macrocyclization, three different ring sizes were obtained and isolated (**7-9**). As the final step, the strain reduced macrocycles were aromatized under reductive conditions yielding [9], [12] and [18]CPP (**10-12**). In the consecutive years different synthetic approaches for the synthesis of CPPs were developed. However, three main strategies can be identified, which differ by the strain-relieving units used for bending (Figure 3). Shortly after Jasti and Bertozzi's synthesis, the group of Itami published their synthesis of [12]CPP,[17] utilizing *syn*-cyclohexanediols, which were already proposed by Vögtle and coworkers.[14] Parekh and Guha, as well as Vögtle followed in their desulfurization attempt the strategy to implement angled linkers, being proposed to be eliminated in the CPP forming step. This idea was used by the group of Yamago forming square-shaped tetra-nuclear platinum complexes as strain reduced macrocycles.[18] In the final step, platinum can be removed under oxidative conditions liberating the nanohoop. More recently, the group of Osakada extended this approach to gold complexes, in order to access other ring-sizes with the same building blocks.[19,20]

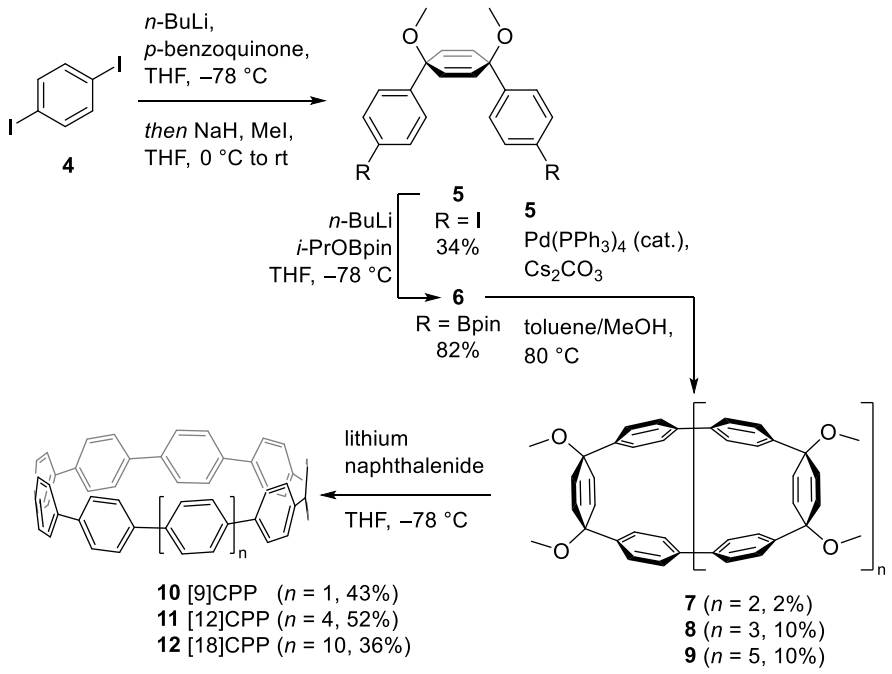

Scheme 2: *The first synthesis of a CPP published by Jasti and Bertozzi in 2008.[16]*

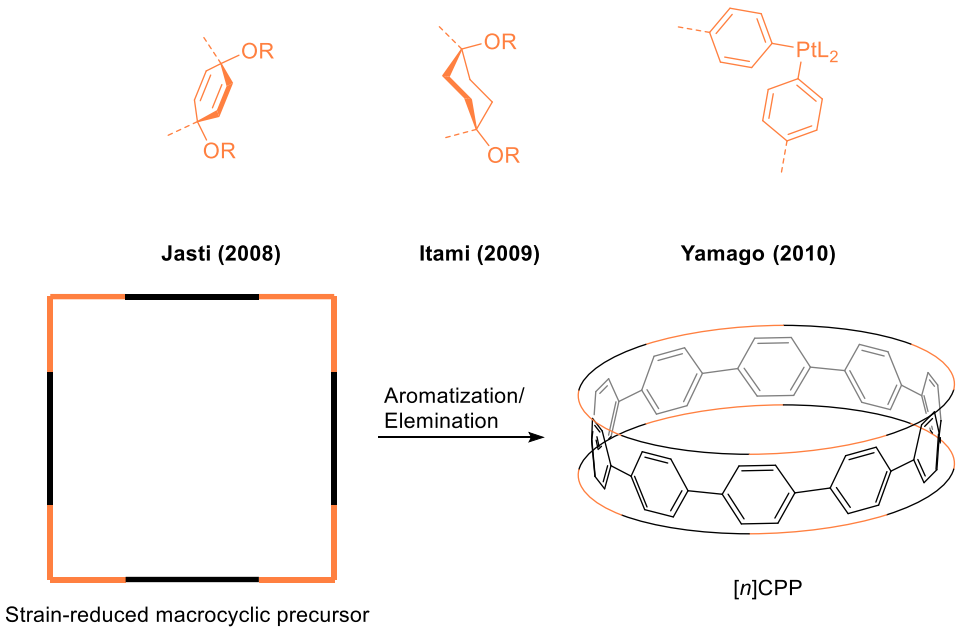

Figure 3: *Representation of the different approaches for the synthesis of strain relieved macrocycles, to form the targeted CPP either by aromatization of the phenyl surrogates (Jasti, Itami),[16,17] or elimination of the metal centers (Yamago).[18]*

Each approach has its benefits and drawbacks, depending on the synthetic target. While the route *via* metal complexes is concise, the flexibility in size is limited and hyper-stoichiometric amounts of precious metal are required. Both other routes, the cyclohexadiene route and the saturated analog are on one hand more flexible regarding accessible patterns and sizes, but on the other hand, the synthetic route is more demanding. The more rigid cyclohexadiene moiety usually gives higher yields in the macrocyclization and aromatization, however, the moiety is prone to side reactions.[21] Based on the above described synthetic paths, a library of syntheses have been developed, differing in size-selectivity[22–28] or being superior in terms of efficiency,[29–31] scale[29,30,32,33] or conditions.[34–37]

Due to their shape, CPPs exhibit specific properties for application in supramolecular chemistry.[38] Alteration of electron density at the concave and convex site makes these compounds excellent hosts for electron deficient guests, as well as guests for electron rich hosts. These supramolecular assemblies, especially with fullerenes, will be an aspect of a following chapter. Besides the contribution to the host-guest properties, their radial π-conjugation, accompanied with the ring strain leads to drastically different (opto)electronic properties compared to the linear oligoparaphenylenes ([*n*]OPPs) (Figure 4). For instance, the energetic gap between the highest occupied molecular orbital (HOMO) and the lowest unoccupied molecular orbital (LUMO) of the cyclic *para*-phenylenes increases with their ring size, approaching the HOMO—LUMO gap of

OPPs.[26] An opposing trend can be observed for the OPPs, in which the HOMO—LUMO gap increases with decreasing size of the aromatic system. Large, and thus, less strained CPPs behave more like their linear analogues than the highly strained smaller CPPs, which is reasonable identifying bending and strain as the major contributors to these properties.

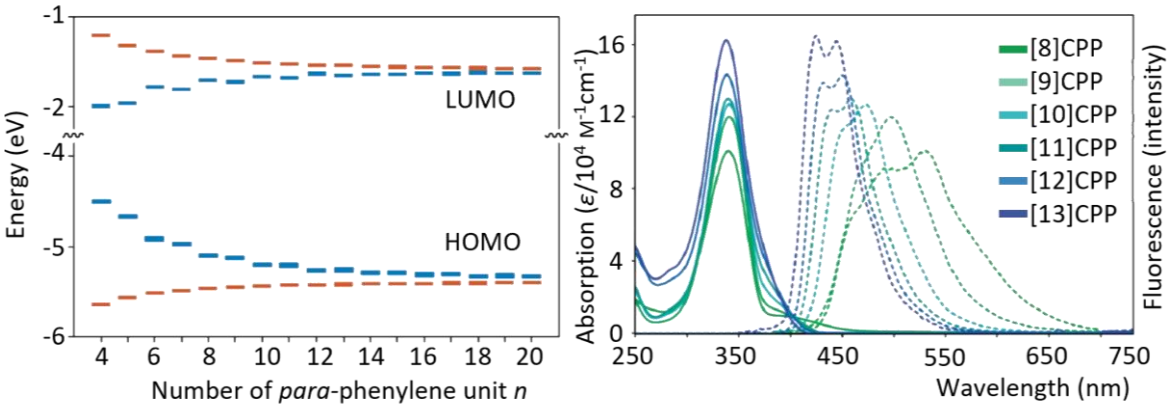

Figure 4: *Left: Density functional theory (DFT, B3LYP/6-31G*) calculated HOMO and LUMO energies for [n]CPPs (blue) and [n]OPPs (orange) in dependence on the number of phenyl units. Right: Absorption (solid lines) and emission (dashed lines) of different sized [n]CPPs. Reprinted with permission from reference [26]. Copyright © 2011 American Chemical Society.*

With respect to the HOMO—LUMO gaps, the absorption spectra are expected to shift hypsochromically by increasing the size of the nanohoop. However, this is not the case, and their absorption is independent of the ring size. A reason for this circumstance was hypothesized by the group of Yamago based on time-dependent density functional theory (TD-DFT, B3LYP/6-31+G*//B3LYP/6-31G*).[26] Due to the centrosymmetry of these nanohoops, the HOMO—LUMO transition is forbidden due to violation of the Laporte rules.[39] Thus, the observed absorption originates from HOMO—LUMO+1/LUMO+2, or HOMO-1/HOMO-2—LUMO transitions, which appear to have a similar energy gap. In contrast to the absorption, the emission is dependent on the ring size, having a larger Stokes shift for smaller CPPs. The group of Irle described the observed size dependency by emission of different exited states.[40] While larger CPPs are emitting from S_2/S_3 Jahn-Teller distorted states (explaining the two maxima in emission and violating Kasha's Rule[41]), smaller CPPs have a higher probability to decay nonradiative to the S_1 state before emission. As the emission from the S_1 state is formally symmetry forbidden, the intensity of emission drops being consistent with the experimental data.[26]

Substituted Cycloparaphenylenes

A more versatile strategy to influence the properties of CPPs than the alteration of size is their functionalization.[42] In this regard, either the backbone of the CPP can be substituted *e.g.,* by exchange of a phenyl unit by another entity like pyridines,[43] dibenzopentalenes[44] and porphyrins[45] (Hybrid-CPPs, Figure 5)[29,46–48], or protons can be exchanged by functional groups.[49–59] As for OPPs, substitution affects the electronic structure of the aromatic system as well as the conjugation between the substituted with the adjacent phenylenes due to an increased dihedral angle, the latter originating from the introduced steric demand.

The synthesis of these substituted nanohoops can either be realized by a bottom-up method, or a post-functionalization of the parent CPP (Figure 5). In principle, post-functionalization offers greater flexibility, as unfunctionalized CPP is derivatized in the final step(s), eliminating the need for a new synthesis for each derivative. However, post-functionalization has proved to be challenging and only a few synthetic approaches have been published, all of which limited in the size of the nanohoop, and/or the degree and pattern of substitution.

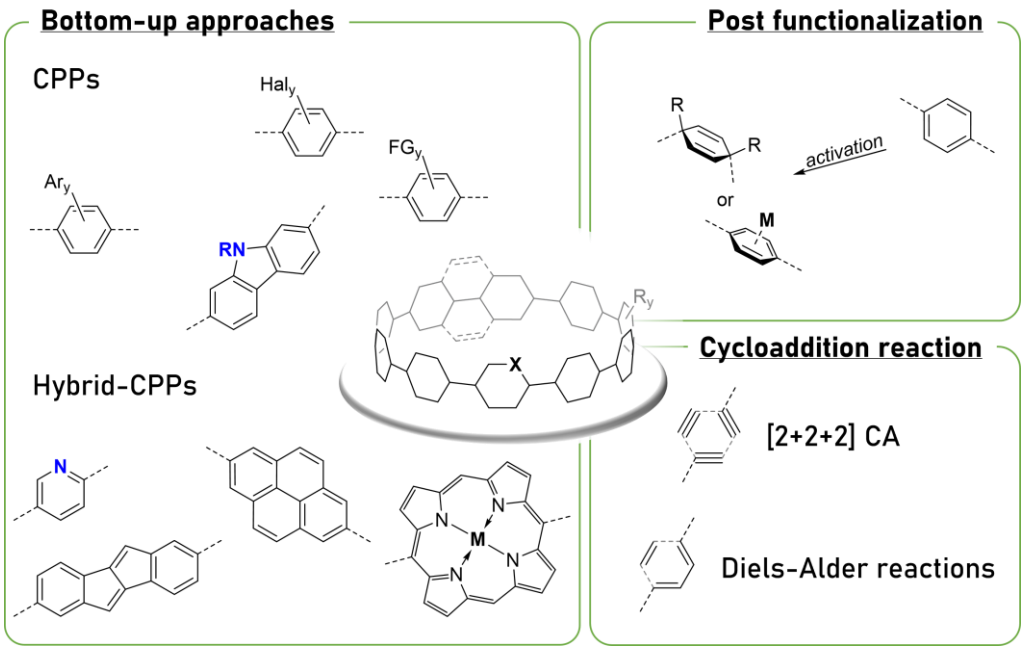

Figure 5: *Representation of the three main approaches toward the functionalization of CPPs: Bottom up approach with various functional groups were attached to the nanohoop,[60–66] or incorporated in the backbone (Hybrid-CPPs).[43–45,67–69] Post-functionalization initiated by covalent[70] or non-covalent[71–73] activation. Application of [2+2+2] cycloaddition reactions (CA)[74–82] or Diels-Alder reactions[83–85].*

A method to post-functionalize CPPs is their bromination.[70] By addition of Br_2 to small sized [*n*]CPPs (*n* = 5, 6, 8, 9), two *para*-phenylenes can be brominated, leading to cyclohexadiene macrocycle **14** (Scheme 3, *n* = 5). The 1,4-cyclohexadienes can either be further brominated or rearranged. The thus obtained CPP surrogates can be aromatized using a phosphazene superbase (P_4-*t*-Bu)[86] to liberate brominated CPPs, as a single product **15** or as a mixture of different bromination patterns **16-18**, depending on the previous treatment. While this example describes a valid method to post-functionalize these nanohoops, the application is finite. On the one hand, the scope is limited to small ring sizes due to the required strain for the initial bromination. On the other hand, the variability in the substitution pattern is restricted, additionally suffering from a lack of selectivity for a higher degree of bromination.

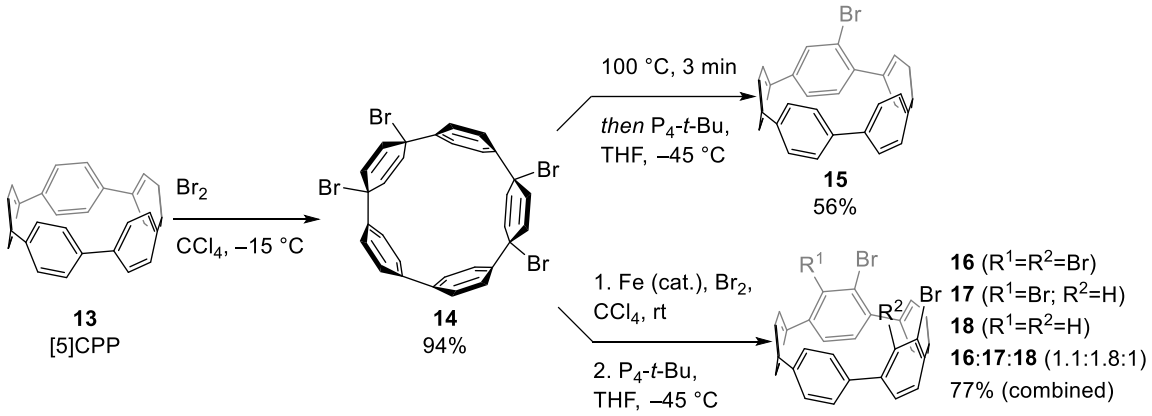

Scheme 3: *Bromination as a post-functionalization method of [5]CPP, reported by Yamago and coworkers.[70] This method yields in different degree and pattern of substitution, depending on the conditions.*

In principle, bromination in the first step is an activation of a phenyl ring for subsequent functionalization, which can also be carried out non-covalently. The group of Itami activated CPPs by converting them into a chromium complex upon addition of chromium hexacarbonyl to [9] or [12]CPP.[72] This η_6-complex with the Lewis acidic metal makes the aromatic ring electron poor, and thus enables deprotonation with *n*-butyllithium (*n*-BuLi). The lithium aryl species can be functionalized with different electrophiles obtaining silylated, borylated or carbonylated nanohoops. In addition to the chromium complexes, η_6-complexes with tungsten, molybdenum and ruthenium were synthesized, however, without covalent functionalization of the CPP.[71–73]

In case other functionalities, patterns or sizes are required, the substituents must be introduced at an earlier stage of the CPP synthesis. Besides the rare examples of post-functionalization, there are several published syntheses about the introduction of substituents during the bottom-up synthesis of the CPP. These strategies differ from parent CPP syntheses in the application of cycloaddition

reactions[74–78,84] or functionalized building blocks,[48,63,87,88] as well as introduction dummy groups,[58,89,90] which can be transferred into desired functionalities.

Introducing substituents within the first building blocks enables precisely to prearrange the degree and pattern of substitution. Nevertheless, the functional groups tolerance of every following reaction step is required. A method to circumvent this issue is the introduction of dummy atoms or groups, which tolerate the conditions of the consecutive steps and can be transferred into the desired functionality at the end of the synthesis. One example in this regard was published by the group of von Delius.[89] To achieve a porphyrin attached CPP, they designed a synthesis of a trimethylsilyl (TMS) substituted CPP derivative **19** (Scheme 4). The TMS group has the advantage of tolerating the conditions of the CPP synthesis and was later exposed to ICl, converting the silane into an iodide, followed by a Sonogashira reaction to finalize the target compound **21** by connecting the porphyrin unit with the nanohoop. In a similar fashion, Jasti and coworkers synthesized a water soluble CPP derivative[58] as well as a catechol embedded nanohoop.[90]

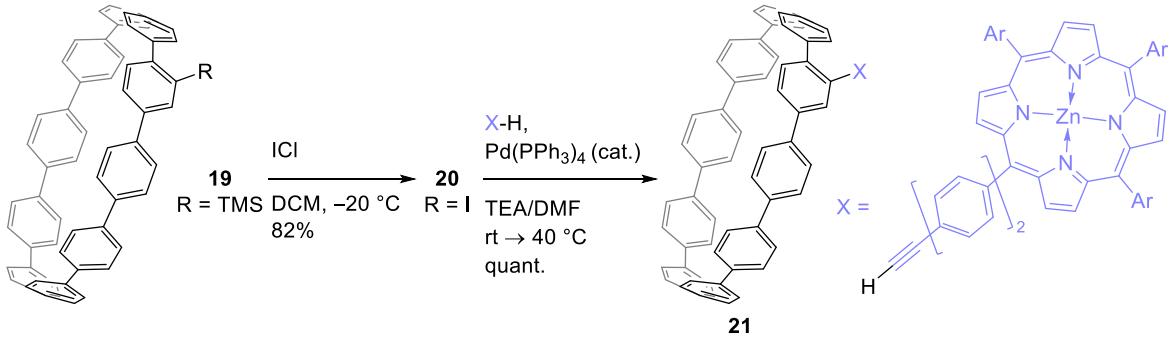

Scheme 4: *Application of a TMS group as dummy to introduce a halide to convert it into a CPP-porphyrin conjugate.*[89]

For the synthesis of nanohoops bearing complex subunits *e.g.,* highly substituted phenyl rings, electrocyclizations or cyclotrimerization reactions can be utilized. While the group of Wang applied a Diels-Alder reaction to introduce naphthyl groups,[83–85] our group,[74,75] as well as the group of Tanaka,[78] used the [2+2+2] cycloaddition (CA) to realize different motifs. It is noteworthy that – even if the nomenclature suggests it – the [2+2+2] CA is only formally a cycloaddition reaction.[91] In this transition metal mediated catalysis three unsaturated bonds are combined to form a cyclic product.[92] The atom efficient reaction allows the construction of complex and highly substituted phenyl rings as well as heteroaromatic compounds and 1,3-cyclohexadienes. Additionally, it was shown by King and coworkers that the [2+2+2] CA is able to build up strained systems, making the reaction valuable for CPP syntheses.[93]

The first CPP synthesis based on a [2+2+2] CA was published by the Wegner group in 2014 (Scheme 5).[75] Two tethered dialkynes were used as [2+2+2] CA precursors, combined with *syn*-cyclohexanediols for the formation of strain reduced macrocycles. The course of synthesis is based on two building blocks, which are combined prior the macrocyclization. First, the

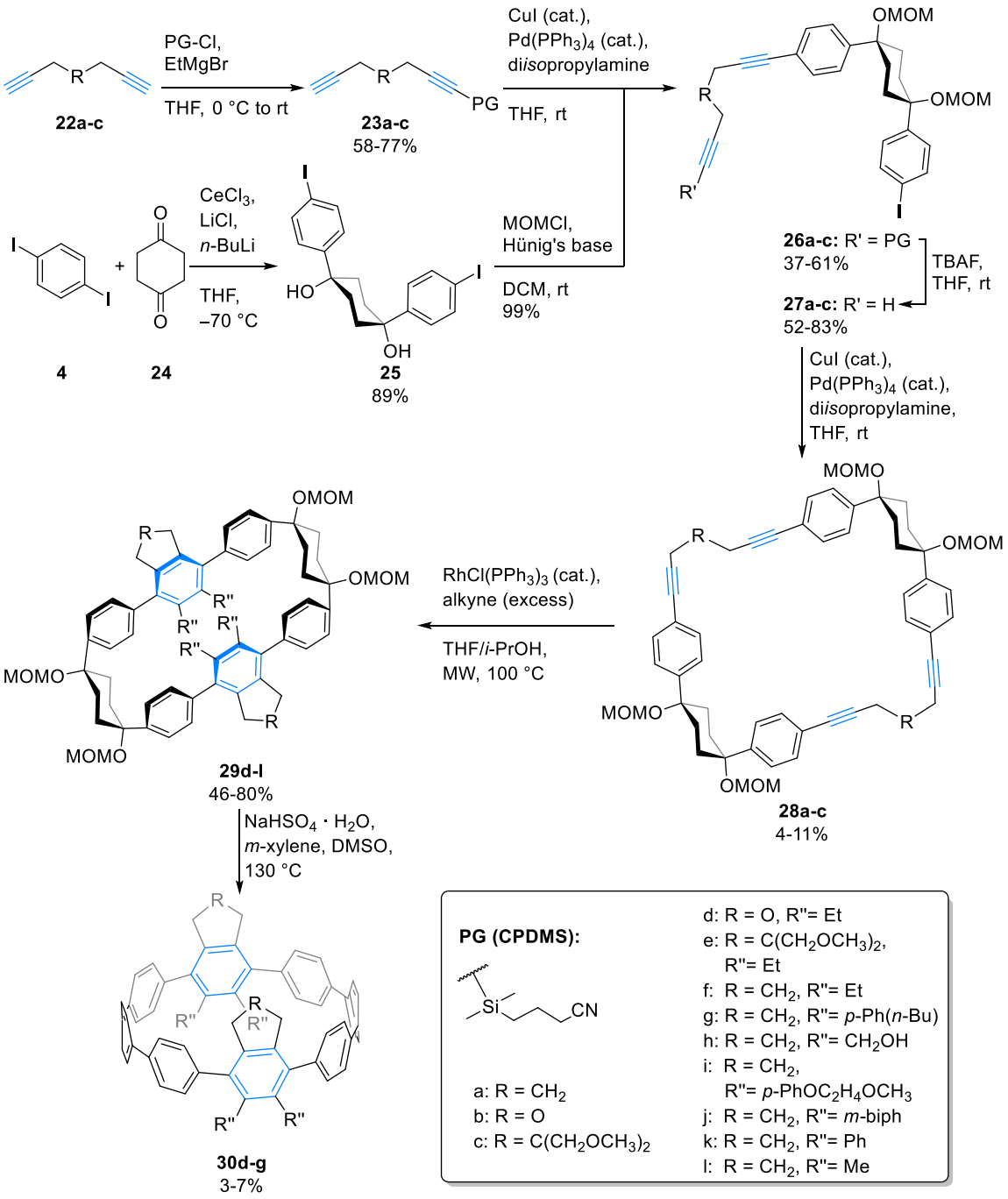

Scheme 5: *Synthesis of a library of tetra-substituted [8]CPPs utilizing the [2+2+2] CA for the introduction of substituents.*[75]

cyclohexane building block is synthesized, according to a literature procedure by Itami yielding in a three-membered building block **25**.[17,94] This was combined with different protected dialkynes **23a-c**, which were synthesized from the parent dialkynes **22a-c** by mono-protection of one terminal alkyne. A Sonogashira reaction of the unprotected terminal alkyne **23a-c**, with the aryl iodide **25** liberated the extended building block **26a-c**. After removal of the protecting group, the building block was applied to a macrocyclization with Sonogashira reaction conditions, liberating the targeted macrocycle **28a-c** in limited yield, presumably originating from the high flexibility of the building block **27a-c**. The dialkyne embedded macrocycle **28a-c** was exposed to a [2+2+2] CA with different symmetric alkynes. In this step, various substituents were introduced by choice of the alkyne (Me, Et, Ph, CH_2OH, *p*-Ph(*n*-Bu), *p*-$PhOCH_2CH_2OCH_3$, *m*-biphenyl), making this route flexible in terms of functionalities. With the [2+2+2] CA product **29d-g** in hand, the remaining cyclohexanediols were aromatized oxidatively yielding in the targeted CPPs **30d-g**. This step shows a disadvantage of the cyclohexanediols as phenyl surrogates: The oxidative aromatization requires harsh conditions, namely elevated temperature, and acid. As the nanohoops have a limited stability in acid,[37] these conditions usually do not allow high yields for the final step of the synthesis.[25]

To put the synthesis in context, the sequence of key steps, particularly the [2+2+2] CA, macrocyclization, and aromatization, is crucial. In the above-described synthesis the [2+2+2] CA was performed within the macrocycle, thus, after the macrocyclization and before the aromatization. This order of steps allows a higher flexibility in substitution due to the late stage cyclotrimerization but decreases the flexibility in ring size as well as the efficiency of the macrocyclization.

The Wegner group focused on the combination of [2+2+2] CA and cross-coupling reactions for CPP syntheses. However, this rhodium catalyzed cross-cyclotrimerization can also combine macrocyclization and introduction of substituents in a single step. This method was developed by the group of Tanaka and utilizes terminal alkynes in combination with cyclohexadienes for the synthesis of ester functionalized CPPs. While different sizes and substitution pattern were realized by the group of Tanaka, their first synthesis is depicted in scheme 6.[78] Starting with building block **5**,[16] first published by Jasti *et al.* the terminal dialkyne **31** was synthesized in a Sonogashira reaction, followed by cleavage of the silyl protecting group. A macrocyclization of this terminal dialkyne with di-*tert*-butyl acetlyenedicarboxylate (**32**) in the presence of Tanaka's Rh^{I}-H_8-binap catalyst[95] liberated the strain reduced macrocycle **33** in 17% yield. The cyclohexadienes were aromatized reductively yielding in a [12]CPP-hexa-carboxylate **34**. On similar routes [8]CPP-octacarboxylate as well as [6]CPP-tetracarboxylate were synthesized.[76,77] By exchanging the

cyclohexadienes by 5,8-dimethoxy-1,4-dihydro-naphthalenes alike in the synthesis of Wang, an electron donating group can be added, leading to a push-pull system embedded CPP.[81]

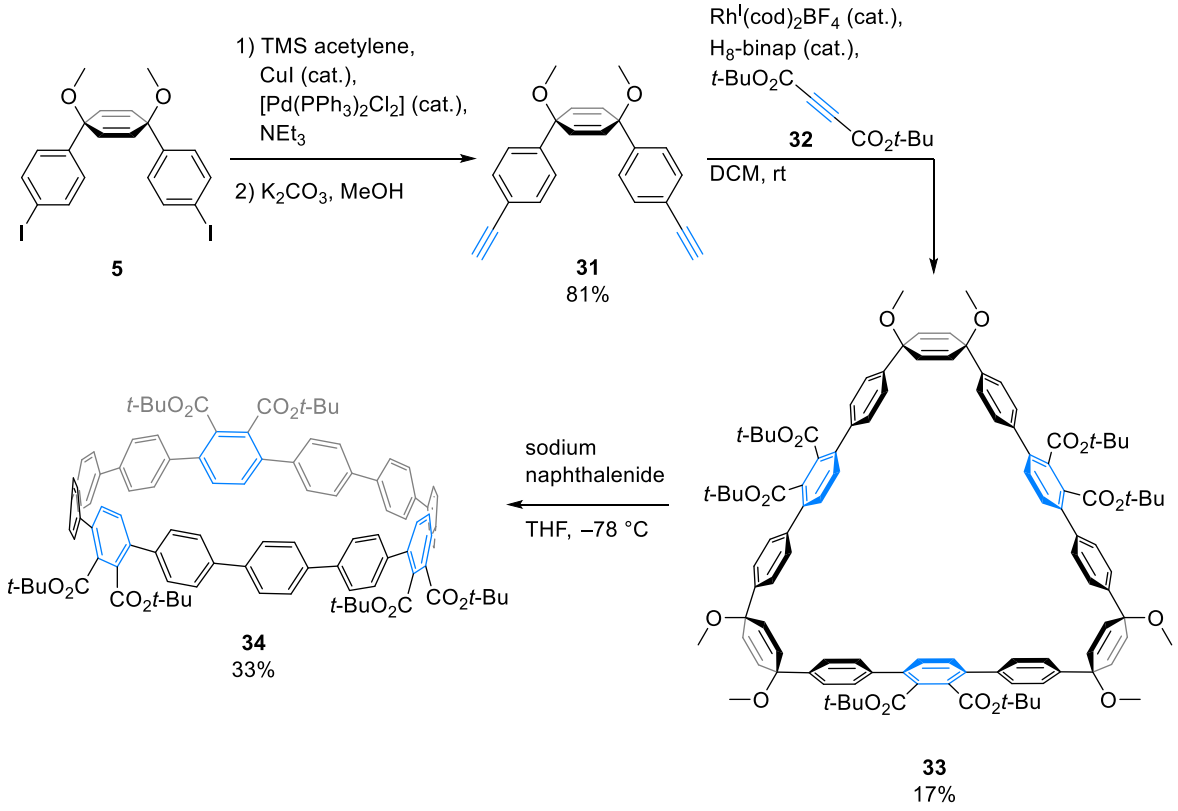

Scheme 6: *Synthesis of a [12]CPP-hexa-carboxylate by the group of Tanaka.[78] The substituents were introduced via a rhodium catalyzed cross-cyclotrimerization.*

The strategy of introducing substituents within the macrocyclization makes the synthesis concise, however, decreases the flexibility in size and pattern. To circumvent this drawback, our group developed a synthesis based on a building block approach by Jasti in combination with Tanaka's method to introduce ester substituents (Scheme 7).[74] Starting with curved alkyne **35** which is readily available in a cost-efficient three step synthesis, a [2+2+2] CA was executed with conditions developed by Tanaka.[95,96] The five-membered key building block **36** and its borylated analog **37a** can be applied to a macrocyclization with Suzuki coupling conditions yielding in a strain reduced macrocycle bearing four ester functionalities. Again, the final step displays the reductive aromatization toward substituted [10]CPP **38**. Besides the coupling with the substituted unit **37a**, unsubstituted three- and five-membered (**37b** and **6**) counter parts can be employed to obtain di-substituted [8] and [10]CPP derivatives **39** and **40**, respectively. Separating the [2+2+2] CA from the

macrocyclization – performed with Suzuki coupling conditions – extends the synthesis by means of steps but increases the modulation capability.

To gain maximum flexibility in terms of a very late-stage introduction of substituents, the group of Tanaka developed a method of combining the aromatization and cyclotrimerization. By synthesis of a dialkyne embedded nanohoop, the [2+2+2] CA can occur at the CPP forming step pushing this concept to a limit.[82] In case all three alkynes for the trimerization are already incorporated to the macrocycle, the synthesis of a nanobelt was possible.[80]

Besides a covalent functionalization of the nanohoops, their properties can be modified by non-covalent functionalization. Before diving into the supramolecular chemistry of CPPs the most important counterpart, the fullerene, will be described in detail.

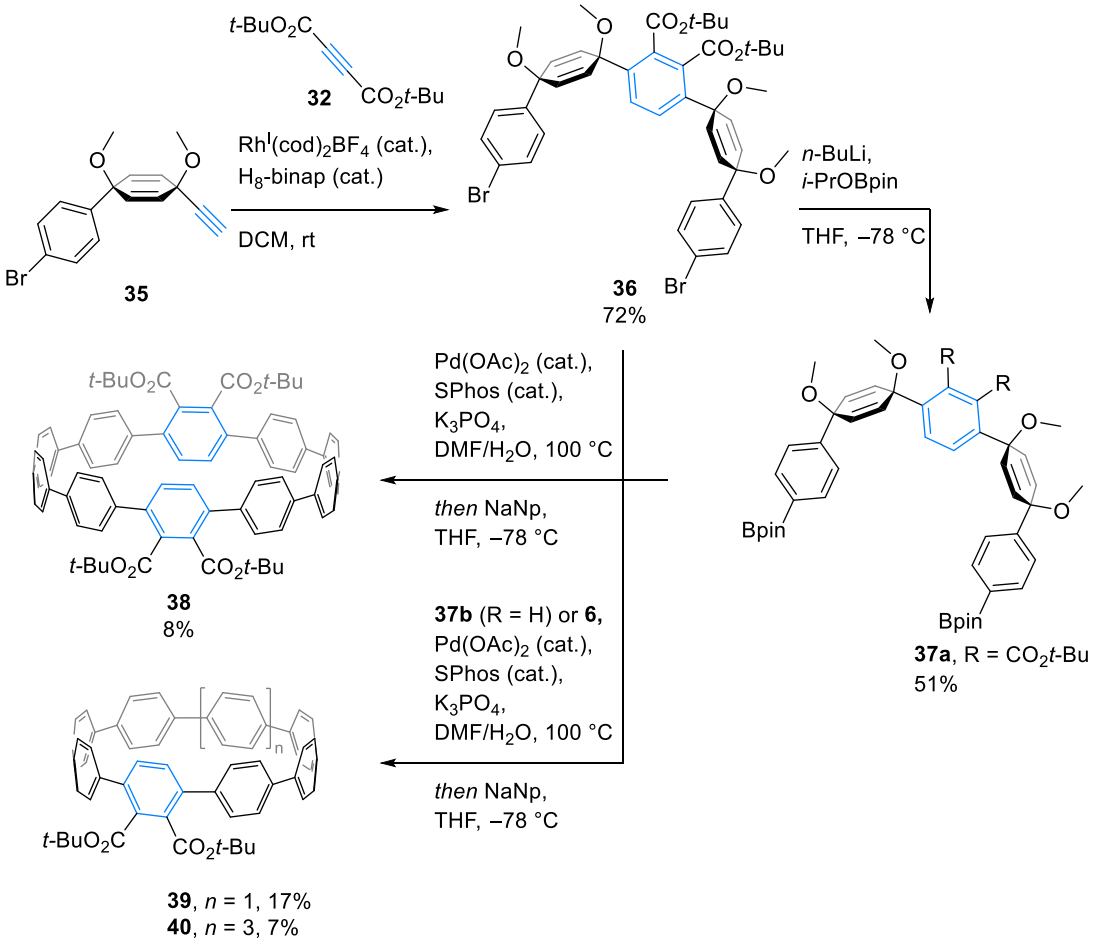

***Scheme 7**: Modular synthesis of di- and tetra-tert-butyl ester functionalized [8] and [10]CPP by the Wegner group.[74]*

1.2 Supramolecular Fullerene Assemblies

Geometry, Electronic Properties, and Functionalization of Fullerenes

Fullerenes belong to the carbon allotropes along with graphite and diamond, among others.[97] This class of molecular carbon allotropes consist of many different members, all being spherical polycyclic molecules consisting of twelve five-membered rings and a variable number *m* of six-membered rings (except for $m = 1$),[98,99] following Euler's theorem.[100,101] The first report postulating the existence of a spherical carbon allotrope was published by Osawa in 1970.[102] 15 Years later, Smalley and coworkers presented the first proof of existence,[103] for which Smalley, Kroto, and Curl where awarded with the Nobel Prize in 1996.[104] By laser vaporization of graphite, cluster with the mass of C_{60} were obtained predominantly (at cluster masses $>C_{40}$), which was rationalized by the spherically truncated icosahedral structure of the "molecular football" (Figure 6). Besides laser vaporization, other graphite vaporization methods toward the formation of fullerenes have been developed[105–108] as well as bottom up approaches.[109,110]

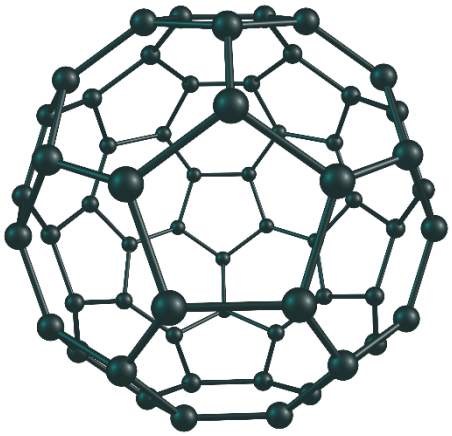

Figure 6: *Structure of buckminsterfullerene (C_{60}).*

Buckminsterfullerene is not only the first reported fullerene, but also the smallest stable homolog having the more precise nomenclature (C_{60}-I_h)[5,6]fullerene.[99] C_{60} describes the composition, I_h the icosahedral point group and [5,6] the embedded ring sizes.[111] The next larger stable fullerene is (C_{70}-D_{5h})[5,6]fullerene, known as C_{70}, followed by the homologs C_{74}, C_{76} and C_{78}. C_{60} consists of pentagons surrounded by hexagons, and thus, bears two different types of bonds, [5,6] and [6,6] bonds. The latter have a higher double bond character, resulting in a shorter C-C bond length and higher reactivity, compared to the [5,6] bond.[112] As a conclusion, C_{60} follows the isolated pentagon rule,[113] embedding [5]radialenes and by that maximizing the number of Kekulé benzene rings.[114]

In general, due to the pyramidalization of the formally sp^2 hybridized carbon atoms in fullerenes, they are electrophilic, which determines the electronic and synthetic properties. C_{60} has a threefold degenerated LUMO,[115] allowing a reduction to its hexaanion by electrochemical (reversible),[116] just as chemical treatment.[117] The electropositive convex surface can be covalently functionalized by nucleophilic addition as well as in electrocyclic reactions.[97] One important example in this regard is the Bingel reaction (Scheme 8),[118] which represents – based on a synthetic method by McCoy[119] – a cyclopropanation of fullerene with a bromo malonate. In case the bromo malonate is synthesized *in situ* by bromination of the parent malonate with CBr_4 in presence of base, this variation is called Bingel-Hirsch reaction.[120] In the first step of the Bingel reaction, the bromo malonate **42** is deprotonated in *α*-position, forming a stabilized malonate anion **A**. This nucleophile adds to the more reactive [6,6] bond of the fullerene **43** to yield the fullerenyl anion **B**. The anion closes the three-membered ring by intramolecular addition to the α-malonyl carbon, releasing bromide as the leaving group.

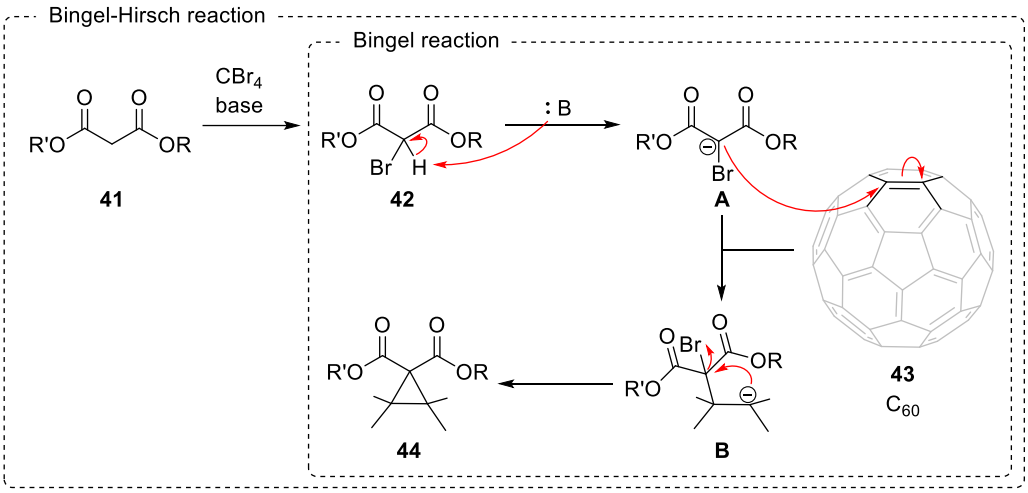

Scheme 8: *Schematic representation of the Bingel reaction[118] and the Bingel-Hirsch variation.[120]*

The electronegativity of fullerenes[116] – resulting from the low-lying LUMO[115] – does not only make them good acceptors for electrons and nucleophiles, but also excellent guests for electron rich hosts in supramolecular assemblies.

Supramolecular Chemistry and Non-Covalent Interactions (NCI)

Supramolecular chemistry is the "chemistry beyond the molecule", and thus, handles species greater than molecules – called supramolecules – which are result of spontaneous association.[121] This field in chemistry is grounded on non-covalent interactions, such as hydrogen bonding[122] or

van-der-Waals interactions.[98,123] The latter family of interactions can be divided into London dispersion interactions (LD, induced dipol – induced dipol),[124,125] Debye interactions (dipol – induced dipol)[126] and Keesom interactions (dipol – dipol).[127] Especially, London dispersion raised attention in the past decades, as this force had been revealed being of underestimated importance in various chemical processes.[128] This underestimation originates from the weak nature when inspecting pair interactions, however, the impact rises rapidly for larger systems bearing multiple pair interactions.[129] Besides the number of pairwise interactions, the polarizability of the counterparts plays a role for interaction strength. Polarizability is the "ease of distortion of the electron cloud" of an entity – a molecule, a functional group, or an atom – by an external electric field.[98] An increased polarizability facilitates the formation of an induced dipole and thus enhances the ability to interact with another (induced) dipole. In organic chemistry LD is often attributed to aliphatic groups, but also plays a significant role in olefinic and aromatic interactions.[130]

The non-covalent interaction between two π-conjugated molecules is called π-π interaction. This generic term is commonly used to describe those interactions, even though the underlying interactions can often be pinpointed to LD or electrostatic (quadrupole) interactions.[131] Stacked π-π interactions lead to the well-known structure of graphite, being further favored by the excellent shape complementarity which allows a homogeneous interaction between the graphene layers.[132] Bending π-conjugated molecules induces changes in the π-orbitals, and thus in the association between bent counterparts. Still, the homogeneity of interaction between a concave and convex surface can be maintained leading to favorable concave-convex π-π interactions (Figure 7).[93] This can be identified as a major force in supramolecular assemblies of fullerenes, alike in multi-walled carbon nanotubes (MWCNTs), which were already described in Iijima's first report of CNTs.[3] Due to the curvature the carbon atoms have a σ-bond hybridization in between sp^2 and sp^3, and therefore, the orbital size alters from the convex to the concave site, being larger on the former site.[133] This phenomenon was thoroughly investigated by Haddon, introducing the π-orbital axis vector (POAV) analysis.[133] By determination of the pyramidalization of the carbon centers the hybridization can be defined helping to understand the orbital geometries of bent π-conjugated molecules. For instance, in buckminsterfullerene the carbon centers have a pyramidalization angle of $(\theta_{\sigma\pi} - 90)\,^\circ = 11.64\,^\circ$ and an average σ-bond hybridization of $sp^{2.278}$.[99,134] Besides the change in orbital geometry, curvature also induces in a dipole moment, giving rise to dipole interactions of those bent π-conjugated molecules.[99]

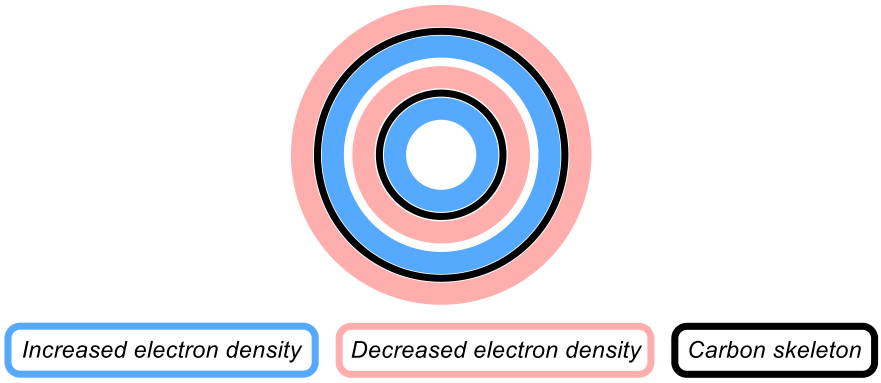

Figure 7: *Representation of the electron density alternation in concave-convex π-π interaction.*[135]

Fullerene Complexes – Catching the Buckyball

A motif, where the encapsulated molecule is not a CNT, but a fullerene was discovered by Luzzi and coworkers in the late 1990s.[136] These fullerene peapods can be obtained by pulsed laser vaporization of graphite yielding in nanotubes with a diameter of 1.3-1.4 nm, surrounding multiple fullerenes C_{60} with a diameter of 0.7 nm (Figure 8). Consequently, the distance between the nanotube and the encapsulated fullerene is ~ 0.3 nm, which resembles the interlayer distance in graphite (0.34 nm) and can be pinpointed as the distance of favorable π-π interaction.[137] An issue of these systems are the difficulties in their analysis. As their method of preparation results in inhomogeneous materials, these fullerene peapods are not suitable for in-depth analyses to understand the underlying interactions.[138]

By application of shorter cutouts of CNTs, the interaction can be mimicked, retaining the desired uniformity in their composition. Even before the first synthesis of CPPs, the group of Oda synthesized carbon nanohoops bearing alternating *para*-phenylenes and acetylenes called [*n*]cycloparaphenyleneacetylenes ([*n*]CPPAs).[139,140] [6]CPPA forms a complex with C_{60} (**45**) having a high association constant of $1.6 \cdot 10^4$ M^{-1} in benzene, which can be attributed to the convex-concave π-π interaction (Figure 9).[141] When comparing the [6]CPPA with the nanotubes of Luzzi, they appear to be similar in size (1.3-1.4 nm for the CNT vs. 1.31 nm for [6]CPPA).[135,136] Thus, the favorable interactions are the result of matching distances within this supramolecular assembly. Additionally, in the study by Oda, they were able to form complexes not only of the [6]CPPA with fullerene, but also between CPPAs of different sizes.[142–145] When mixing [6]CPPA with [9]CPPA, a ring-in-ring complex **46** was observed with an association constant of ~ 40 M^{-1} in chloroform. The drastically reduced binding constant, with regard to the [6]CPPA⊃C_{60} (**45**), is likely to originate from

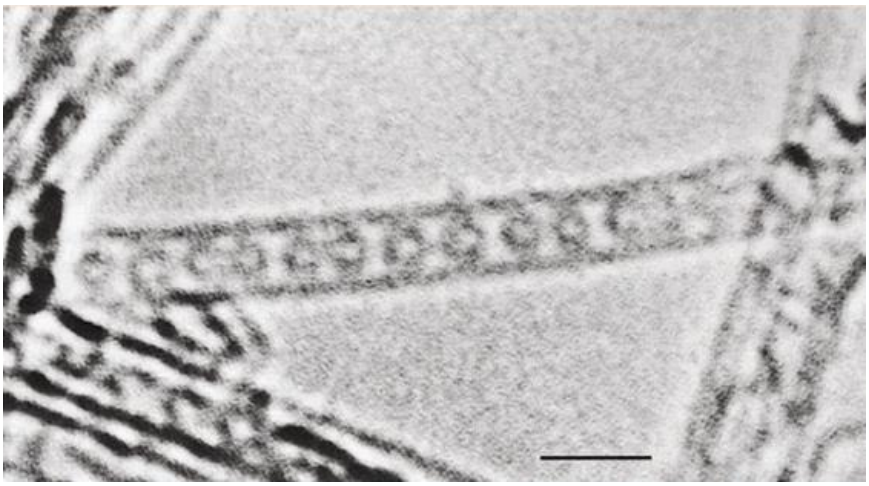

Figure 8: *C_{60} filling the cavity of a single walled carbon nanotube (SWCNT). High-resolution transmission electron microscopy image of the fullerene peapod reported by the group of Luzzi. Scale bar 2.0 nm.[136] Reprinted with permission. Copyright © 1998 Springer Nature.*

the decreased π-interactions as well as the fact that the ring-in-ring association is only effective when both rings are overlapping. Consequently, there is an entropic penalty reducing the association energy and thereby the association constant. By extension of the *para*-phenylenes to 1,4-naphthalenes the association constant could be increased, which shows the possibility of tuning the binding behavior with substituents, *e.g.,* aromatic pendants. These motifs can be pushed to even more ambitious assemblies by the formation of an onion-like complex, also known as Russian-doll complex.[142] By combination of the ring-in-ring with the fullerene complex, an assembly bearing a C_{60} core surrounded by [6]CPPA surrounded by [9]CPPA can be obtained mimicking a MWCNT (**47**, Figure 9, right).

As already mentioned in case of CPPAs, the substitution on the nanohoop influences the association behavior, rationalized by changing area or strength of interaction. An often-used host for buckminsterfullerene is calix[5]arene, allowing to study the influence of substitution systematically.[135] A review by Kurata and Kawase summarized published data on the association of the calixarene-fullerene complex in toluene (Figure 10).[135] In general, the unsubstituted calixarene **48a** appears to be too small for an efficient encapsulation.[146] By adding methyl groups additional CH-π interactions increase the association constant to $1.7 \cdot 10^3$ M^{-1} (**48b**).[146] The partial exchange of CH_3 groups with better polarizable iodide (**48c**) increased the association constant further, showing a stronger interaction.[147] Equipping the calixarenes with aromatic pendants, such as benzyl (Bn, **48d**)[148] and phenyl groups (Ph, **48e**),[149] increases the binding even further and also the formation of 2:1 complexes (**48d**)$_2\supset C_{60}$ and (**48e**)$_2\supset C_{60}$ were reported. In these trimeric

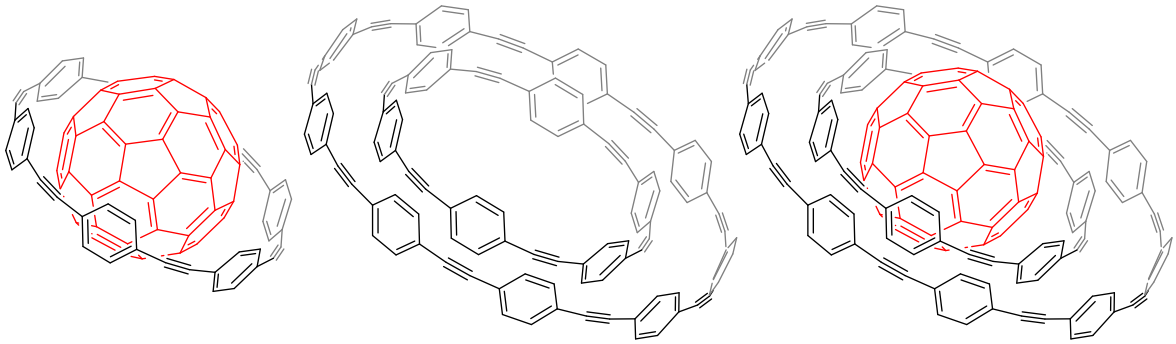

45
[6]CPPA⊃C_{60}

46
[9]CPPA⊃[6]CPPA

47
[9]CPPA⊃[6]CPPA⊃C_{60}

Figure 9: *Supramolecular assemblies of Buckminsterfullerene and/or [n]CPPAs, forming orbit- and onion-like structures.*[141,142]

complexes, two bowl-shaped calixarenes form a capsule binding the fullerene in their cavity. Noteworthy, with second binding constants of K_2(**48d**, Bn) = 230 M^{-1} and K_2(**48e**, Ph) = 250 M^{-1}, in both cases the cooperativity factor α is smaller than 1, indicating hindrance of the second association by the first (EQ 1). In case the host or the guest possesses more than one binding site, the cooperativity factor α displays the influence of one binding event on the other.[150] For a complexation in a 2:1 or 1:2 fashion, $\alpha = 1$ indicates two independent binding sites, while a cooperativity factor of $\alpha > 1$ and $\alpha < 1$ display a positive or negative influence on the second binding event, respectively.[151]

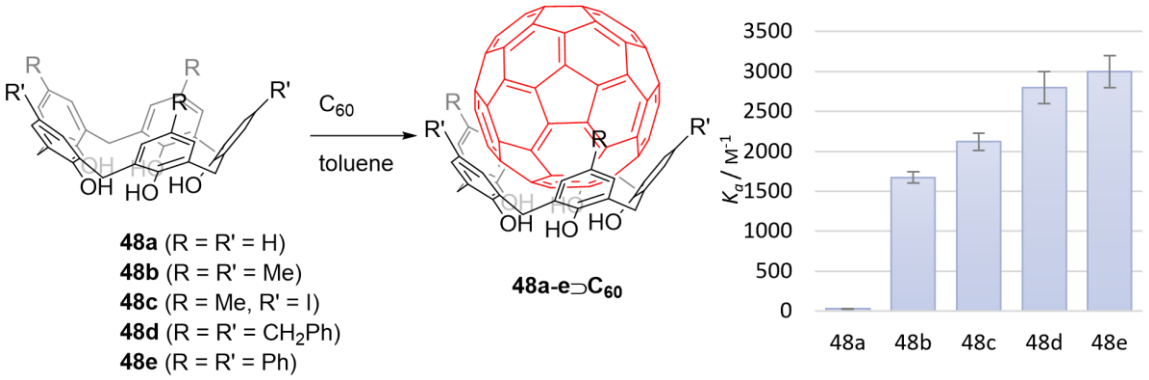

Figure 10: *Binding constants of different functionalized calix[5]arenes with C_{60} in toluene. The data were obtained from different publications and summed up in a review by Kurata and Kawase.*[135,146–149]

$$\alpha = \frac{4K_2}{K_1} \qquad \text{(EQ 1)}$$

CPP-Fullerene Complexes – Properties, Substitution Effects, and Application

Besides extending the *para*-phenylenes to naphthalenes in CPPAs, as done by Oda and coworkers, the π-surface can be increased by exchanging the acetylenes with *para*-phenylenes, or more precisely, by using CPPs. Alike in CPPA complexes the concave-convex π-π interaction is the most important interaction in supramolecular CPP architectures,[38,152] however, also assemblies dominated by CH-π interactions are reported in literature.[153–155] The first report of a fullerene complex with a CPP was published by the group of Yamago in 2011.[156] Addition of excess solid C_{60} to a mixture of [8]-[12]CPP in deuterated chloroform, induced a ^{1}H NMR shift of [10]CPP resulting from the deshielding effect of C_{60} (Figure 11). The signal for [8], [9], [11] and [12]CPPs remained unchanged showing the size-selective encapsulation of [10]CPP. When comparing the diameter of [10]CPP and C_{60}, the difference in diameter is 0.68 nm, which results in a CPP-fullerene distance of 0.34 nm, being the ideal distance for π-π interactions.[32] This match in size and shape leads to an extraordinarily high association constant of $8.40 \cdot 10^6$ M^{-1} in toluene and $2.5–8.1 \cdot 10^5$ M^{-1} in *o*-DCB (depending on the experimental technique).[157]

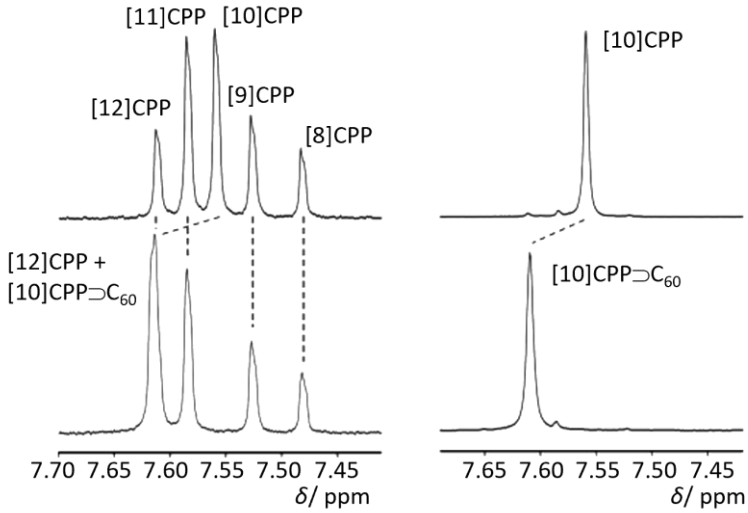

Figure 11: *^{1}H NMR ($CDCl_3$) executed by Yamago and coworkers.[156] In a mixture of different CPPs, [10]CPP selectively shifts downfield upon addition of fullerene C_{60} (left). The protons of [10]CPP are deshielded when buckminsterfullerene is placed in the cavity of the nanohoop (right). Reprinted with permission. Copyright © 2011 Wiley-VCH Verlag GmbH & Co. KGaA.*

Fullerenes C_{70} and C_{60} share the diameter along the short axis, and thus, it is comprehensible that this ellipsoidal fullerene can also be encapsulated with [10]CPP. By executing the same experiment with C_{70}, which was described above for C_{60}, not only the signal for [10]CPP shifts, but also the signal corresponding to [11]CPP (Figure 12).[158] This originates from the two different diameters of C_{70}

along the two axes, where the larger diameter fits the cavity of [11]CPP. Interestingly, the effect of the encapsulation on the NMR-shift is opposing. While [10]CPP experiences a shielding effect, the protons of [11]CPP are deshielded, resulting from the opposite magnetic anisotropy. Besides the magnetic effects of the binding, the association constants in toluene were determined, being $K_a = 8.4 \cdot 10^4$ M^{-1} and $K_a = 1.5 \cdot 10^5$ M^{-1} for [10]CPP⊃C_{70} and [11]CPP⊃C_{70}, respectively. The reduced association constants compared to [10]CPP⊃C_{60} can be attributed to the reduced degrees of rotational freedom of C_{70} in the complexes as well as slight deformation of the nanohoop in [11]CPP⊃C_{70} (Figure 12, bottom right). While in case of C_{60} the fullerene can rotate along all axes without leaving or deforming the cavity, this rotation is reduced by one degree of freedom (one axis) in case of both discussed C_{70} complexes. Similarly, a substitution of fullerene C_{60} – such as in case of [6,6]-phenyl-C_{61}-butyric acid methyl ester (PCBM, **49**, Figure 13) – reduces the freedom of rotation and leads to a decrease in the association constant ($K_a = 3.7 \cdot 10^5$ M^{-1} for [10]CPP⊃PCBM) with respect to parent C_{60}.[89,158]

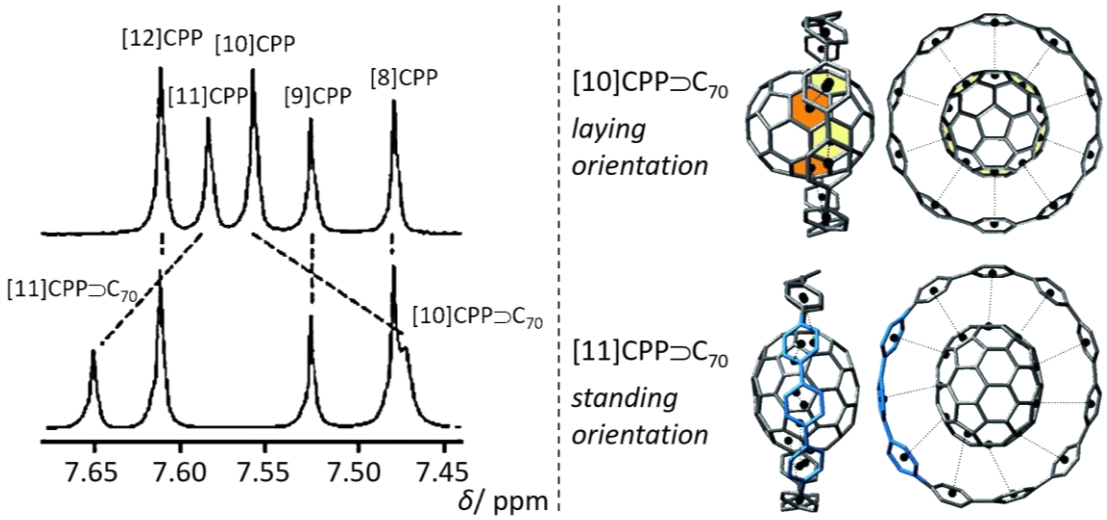

Figure 12: *^{1}H NMR ($CDCl_3$) executed by Yamago and coworkers.[158] In a mixture of different CPPs, [10]CPP and [11]CPP selectively shifted upon addition of fullerene C_{70}, having the opposite effect on the magnetic anisotropy (left). Calculated geometries of [10]CPP⊃C_{70} in its lying and the [11]CPP⊃C_{70} in its standing fashion (M06-2X/6-31G*; right). Reprinted with permission. Copyright © 2013 Wiley-VCH Verlag GmbH & Co. KGaA.*

The motif of a functionalized fullerene encapsulated by [10]CPP was also used by the group of von Delius for the synthesis of a rotaxane.[159] In this study, [10]CPP encapsulated fullerene was functionalized with very bulky groups on both poles to prohibit the release of the nanohoop. By that, a supramolecular CPP assembly was formed, having a formally infinite association constant. Besides in rotaxanes,[160] these infinite association constants can be achieved in catenanes.[161–163]

Another way of increasing the association in CPP-fullerene complexes is the π-extension of the nanohoop.[164,165] Even though this does not result in an infinite association constant, the association can be improved. For instance, the group of Du reported the encapsulation of C_{70} by a π-extended [12]CPP, namely a [4]cyclohexa-peri-hexabenzocoronene (**50**, Figure 13).[108] While an association between parent [12]CPP and C_{70} is not reported, this nanotube segment has a remarkable association constant of $K_a = 1.07 \cdot 10^6$ м$^{-1}$ in toluene.

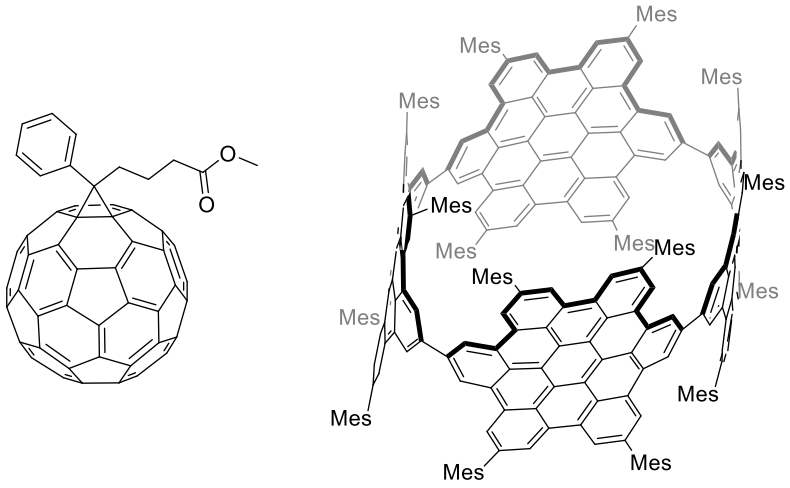

49
PCBM

50
[4]cyclohexa-peri-hexabenzocoronene

Figure 13: *[6,6]-phenyl-C_{61}-butyric acid methyl ester (PCBM, left) and [4]cyclohexa-peri-hexabenzocoronene*[166] *(right).*

In the examples of functionalized fullerenes described above, functionalization led to a reduction in association. Moreover, modifications offer the possibility of additional interactions, either with the surrounding nanohoop or another molecule. One possibility of functionalization is to substitute with another fullerene, and thus, forming fullerene dimers[167] like bisazafullerene $(C_{59}N)_2$, among others.[89,157] In azafullerene one carbon atom in C_{60} is exchanged by nitrogen atom resulting in a vacancy of the adjacent carbon, which is filled by dimerization.[168,169] Addition of [10]CPP to this dimer, leads to a 2:1 complex, where each CPP hosts one sphere (Scheme 9).[170] The association constant for the first binding is $K_1 = 8.4 \cdot 10^6$ м$^{-1}$ being similar to the parent [10]CPP⊃C_{60} complex.[170] The second association has a binding constant of $K_2 = 3.0 \cdot 10^6$ м$^{-1}$ and thus a positive cooperativity (cooperativity factor $\alpha > 1$). By DFT calculations (AIMPRO, utilizing 38 independent Gaussian-based functions are used as basis set for carbon, 12 for hydrogen, 40 for nitrogen), the positive cooperativity was attributed to additional London dispersion and CH-π interactions between the two nanohoops.

Furthermore, it was possible to homolytically cleave the spheres-connecting single bond by irradiation of the of the bisazafullerene complex **54** in solution. Although the homolysis of parent $(C_{59}N)_2$ dimer was already known, the stability of the formed radicals was drastically improved by the surrounding nanohoop (increased lifetime by factor of 10^8).[171]

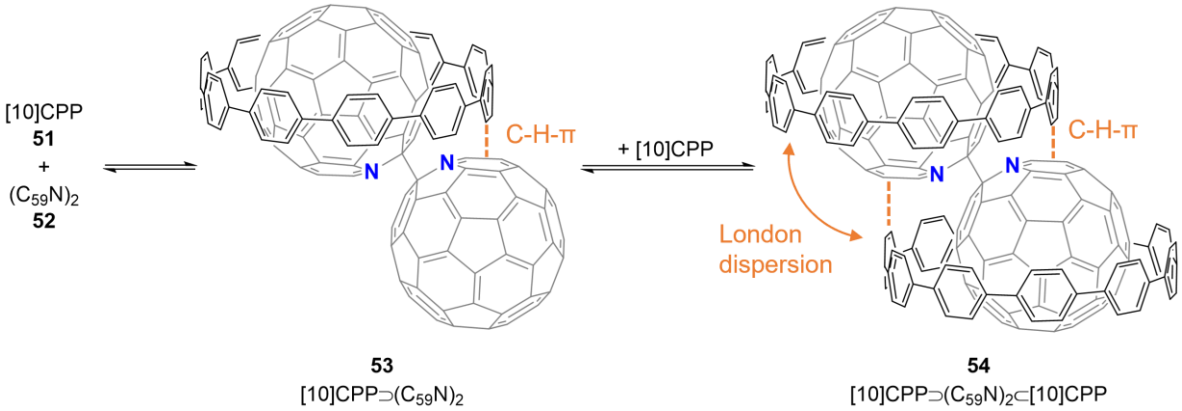

Scheme 9: *Binding of bisazafullerene in the cavities of two [10]CPPs. The association is assisted by additional CH-π and London dispersion interactions.*[170]

While the encapsulated azafullerenyl radical is a valid candidate for qubits,[171] the supramolecular assemblies of CPPs can also be utilized for the selective functionalization of fullerenes,[159,162,172] as well as purification[173] and tuning[174–176] of metallofullerenes.

The attributes of CPPs, which were discussed above, in addition to the remarkable characteristics and potential applications of their supramolecular assemblies make new syntheses of the nanohoops and an enhanced understanding of their behavior in supramolecular complexes valuable. Fullerene complexes with substituted CPPs offer new properties, and the influence of substituents in supramolecular CPP-fullerene architectures remains a blind spot.

2 Motivation and Outlook

Cycloparaphenylenes and their fullerene complexes have unusual properties with potential application in molecular electronics and materials science.[9,171] To extend the knowledge about those properties and their applications, these nanohoops have to be available in a certain quantity and a bottleneck remains the challenging synthesis and hence, costly production of the nanohoops. As functionalization of CPPs allows alteration of their properties, elegant syntheses of CPPs with novel substitution patterns are desirable.

As the first part of this thesis, a new strategy for the synthesis of a substituted [10]CPP derivative was developed (Figure 14).[177] A [2+2+2] CA was utilized as an efficient tool to introduce substituents during the synthesis, yielding in a diethyl phthalane incorporated [10]CPP. The motivation for this synthesis originates from drawbacks of reported synthetic methods, lacking efficiency in the key steps ([2+2+2] CA, macrocyclization, and aromatization). Grounded on synthetic strategies by the groups of Tanaka (Scheme 6) and Wegner (Scheme 5), a synthesis was developed which combines the advantages, and circumvents the disadvantages of both syntheses. A [10]CPP derivative was targeted, as its size allows efficient encapsulation of the fullerenes C_{60} and C_{70}, in order to investigate the influence of substitution in these supramolecular assemblies.

The reported synthesis provided the targeted nanohoop in 8% overall yield. Especially the efficiency of the key steps was enhanced, making this synthesis a valuable improvement in the field of nanohoops and a step forward to the application and in-depth understanding of CPPs. Furthermore, the application of a [2+2+2] CA enables the introduction of various substituents to precisely control the properties of the nanohoop, increasing the potential application of this synthetic approach.

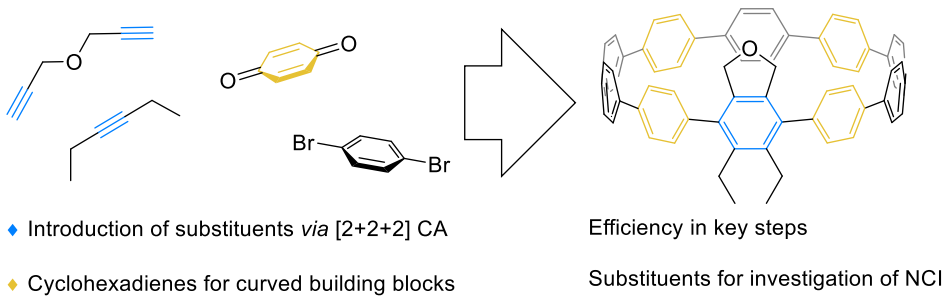

***Figure 14**: Synthetic strategy for the synthesis of a diethyl phthalane [10]CPP.*

In two consecutive studies the influence of substitution on the binding behavior with fullerenes was investigated (Figure 15). While binding constants of nanohoops with fullerene C_{60} are regularly determined along with their synthesis,[178] a systematic study on the substitution effects remained

unaddressed. As substitution of the nanohoops is a versatile tool to alter the binding behavior and, by that, access desired properties, an in-depth understanding on the influence of degree and kind of substitution is desirable. A systematic approach is of particular importance as the determination of binding constants – being the crucial quantity in this regard – is prone to errors originating from differences in the spectroscopic measurements or shortcuts in data analysis[179] (*e.g.,* comparison of binding constants reported for [10]CPP⊃C_{60}).[156,157,180] Hence, interpretation based on values obtained from different sources is rarely possible.

A systematic study on the interactions between alkyl substituents on both [10]CPP and fullerene C_{60} revealed an interplay between stabilizing and destabilizing effects. These were assigned to London dispersion and Pauli repulsion, showing an overall stabilizing effect which is partly compensated in sterically demanding methanofullerenes.[180]

Furthermore, the effects of CPP substitution on the association with the fullerenes C_{60} and C_{70} were investigated.[181] In this study, three substituted CPPs were applied bearing different substituents and degrees of substitution. The studies revealed that the ellipsoid shape of C_{70} allows a relative stabilization of substituted CPP complexes in comparison to the C_{60} complexes. This observation can be rationalized by the shape of C_{70}, enabling additional favorable substituent-fullerene interactions.

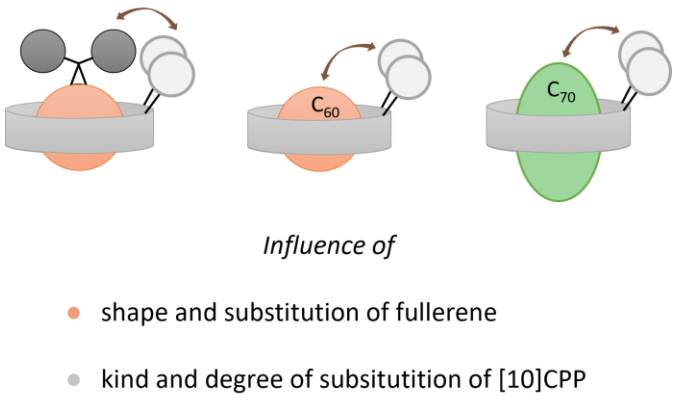

Figure 15: *Overview of the analyzed and compared interactions in the binding studies.*

The results of these systematic studies shine light on the binding behavior of substituted CPPs, giving rise to decisive manipulation of the binding energy by choice of kind and degree of substitution on the CPP. While substitution enables additional stabilizing interactions, energetic penalties of reduced entropy or increased dihedral strain outnumbers these stabilizing forces. Thus, substituted CPPs with an increased diameter should be applied in further studies as they promise similar stabilizing effects and a better complementarity in size. Additionally, the precise

determination of binding constants *via* fluorescence quenching – as shown in both projects – can be utilized to study interactions between the binding partners.

3 REFERENCES

[1] L. Pauling, *J. Am. Chem. Soc.* **1931**, *53*, 1367.

[2] E. H. L. Falcao, F. Wudl, *J. Chem. Technol. Biotechnol.* **2007**, *82*, 524.

[3] L. V. Radushkevich, V. M. Lukyanovich, *Zurn. Fisic. Chim.* **1952**, *26*, 88.

[4] S. Iijima, *Nature* **1991**, *354*, 56.

[5] M. S. Dresselhaus, G. Dresselhaus, R. Saito, *Carbon* **1995**, *33*, 883.

[6] A. K.-T. Lau, D. Hui, *Compos. B. Eng.* **2002**, *33*, 263.

[7] K. Müllen, M. Antonietti, *Chemical synthesis and applications of graphene and carbon materials*, Wiley-VCH, Weinheim, Germany, **2017**.

[8] U. Vohrer, N. Zschoerper, *VIP* **2007**, *19*, 22.

[9] S. E. Lewis, *Chem. Soc. Rev.* **2015**, *44*, 2221.

[10] H. Omachi, T. Nakayama, E. Takahashi, Y. Segawa, K. Itami, *Nat. Chem.* **2013**, *5*, 572.

[11] D. Wu, W. Cheng, X. Ban, J. Xia, *Asian J. Org. Chem.* **2018**, *7*, 2161.

[12] U. H. F. Bunz, S. Menning, N. Martín, *Angew. Chem. Int. Ed.* **2012**, *51*, 7094.

[13] V. C. Parekh, P. C. Guha, *J. Indian Chem. Soc.* **1934**, *11*, 95.

[14] R. Friederich, M. Nieger, F. Vögtle, *Chem. Ber.* **1993**, *126*, 1723.

[15] A.-F. Tran-Van, H. A. Wegner, *Beilstein J. Nanotechnol.* **2014**, *5*, 1320.

[16] R. Jasti, J. Bhattacharjee, J. B. Neaton, C. R. Bertozzi, *J. Am. Chem. Soc.* **2008**, *130*, 17646.

[17] H. Takaba, H. Omachi, Y. Yamamoto, J. Bouffard, K. Itami, *Angew. Chem. Int. Ed.* **2009**, *48*, 6112.

[18] S. Yamago, Y. Watanabe, T. Iwamoto, *Angew. Chem. Int. Ed.* **2010**, *49*, 757.

[19] Y. Yoshigoe, Y. Tanji, Y. Hata, K. Osakada, S. Saito, E. Kayahara, S. Yamago, Y. Tsuchido, H. Kawai, *JACS Au* **2022**, *2*, 1857.

[20] Y. Tsuchido, R. Abe, T. Ide, K. Osakada, *Angew. Chem. Int. Ed.* **2020**, *59*, 22928.

[21] R. B. Kręcijasz, J. Malinčík, T. Šolomek, *Synthesis* **2023**, *55*, 1355.

[22] E. R. Darzi, T. J. Sisto, R. Jasti, *J. Org. Chem.* **2012**, *77*, 6624.

[23] T. J. Sisto, M. R. Golder, E. S. Hirst, R. Jasti, *J. Am. Chem. Soc.* **2011**, *133*, 15800.

[24] J. Xia, R. Jasti, *Angew. Chem. Int. Ed.* **2012**, *51*, 2474.

[25] Y. Ishii, Y. Nakanishi, H. Omachi, S. Matsuura, K. Matsui, H. Shinohara, Y. Segawa, K. Itami, *Chem. Sci.* **2012**, *3*, 2340.

[26] T. Iwamoto, Y. Watanabe, Y. Sakamoto, T. Suzuki, S. Yamago, *J. Am. Chem. Soc.* **2011**, *133*, 8354.

[27] E. Kayahara, T. Iwamoto, T. Suzuki, S. Yamago, *Chem. Lett.* **2013**, *42*, 621.

[28] E. Kayahara, V. K. Patel, S. Yamago, *J. Am. Chem. Soc.* **2014**, *136*, 2284.

[29] J. H. Griwatz, M. L. Kessler, H. A. Wegner, *Chem. Eur. J.* **2023**, e202302173.

[30] J. H. Griwatz, H. A. Wegner, *Organic Materials* **2020**, *2*, 306.

[31] E. Kayahara, Y. Sakamoto, T. Suzuki, S. Yamago, *Org. Lett.* **2012**, *14*, 3284.

[32] J. Xia, J. W. Bacon, R. Jasti, *Chem. Sci.* **2012**, *3*, 3018.

[33] H. Kim, H.-J. Lee, D.-P. Kim, *Angew. Chem. Int. Ed.* **2016**, *55*, 1422.

[34] E. R. Darzi, B. M. White, L. K. Loventhal, L. N. Zakharov, R. Jasti, *J. Am. Chem. Soc.* **2017**, *139*, 3106.

[35] P. J. Evans, E. R. Darzi, R. Jasti, *Nat. Chem.* **2014**, *6*, 404.

[36] Y. Segawa, T. Kuwabara, K. Matsui, S. Kawai, K. Itami, *Tetrahedron* **2015**, *71*, 4500.

[37] V. K. Patel, E. Kayahara, S. Yamago, *Eur. J. Org. Chem.* **2015**, *21*, 5742.

[38] Y. Xu, M. von Delius, *Angew. Chem. Int. Ed.* **2020**, *59*, 559.

[39] O. Laporte, W. F. Meggers, *J. Opt. Soc. Am.* **1925**, *11*, 459.

[40] C. Camacho, T. A. Niehaus, K. Itami, S. Irle, *Chem. Sci.* **2013**, *4*, 187.

[41] M. Kasha, *Discuss. Faraday Soc.* **1950**, *9*, 14.

[42] S. Beeck, H. A. Wegner, *Synlett* **2017**, *28*, 1018.

[43] K. Matsui, Y. Segawa, K. Itami, *Org. Lett.* **2012**, *14*, 1888.

[44] J. S. Wössner, D. Wassy, A. Weber, M. Bovenkerk, M. Hermann, M. Schmidt, B. Esser, *J. Am. Chem. Soc.* **2021**, *143*, 12244.

[45] W. Stawski, J. M. van Raden, C. W. Patrick, P. N. Horton, S. J. Coles, H. L. Anderson, *Org. Lett.* **2023**, *25*, 378.

[46] J. Batson, T. Swager, *Synlett* **2013**, *24*, 2545.

[47] M. R. Golder, C. E. Colwell, B. M. Wong, L. N. Zakharov, J. Zhen, R. Jasti, *J. Am. Chem. Soc.* **2016**, *138*, 6577.

[48] A. Yagi, Y. Segawa, K. Itami, *J. Am. Chem. Soc.* **2012**, *134*, 2962.

[49] S. Wang, Q. Huang, J. Wang, P. Huang, P. Fang, P. Du, *Chem. Commun.* **2021**, *57*, 11867.

[50] N. Grabicki, K. T. D. Nguyen, S. Weidner, O. Dumele, *Angew. Chem. Int. Ed.* **2021**, *60*, 14909.

[51] S. Li, M. Aljhdli, H. Thakellapalli, B. Farajidizaji, Y. Zhang, N. G. Akhmedov, C. Milsmann, B. V. Popp, K. K. Wang, *Org. Lett.* **2017**, *19*, 4078.

[52] S. Cui, G. Zhuang, J. Wang, Q. Huang, S. Wang, P. Du, *Org. Chem. Front.* **2019**, *6*, 1885.

[53] P. Della Sala, C. Talotta, M. de Rosa, A. Soriente, S. Geremia, N. Hickey, P. Neri, C. Gaeta, *J. Org. Chem.* **2019**, *84*, 9489.

[54] E. Kayahara, M. Nakano, L. Sun, K. Ishida, S. Yamago, *Chem. Asian J.* **2020**, *15*, 2451.

[55] E. Kayahara, L. Sun, H. Onishi, K. Suzuki, T. Fukushima, A. Sawada, H. Kaji, S. Yamago, *J. Am. Chem. Soc.* **2017**, *139*, 18480.

[56] E. J. Leonhardt, J. M. van Raden, D. Miller, L. N. Zakharov, B. Alemán, R. Jasti, *Nano Lett.* **2018**, *18*, 7991.

[57] D. Lu, G. Zhuang, H. Jia, J. Wang, Q. Huang, S. Cui, P. Du, *Org. Chem. Front.* **2018**, *5*, 1446.

[58] B. M. White, Y. Zhao, T. E. Kawashima, B. P. Branchaud, M. D. Pluth, R. Jasti, *ACS Cent. Sci.* **2018**, *4*, 1173.

[59] Y. Xu, F. Steudel, M.-Y. Leung, B. Xia, M. von Delius, V. W.-W. Yam, *Angew. Chem. Int. Ed.* **2023**, *62*, e202302978.

[60] H. Shudo, M. Kuwayama, M. Shimasaki, T. Nishihara, Y. Takeda, N. Mitoma, T. Kuwabara, A. Yagi, Y. Segawa, K. Itami, *Nat. Commun.* **2022**, *13*, 3713.

[61] S. Hashimoto, E. Kayahara, Y. Mizuhata, N. Tokitoh, K. Takeuchi, F. Ozawa, S. Yamago, *Org. Lett.* **2018**, *20*, 5973.

[62] Y. Kuroda, Y. Sakamoto, T. Suzuki, E. Kayahara, S. Yamago, *J. Org. Chem.* **2016**, *81*, 3356.

[63] J. Xia, M. R. Golder, M. E. Foster, B. M. Wong, R. Jasti, *J. Am. Chem. Soc.* **2012**, *134*, 19709.

[64] T. C. Lovell, Z. R. Garrison, R. Jasti, *Angew. Chem. Int. Ed.* **2020**, *59*, 14363.

[65] F. E. Golling, S. Osella, M. Quernheim, M. Wagner, D. Beljonne, K. Müllen, *Chem. Sci.* **2015**, *6*, 7072.

[66] F. E. Golling, M. Quernheim, M. Wagner, T. Nishiuchi, K. Müllen, *Angew. Chem. Int. Ed.* **2014**, *126*, 1551.

[67] M. J. Heras Ojea, J. M. van Raden, S. Louie, R. Collins, D. Pividori, J. Cirera, K. Meyer, R. Jasti, R. A. Layfield, *Angew. Chem. Int. Ed.* **2021**, *60*, 3515.

[68] T. Iwamoto, E. Kayahara, N. Yasuda, T. Suzuki, S. Yamago, *Angew. Chem. Int. Ed.* **2014**, *53*, 6430.

[69] S. Kammermeier, P. G. Jones, R. Herges, *Angew. Chem. Int. Ed.* **1996**, *35*, 2669.

[70] E. Kayahara, R. Qu, S. Yamago, *Angew. Chem. Int. Ed.* **2017**, *56*, 10428.

[71] K. Ypsilantis, T. Tsolis, A. Garoufis, *Inorg. Chem. Commun.* **2021**, *134*, 108992.

[72] N. Kubota, Y. Segawa, K. Itami, *J. Am. Chem. Soc.* **2015**, *137*, 1356.

[73] E. Kayahara, V. K. Patel, A. Mercier, E. P. Kündig, S. Yamago, *Angew. Chem. Int. Ed.* **2016**, *128*, 310.

[74] D. Kohrs, J. Becker, H. A. Wegner, *Chem. Eur. J.* **2022**, *28*, e202104239.

[75] A.-F. Tran-Van, E. Huxol, J. M. Basler, M. Neuburger, J.-J. Adjizian, C. P. Ewels, H. A. Wegner, *Org. Lett.* **2014**, *16*, 1594.

[76] N. Hayase, Y. Miyauchi, Y. Aida, H. Sugiyama, H. Uekusa, Y. Shibata, K. Tanaka, *Org. Lett.* **2017**, *19*, 2993.

[77] N. Hayase, H. Sugiyama, H. Uekusa, Y. Shibata, K. Tanaka, *Org. Lett.* **2019**, *21*, 3895.

[78] Y. Miyauchi, K. Johmoto, N. Yasuda, H. Uekusa, S. Fujii, M. Kiguchi, H. Ito, K. Itami, K. Tanaka, *Chem. Eur. J.* **2015**, *21*, 18900.

[79] S. Nishigaki, Y. Shibata, A. Nakajima, H. Okajima, Y. Masumoto, T. Osawa, A. Muranaka, H. Sugiyama, A. Horikawa, H. Uekusa et al., *J. Am. Chem. Soc.* **2019**, *141*, 14955.

[80] J. Nogami, Y. Nagashima, H. Sugiyama, K. Miyamoto, Y. Tanaka, H. Uekusa, A. Muranaka, M. Uchiyama, K. Tanaka, *Angew. Chem. Int. Ed.* **2022**, *61*, e202200800.

[81] S. Nishigaki, M. Fukui, H. Sugiyama, H. Uekusa, S. Kawauchi, Y. Shibata, K. Tanaka, *Chem. Eur. J.* **2017**, *23*, 7227.

[82] L.-H. Wang, Y. Nagashima, M. Abekura, H. Uekusa, G.-I. Konishi, K. Tanaka, *Chem. Eur. J.* **2022**, *28*, e202200064.

[83] B. Farajidizaji, H. Thakellapalli, N. G. Akhmedov, K. K. Wang, *J. Org. Chem.* **2018**, *83*, 1216.

[84] C. Huang, Y. Huang, N. G. Akhmedov, B. V. Popp, J. L. Petersen, K. K. Wang, *Org. Lett.* **2014**, *16*, 2672.

[85] H. Thakellapalli, B. Farajidizaji, S. Li, J. C. Heller, Y. Zhang, N. G. Akhmedov, C. Milsmann, J. L. Petersen, K. K. Wang, *J. Org. Chem.* **2018**, *83*, 2455.

[86] R. Schwesinger, H. Schlemper, C. Hasenfratz, J. Willaredt, T. Dambacher, T. Breuer, C. Ottaway, M. Fletschinger, J. Boele, H. Fritz et al., *Liebigs Ann.* **1996**, *1996*, 1055.

[87] J. M. van Raden, E. J. Leonhardt, L. N. Zakharov, A. Pérez-Guardiola, A. J. Pérez-Jiménez, C. R. Marshall, C. K. Brozek, J. C. Sancho-García, R. Jasti, *J. Org. Chem.* **2020**, *85*, 129.

[88] H. Omachi, Y. Segawa, K. Itami, *Org. Lett.* **2011**, *13*, 2480.

[89] Y. Xu, B. Wang, R. Kaur, M. B. Minameyer, M. Bothe, T. Drewello, D. M. Guldi, M. von Delius, *Angew. Chem. Int. Ed.* **2018**, *57*, 11549.

[90] A. A. Kamin, T. D. Clayton, C. E. Otteson, P. M. Gannon, S. Krajewski, W. Kaminsky, R. Jasti, D. J. Xiao, *Chem. Sci.* **2023**, *14*, 9724.

[91] P. R. Chopade, J. Louie, *Adv. Synth. Catal.* **2006**, *348*, 2307.

[92] G. Domínguez, J. Pérez-Castells, *Chem. Soc. Rev.* **2011**, *40*, 3430.

[93] R. Bhola, T. Bally, A. Valente, M. K. Cyrański, Ł. Dobrzycki, S. M. Spain, P. Rempała, M. R. Chin, B. T. King, *Angew. Chem. Int. Ed.* **2010**, *49*, 399.

[94] H. Omachi, S. Matsuura, Y. Segawa, K. Itami, *Angew. Chem. Int. Ed.* **2010**, *49*, 10202.

[95] K. Tanaka, K. Shirasaka, *Org. Lett.* **2003**, *5*, 4697.

[96] K. Tanaka, H. Sagae, K. Toyoda, K. Noguchi, M. Hirano, *J. Am. Chem. Soc.* **2007**, *129*, 1522.

[97] X. Lu, T. Akasaka, Z. Slanina (Eds.) *Handbook of Fullerene Science and Technology*, Springer Singapore, Singapore, **2021**.

[98] V. Gold, *The IUPAC Compendium of Chemical Terminology*, International Union of Pure and Applied Chemistry (IUPAC), Research Triangle Park, NC, United States, **2019**.

[99] A. Hirsch, M. Brettreich, *Fullerenes*, Wiley-VCH, Weinheim, Germany, **2004**.

[100] M. Friedman, *A history of folding in mathematics*. *Mathematizing the margins*, Birkhäuser, Basel, Switzerland, **2018**.

[101] L. Euler, *Elementa doctrinae solidorum*, University of the Pacific Scholarly Commons, Stockton, CA, United States, **1758**.

[102] E. Osawa, *Kagaku* **1970**, *25*, 854.

[103] H. W. Kroto, J. R. Heath, S. C. O'Brien, R. F. Curl, R. E. Smalley, *Nature* **1985**, *318*, 162.

[104] "The Nobel Prize in Chemistry 1996. NobelPrize.org.", can be found under www.nobelprize.org/prizes/chemistry/1996/summary/ (30.08.2023).

[105] A. S. Koch, K. C. Khemani, F. Wudl, *J. Org. Chem.* **1991**, *56*, 4543.

[106] W. Krätschmer, L. D. Lamb, K. Fostiropoulos, D. R. Huffman, *Nature* **1990**, *347*, 354.

[107] R. E. Haufler, J. Conceicao, L. P. F. Chibante, Y. Chai, N. E. Byrne, S. Flanagan, M. M. Haley, S. C. O'Brien, C. Pan, et al., *J. Phys. Chem.* **1990**, *94*, 8634.

[108] G. Peters, M. Jansen, *Angew. Chem. Int. Ed.* **1992**, *31*, 223.

[109] Y. Rubin, *Chem. Eur. J.* **1997**, *3*, 1009.

[110] L. T. Scott, M. M. Boorum, B. J. McMahon, S. Hagen, J. Mack, J. Blank, H. A. Wegner, A. de Meijere, *Science* **2002**, *295*, 1500.

[111] W. H. Powell, F. Cozzi, G. P. Moss, C. Thilgen, R. J.-R. Hwu, A. Yerin, *Pure Appl. Chem.* **2002**, *74*, 629.

[112] M. Bühl, A. Hirsch, *Chem. Rev.* **2001**, *101*, 1153.

[113] E. Campbell, P. W. Fowler, D. Mitchell, F. Zerbetto, *Chem. Phys. Lett.* **1996**, *250*, 544.

[114] H. W. Kroto, *Nature* **1987**, *329*, 529.

[115] A. Haymet, *Chem. Phys. Lett.* **1985**, *122*, 421.

[116] L. Echegoyen, L. E. Echegoyen, *Acc. Chem. Res.* **1998**, *31*, 593.

[117] Y. Ederlé, C. Mathis, *Macromolecules* **1997**, *30*, 4262.

[118] C. Bingel, *Chem. Ber.* **1993**, *126*, 1957.

[119] L. L. McCoy, *J. Am. Chem. Soc.* **1958**, *80*, 6568.

[120] X. Camps, A. Hirsch, *J. Chem. Soc., Perkin Trans. 1* **1997**, 1595.

[121] J. M. Lehn, *Science* **1993**, *260*, 1762.

[122] M. L. Huggins, *Angew. Chem. Int. Ed.* **1971**, *10*, 147.

[123] J. D. van der Waals, *Over de continuiteit van de gas- en vloeistoftoestand.*, Universität Leiden, **1873**.

[124] R. Eisenschitz, F. London, *Z. Physik* **1930**, *60*, 491.

[125] F. London, *Z. Physik* **1930**, *63*, 245.

[126] P. Debye, *Phys. Z.* **1912**, *13*, 97.

[127] W. H. Keesom, *KNAW Proceedings* **1915**, *18*, 636.

[128] J. P. Wagner, P. R. Schreiner, *Angew. Chem. Int. Ed.* **2015**, *54*, 12274.

[129] G. Frenking, S. Shaik (Eds.) *The chemical bond*. *Chemical bonding across the perodic table*, Wiley-VCH Verlag GmbH & Co, Weinheim, Germany, **2014**.

[130] P. R. Schreiner, L. V. Chernish, P. A. Gunchenko, E. Y. Tikhonchuk, H. Hausmann, M. Serafin, S. Schlecht, J. E. P. Dahl, R. M. K. Carlson, A. A. Fokin, *Nature* **2011**, *477*, 308.

[131] S. Grimme, *Angew. Chem. Int. Ed.* **2008**, *47*, 3430.

[132] E. Riedel, C. Janiak, *Anorganische Chemie*, De Gruyter, Berlin, Boston, **2022**.

[133] R. C. Haddon, *J. Am. Chem. Soc.* **1986**, *108*, 2837.

[134] a) R. C. Haddon, *Science* **1993**, *261*, 1545; b) R. C. Haddon, *Acc. Chem. Res.* **1988**, *21*, 243.

[135] T. Kawase, H. Kurata, *Chem. Rev.* **2006**, *106*, 5250.

[136] B. W. Smith, M. Monthioux, D. E. Luzzi, *Nature* **1998**, *396*, 323.

[137] D. D. L. Chung, *J. Mat. Sci.* **2002**, *37*, 1475.

[138] J.-F. Nierengarten, N. Martín, *Supramolecular chemistry of fullerenes and carbon nanotubes*, Wiley-VCH, Weinheim, Germany, **2012**.

[139] T. Kawase, H. R. Darabi, M. Oda, *Angew. Chem. Int. Ed.* **1996**, *35*, 2664.

[140] T. Kawase, N. Ueda, K. Tanaka, Y. Seirai, M. Oda, *Tetrahedron Lett.* **2001**, *42*, 5509.

[141] T. Kawase, K. Tanaka, N. Fujiwara, H. R. Darabi, M. Oda, *Angew. Chem. Int. Ed.* **2003**, *42*, 1624.

[142] T. Kawase, K. Tanaka, N. Shiono, Y. Seirai, M. Oda, *Angew. Chem. Int. Ed.* **2004**, *43*, 1722.

[143] T. Kawase, Y. Nishiyama, T. Nakamura, T. Ebi, K. Matsumoto, H. Kurata, M. Oda, *Angew. Chem. Int. Ed.* **2007**, *46*, 1086.

[144] K. Miki, K. Saiki, T. Umeyama, J. Baek, T. Noda, H. Imahori, Y. Sato, K. Suenaga, K. Ohe, *Small* **2018**, *14*, 1800720.

[145] K. Miki, T. Matsushita, Y. Inoue, Y. Senda, T. Kowada, K. Ohe, *Chem. Commun.* **2013**, *49*, 9092.

[146] J. Wang, C. D. Gutsche, *J. Am. Chem. Soc.* **1998**, *120*, 12226.

[147] T. Haino, M. Yanase, Y. Fukazawa, *Angew. Chem. Int. Ed.* **1997**, *36*, 259.

[148] J. L. Atwood, L. J. Barbour, P. J. Nichols, C. L. Raston, C. A. Sandoval, *Chem. Eur. J.* **1999**, *5*, 990.

[149] M. Makha, M. J. Hardie, C. L. Raston, *Chem. Commun.* **2002**, *38*, 1446.

[150] D. Brynn Hibbert, P. Thordarson, *Chem. Commun.* **2016**, *52*, 12792.

[151] P. Thordarson, *Chem. Soc. Rev.* **2011**, *40*, 1305.

[152] T. Kawase, Y. Seirai, H. R. Darabi, M. Oda, Y. Sarakai, K. Tashiro, *Angew. Chem. Int. Ed.* **2003**, *42*, 1621.

[153] H. Kwon, C. J. Bruns, *Nano Res.* **2022**, *15*, 5545.

[154] H. Kwon, B. S. Newell, C. J. Bruns, *Nanoscale* **2022**, *14*, 14276.

[155] T. Matsuno, M. Fujita, K. Fukunaga, S. Sato, H. Isobe, *Nat. Commun.* **2018**, *9*, 3779.

[156] T. Iwamoto, Y. Watanabe, T. Sadahiro, T. Haino, S. Yamago, *Angew. Chem. Int. Ed.* **2011**, *50*, 8342.

[157] I. Solymosi, J. Sabin, H. Maid, L. Friedrich, E. Nuin, M. E. Pérez-Ojeda, A. Hirsch, *Organic Materials* **2022**, *4*, 73.

[158] T. Iwamoto, Y. Watanabe, H. Takaya, T. Haino, N. Yasuda, S. Yamago, *Chem. Eur. J.* **2013**, *19*, 14061.

[159] Y. Xu, R. Kaur, B. Wang, M. B. Minameyer, S. Gsänger, B. Meyer, T. Drewello, D. M. Guldi, M. von Delius, *J. Am. Chem. Soc.* **2018**, *140*, 13413.

[160] J. M. van Raden, B. M. White, L. N. Zakharov, R. Jasti, *Angew. Chem. Int. Ed.* **2019**, *58*, 7341.

[161] A. Bu, Y. Zhao, H. Xiao, C.-H. Tung, L.-Z. Wu, H. Cong, *Angew. Chem. Int. Ed.* **2022**, *61*, e202209449.

[162] F. M. Steudel, E. Ubasart, L. Leanza, M. Pujals, T. Parella, G. M. Pavan, X. Ribas, M. von Delius, *Angew. Chem. Int. Ed.* **2023**, e202309393.

[163] J. H. May, J. M. van Raden, R. L. Maust, L. N. Zakharov, R. Jasti, *Nat. Chem.* **2023**, *15*, 170.

[164] K. Tashiro, T. Aida, J.-Y. Zheng, K. Kinbara, K. Saigo, S. Sakamoto, K. Yamaguchi, *J. Am. Chem. Soc.* **1999**, *121*, 9477.

[165] Z. Xia, S. H. Pun, H. Chen, Q. Miao, *Angew. Chem. Int. Ed.* **2021**, *60*, 10311.

[166] D. Lu, G. Zhuang, H. Wu, S. Wang, S. Yang, P. Du, *Angew. Chem. Int. Ed.* **2017**, *56*, 158.

[167] T. Matsuno, S. Kamata, S. Sato, A. Yokoyama, P. Sarkar, H. Isobe, *Angew. Chem. Int. Ed.* **2017**, *129*, 15216.

[168] J. C. Hummelen, B. Knight, J. Pavlovich, R. González, F. Wudl, *Science* **1995**, *269*, 1554.

[169] J. C. Hummelen, M. Prato, F. Wudl, *J. Am. Chem. Soc.* **1995**, *117*, 7003.

[170] J. Rio, S. Beeck, G. Rotas, S. Ahles, D. Jacquemin, N. Tagmatarchis, C. Ewels, H. A. Wegner, *Angew. Chem. Int. Ed.* **2018**, *57*, 6930.

[171] A. Stergiou, J. Rio, J. H. Griwatz, D. Arčon, H. A. Wegner, C. P. Ewels, N. Tagmatarchis, *Angew. Chem. Int. Ed.* **2019**, *58*, 17745.

[172] E. Ubasart, O. Borodin, C. Fuertes-Espinosa, Y. Xu, C. García-Simón, L. Gómez, J. Juanhuix, F. Gándara, I. Imaz, D. Maspoch et al., *Nat. Chem.* **2021**, *13*, 420.

[173] Y. Nakanishi, H. Omachi, S. Matsuura, Y. Miyata, R. Kitaura, Y. Segawa, K. Itami, H. Shinohara, *Angew. Chem. Int. Ed.* **2014**, *53*, 3102.

[174] M. Freiberger, I. Solymosi, E. M. Freiberger, A. Hirsch, M. E. Pérez-Ojeda, T. Drewello, *Nanoscale* **2023**, *15*, 5665.

[175] T. Iwamoto, Z. Slanina, N. Mizorogi, J. Guo, T. Akasaka, S. Nagase, H. Takaya, N. Yasuda, T. Kato, S. Yamago, *Eur. J. Org. Chem.* **2014**, *20*, 14403.

[176] H. Ueno, T. Nishihara, Y. Segawa, K. Itami, *Angew. Chem. Int. Ed.* **2015**, *54*, 3707.

[177] J. Volkmann, D. Kohrs, F. Bernt, H. A. Wegner, *Eur. J. Org. Chem.* **2022**, *2022*, e202101357.

[178] B. Esser, J. S. Wössner, M. Hermann, *Synlett* **2022**, *33*, 737.

[179] P. Thordarson (Ed.) *Binding Constants and Their Measurement*, Wiley-VCH, Weinheim, Germany, **2012**.

[180] J. Volkmann, D. Kohrs, H. A. Wegner, *Chem. Eur. J.* **2023**, *29*, e202300268.

[181] D. Kohrs, J. Volkmann, H. A. Wegner, *Eur. J. Org. Chem.* **2023**, e202300575.

4 CONTRIBUTIONS TO THE LITERATURE

4.1 Synthesis of a Substituted [10]Cycloparaphenylene through [2+2+2] Cycloaddition

Reference: J. Volkmann, D. Kohrs, F. Bernt, H. A. Wegner, *Eur. J. Org. Chem.* **2022**, *2022*, e202101357.

DOI: 10.1002/ejoc.202101357

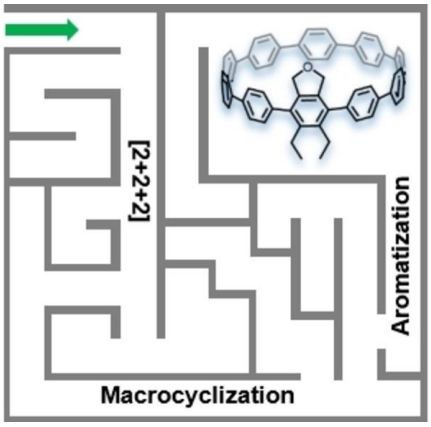

"The efficient synthesis of a *tetra*-substituted [10]cycloparaphenylene (CPP) is reported. The introduction of a diethylphthalane gives valuable insight into the incorporation of highly substituted units into these nanohoops. Finally, a seven-step synthesis with an overall yield of 8% provided the target compound while different expected and unexpected obstacles were overcome."

Front Cover: Synthesis of a Substituted [10]Cycloparaphenylene through [2+2+2] Cycloaddition (Eur. J. Org. Chem. 4/2022)

Reference: J. Volkmann, D. Kohrs, F. Bernt, H. A. Wegner, *Eur. J. Org. Chem.* **2022**, *2022*, e202200044.

DOI: 10.1002/ejoc.202200044

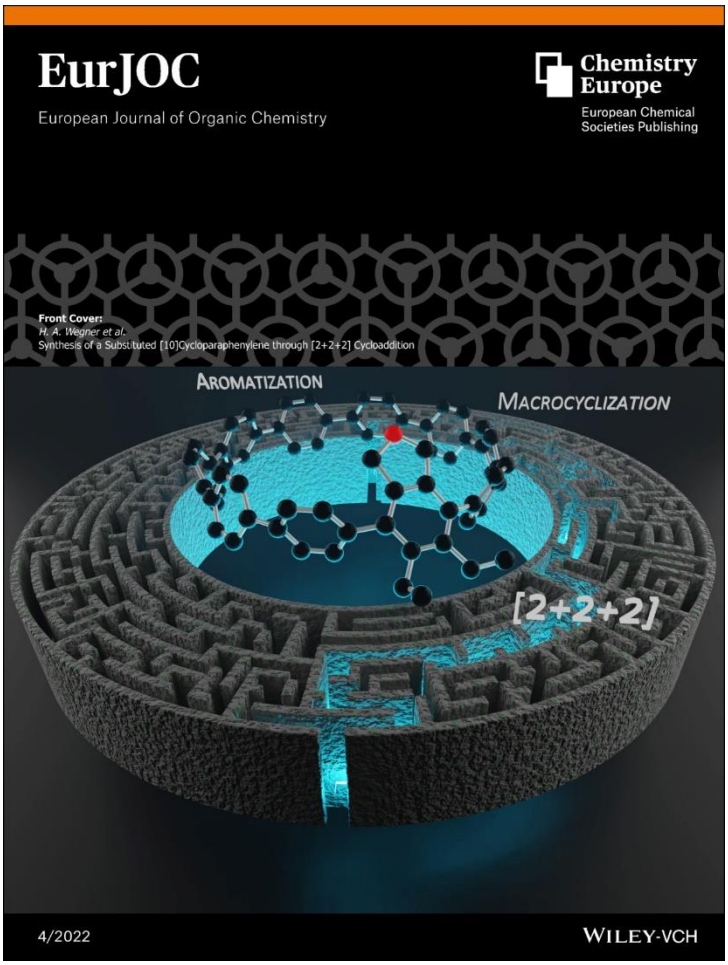

"The Front Cover illustrates a maze through which the authors went facing challenges to overcome targeting a substituted [10]cycloparaphenylene derivative. Designing new synthetic strategies towards new molecules is often connected to difficulties and dead ends. With the chemist's manifold toolbox of reactions and reagents, this maze was solved, and the target compound obtained. Cover design by Felix Bernt".

Check for updates

EurJOC
European Journal of Organic Chemistry

Research Article
doi.org/10.1002/ejoc.202101357

Chemistry Europe
European Chemical Societies Publishing

www.eurjoc.org

VIP *Very Important Paper*

Special Collection

Synthesis of a Substituted [10]Cycloparaphenylene through [2+2+2] Cycloaddition

Jannis Volkmann,[a, b] Daniel Kohrs,[a, b] Felix Bernt,[a, b] and Hermann A. Wegner*[a, b]

Herein, we report the synthesis and investigation of a substituted [10]cycloparaphenylene (CPP) incorporating a diethylphthalane unit. An efficient strategy relying on a symmetric built-up starting with propargyl ether as [2+2+2] cycloaddition precursor was developed. The straightforward synthesis required overcoming unexpected obstacles within the [2+2+2] cycloaddition, protection and aromatization. These results give valuable insights for accessing CPPs with highly substituted subunits. Finally, a seven-step synthesis with an overall yield of 8% provided the target nanoring, including good to excellent yields for the critical macrocyclization and aromatization. The synthesized nanohoop exhibits a hypsochromic shift in fluorescence and absorption, compared to the unsubstituted [10]CPP. This observation is proposedly caused by an increased torsion angle between the bivalent substituted phenyl moieties and the adjacent units.

Introduction

Cycloparaphenylenes (CPPs), the shortest cutout of an armchair carbon nanotube, attract attention in the fields of organic synthesis, as well as molecular materials:[1,2] The distortion of their radially oriented π-systems in these nanohoops result in unique optoelectronic as well as supramolecular properties, which are not only dependent on the ring size, but also on the substituents.[3] The extraordinary structure of these nanorings makes the development of new syntheses still an ambitious task. Hence, general access to CPPs with a high degree of substitution represents still an unsolved challenge. In recent years, different strategies were explored to introduce manifold substituents and substitutional pattern to CPPs (Figure 1).[2,4,5–8] Two major approaches can be distinguished: The post functionalization of non-substituted CPPs[9–12] and the introduction of substituents within the first building blocks.[13–15] The first principally offers the largest flexibility as unsubstituted CPPs are modified in the last step(s) of their synthesis. However, this method is restricted by its low selectivity and suffers from a low substrate tolerance (*i.e.* ring size).[11] Besides this, the accessible degree and pattern of substitution is still strongly limited. Therefore, this approach is not practical to access a broad variety of functionalized nanohoops.

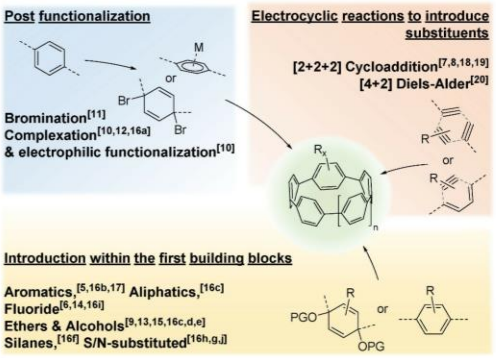

Figure 1. Summary of strategies to access for substituted CPPs, classified by their synthetic methodology.[5–20]

The introduction of substituents within the first steps of the synthesis, on the other hand, is restricted by the requirement, that the introduced substituents have to tolerate every applied reaction condition within the synthesis. This drawback can be partially circumvent by using a dummy, which tolerates these conditions and can be easily transferred into the desired functionality.[17] Nevertheless, this approach is again limited to specific substitution pattern and functionalities.

An alternative to these approaches is the introduction of substituents at a more advanced stage of the synthesis. Here, electrocyclic reactions,[20] as well as transition metal-catalyzed [2+2+2] cycloaddition reactions (CA) have proven their feasibility.[8,18,19] In general, the [2+2+2] CA is a highly efficient method to synthesize substituted aromatic rings in a regioselective fashion.[21] This methodology showed its potential in the

[a] *J. Volkmann, D. Kohrs, F. Bernt, Prof. Dr. H. A. Wegner*
Institute of Organic Chemistry,
Justus Liebig University Giessen
Heinrich-Buff-Ring 17, 35392 Giessen, Germany
E-mail: hermann.a.wegner@org.chemie.uni-giessen.de
https://www.uni-giessen.de/fbz/fb08/Inst/organische-chemie/Wegner
[b] *J. Volkmann, D. Kohrs, F. Bernt, Prof. Dr. H. A. Wegner*
Center for Material Research (ZfM/LaMa),
Justus Liebig University Giessen
Heinrich-Buff-Ring 16, 35392 Giessen, Germany
https://www.uni-giessen.de/fbz/zentren/lama/AGOrdner/personen/personen-layouts/q-z/wegner_hermann_layout

Supporting information for this article is available on the WWW under https://doi.org/10.1002/ejoc.202101357

Part of the "Carbon Allotropes" Special Collection.

EurJOC
European Journal of Organic Chemistry

Research Article
doi.org/10.1002/ejoc.202101357

Chemistry Europe
European Chemical Societies Publishing

preparation of substituted CPPs with either twofold,[7] or fourfold[8] functionalized phenyl units. Tanaka and coworkers, as well as our group exploited the strength of this reaction for the synthesis of substituted CPPs, introducing different functionalities, such as esters, ethers, aliphatic and aromatic side chains (Figure 1).[7,8] Furthermore, highly complex structural motifs such as a Möbius-shaped nanoring has been accessed via the [2+2+2] CA.[22]

In 2014, our group realized the incorporation of diethylphthalane units in [8]CPPs.[8] The steric demand of the annulated ring systems and the two substituents on the opposite side of the phenyl unit led to a significant increase in the torsion angle with their neighboring rings. As a consequence, the extinction coefficient decreased significantly, while the absorption maximum λ_{max} was hypsochromically shifted. This large torsion angle, as well as the tetravalent substitution pattern are of particular interest as design elements to control the optoelectronic and non-covalent interaction properties of these nanohoops. Even though the developed synthesis furnished a variety of novel, diverse [8]CPPs, the efficiency to access these substitution pattern for further use and investigation has to be improved.

Results and Discussion

Synthesis

In view of the drawbacks of the above discussed synthesis of substituted [8]CPPs *via* [2+2+2] CA, the new strategy towards such valuable tetra-substituted [10]CPP **1** was designed. By slicing the CPP in two equal parts, two symmetric five-membered building blocks (Scheme 1, **4** and **3**) would be obtained as precursors for a strain-reduced macrocyclic precursor **2**. While the unsubstituted building block **4** can be synthesized *via* a literature known procedure,[23] the substituted coupling partner **3** should be accessible *via* a [2+2+2] CA with 3-hexyne (**7**). This reaction could either be performed in the completing step of the building block synthesis towards **3** (path A), or one step in advance, forming a three-membered building block **5** (path B). The former approach is preferable, as one protection step is sufficient, while the latter approach requires a successive two-step protection. Further, only a bulky protecting group is suitable in path B to obtain a *syn*-selectivity within the formation of **3**. However, in path A the [2+2+2] CA is executed with a more sterically encumbered substrate, which might hamper the formation of the substituted core unit. Both described paths have their origin in the tethered diquinone derivative **8**. This substrate already contains the cyclohexadienes, which ensure the angular arrangement in the U-shaped

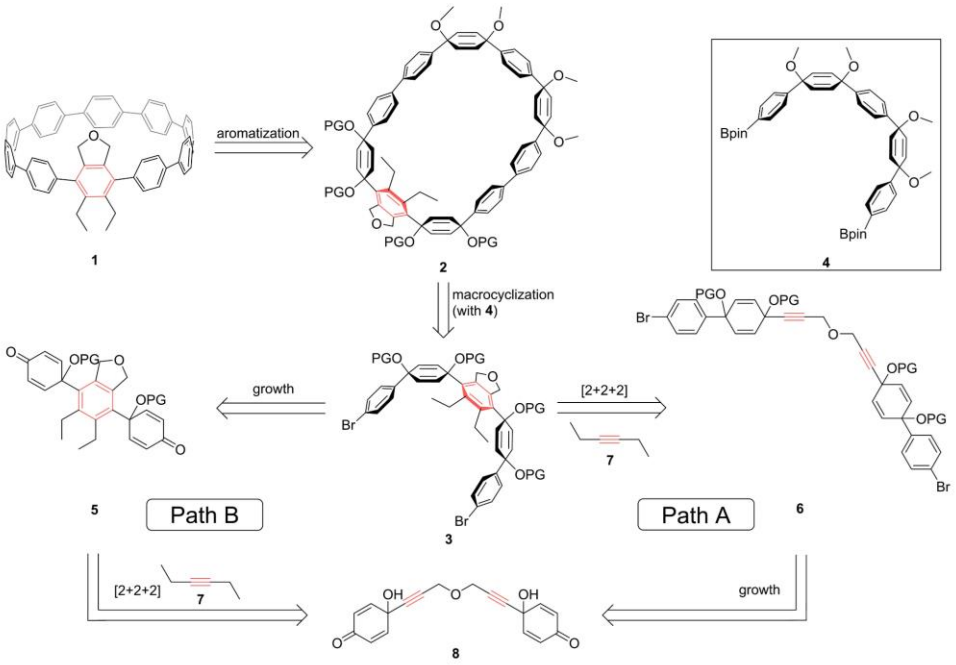

Scheme 1. Retrosynthetic perspective for the synthesis of target compound **1**. Two synthetic paths were followed, whereat the order of steps is changed, resulting in a difference in reactivity.

EurJOC
European Journal of Organic Chemistry

Research Article
doi.org/10.1002/ejoc.202101357

Chemistry Europe
European Chemical Societies Publishing

building block **3** enabling the formation of strain reduced macrocycle **2**. Dialkyne **8** is conveniently accessible from the commercially available propargyl ether **9** and 1,4-benzoquinone.

In the first step the propargyl ether **9** was deprotonated, followed by the addition of 1,4-benzoquinone forming the diketone **8** with a moderate yield of 37% (Scheme 2). Increasing the amount of benzoquinone from 2.35 eq. to 3.52 eq. raised the yield to 53%. The main side product was the mono addition product. However, increasing the amount of benzoquinone improved the ratio between double and single addition only marginally. In the following step, the extension of the building block was targeted (path A). Monolithiation of 1,4-dibromobenzene (**10**) and subsequent addition to the deprotonated diol **7** provided the tetraalcohol. As expected, one diastereomer was obtained in large excess.[24] At this point, it was not possible to remove traces of other diastereomers. Hence, the mixture of diastereomers was exposed directly to the protection toward tetra methyl ether **6-Me**. During a protection using NaH and iodomethane without an additive, no consumption of the diol

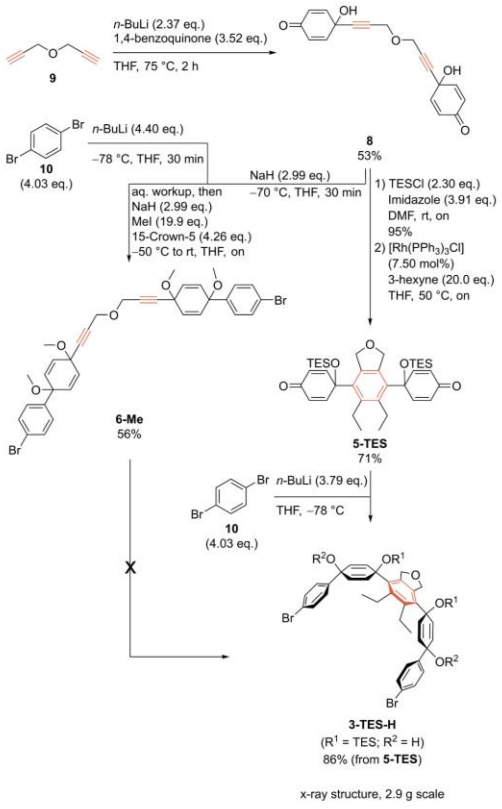

Scheme 2. Synthetic routes A & B toward five membered building block **3-TES-H**.

was observed. A proton-deuterium exchange experiment proved the efficient deprotonation with sodium hydride (see Supporting Information Figure S1). Hence, the following nucleophilic attack of the sodium alcoholate emerged to be too hindered. Only by addition of 15-crown-5 in this protection the [2+2+2] precursor was accessed. The crown ether complexing the sodium increased the nucleophilicity of the alcoholate and thus enabled the completion of the ether synthesis of **6-Me**.

The following [2+2+2] CA was executed with 3-hexyne (**7**). Different temperatures and catalytic systems, as well as reactions in a microwave and a pressure tube were tested for this reaction (for further information see Supporting Information Table S1 and Table S2). However, the product was only obtained in traces. To elucidate this low reactivity, ^{1}H NMR experiments with stoichiometric and hyperstoichiometric amounts of Wilkinson's catalyst were performed (see Supporting Information Figure S3). The addition of a stoichiometric amount of the catalyst led to the formation of a new set of ^{1}H NMR signals with a ratio of 1:1 with respect to the signals of the starting material **6-Me**. Upon addition of a second equivalent of the catalyst, the signals of the starting material vanished. This result indicates the formation of an undesired 1:2 species of the dialkyne and the catalyst which did not proceed to the desired [2+2+2] cycloadduct.

As this strategy (path A) did not proceed as desired, the alternative pathway (path B) was followed. Here it was expected that the strongly reduced steric hindrance arising from the two *para*-bromophenyl groups should facilitate the [2+2+2] cycloaddition, more precisely the coordination and subsequent insertion of the third alkyne. Therefore, diol **8** was protected as di(triethylsilyl) ether in excellent yield. This protection prohibits undesired interactions of the hydroxyl group in the [2+2+2] cycloaddition, as well as ensures the *syn*-selectivity for the subsequent addition. Indeed, the [2+2+2] CA with 3-hexyne (**7**) and Wilkinson's catalyst (7.5 mol%) gave phthalane **5-TES** in 71% yield. When the catalyst loading was lowered to 5.2 mol% the yield also decreased to 54%. Next, 1,4-dibromobenzene (**10**) was lithiated and added to diketone **5-TES** providing the desired 5-membered building block **3-TES-H**. Suitable crystals for *X*-ray analysis of this key intermediate were obtained by layering a solution of **3-TES-H** in dichloromethane with *n*-pentane. The obtained solid-state structure shows a U-shape arrangement which is ideally oriented for the dimerization forming the ten-membered macrocycle **2** (Figure 2).

The remaining two hydroxyl groups in **3-TES-H** should be protected, either as their methyl or silyl ethers to prevent side reactions in the following steps. However, this protection emerged to be an unexpected challenge. Different strong bases, as well as protection agents were applied but the protection was not achieved. In the majority of cases, starting material was re-isolated, while harsh conditions led to decomposition. Proton-deuterium exchange ^{1}H-NMR experiments were performed, whereat no deprotonation with NaH was observed (see Supporting Information Figure S2). This finding is remarkable as there should be a difference in *p*Ka values of approximately 20–25 orders of magnitude between the tertiary alcohol and the corresponding acid of the applied base (based on the *p*Ka value

EurJOC
European Journal of Organic Chemistry

Research Article
doi.org/10.1002/ejoc.202101357

Chemistry Europe
European Chemical Societies Publishing

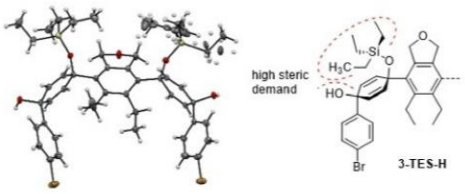

Figure 2. a) Solid state structure of the TES/OH-building block **3-TES-H** (ORTEP drawing, solvent molecules were omitted). b) Illustration of the proposed sterically shielding of the alcohol moieties by the bulky protecting group.

of known tertiary alcohols).[25] One explanation could be the strong steric hindrance of the tertiary alcohol with the large TES group in close proximity (Figure 2). The substituted phenyl ring thrusts the silyl ether toward the cyclohexadienes, where the bulky and flexible protecting group shields the free alcohol. Indeed, the crystal structure shows a proximity between protection group and the alcohols. Nevertheless, the hindrance to such a degree is surprising. The free and flexible rotation of the protecting group could increase this shielding drastically and therefore might explain the observed inertness. Despite the initial doubts the macrocyclization between substituted dibromide **3-TES-H** and non-substituted diboronic ester **4** was performed without protection using $Pd_2(dba)_3$ and the Buchwald ligand S-Phos (Scheme 3). The Suzuki coupling led to the macrocycle in an unexpectedly high yield of 31%. Deprotection with TBAF provided the mixed OH/OMe-macrocycle. For the final step, H_2SnCl_4, as well as sodium naphthalenide were tested to form the desired CPP **1**. While an aromatization with H_2SnCl_4 gave the product in traces, the product was not observed *via* single-electron reduction with sodium naphthalenide. This circumstance is presumably caused by the combination of cyclo-hexadienols, as well as their methyl ethers for the aromatization. In literature, the stannane-ate complex is majorly used for the aromatization of cyclohexadienols,[26] while, to the best of our knowledge, an aromatization with naphthalenide is only reported for the methyl ethers.

Based on this rationale, the all-methyl protected macrocycle **2-Me** was targeted. Therefore, the protection of the five-membered building block **3-TES-H** was resumed. The silyl ether was quantitatively cleaved with TBAF to the tetraalcohol. By applying NaH as base and iodomethane as the electrophile, the fourfold methyl protected building block **3-Me** was obtained in 81% over two steps. The fact, that this protection was successful, strengthens the assumption that the deprotonation of **3-TES-H** was sterically strongly hindered by the large silyl protecting group. With building block **3-Me** and non-substituted diboronic ester **4** in hand, again, a macrocyclization with similar conditions was executed, yielding the fully protected macrocycle in an even better yield of 46%. As expected, the aromatization with an excess of sodium naphthalenide led to the desired diethylphthalane incorporated [10]CPP **1**. In contrast to the previous aromatization attempts of macrocycle **2-TES-H**, the outcome was strongly improved to a yield of 70%. In total, an overall yield of 8% was achieved for this seven-step synthesis. This displays an exceedingly increase in yield compared to our previously reported synthesis of a similarly

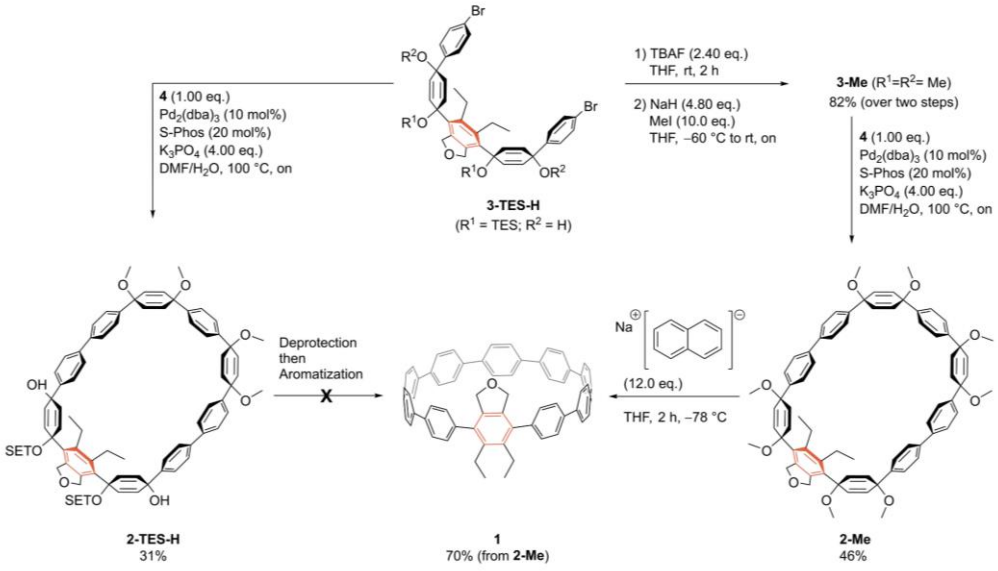

Scheme 3. Completion of the synthesis. The faster synthesis without protection yielded in the desired macrocycle, but not in the targeted CPP (left path), while a de- and reprotection of the five-membered building block **3-TES-H** provided the substituted CPP after a successful macrocyclization (right path).

EurJOC
European Journal of Organic Chemistry

Research Article
doi.org/10.1002/ejoc.202101357

Chemistry Europe
European Chemical Societies Publishing

substituted [8]CPP (0.01 % yield).[8] Especially the critical steps, the macrocyclization and the aromatization have been greatly improved. By using a rigid U-shaped building block, the macrocyclization is significantly enhanced in contrast to the reaction with flexible building blocks. Furthermore, the use of cyclohexadienes proved to be more efficient to aromatize compared to cyclohexanes.[7,27]

Optoelectronic properties

Compound **1** exhibits an absorption maximum at 326 nm, as well as a broad shoulder between 350 and 425 nm (Figure 3), displaying a hypsochromic shift compared to [10]CPP (340 nm). This blue shift can be rationalized by the larger torsion angle in the substituted case resulting in a reduced conjugation. This structural change has been well characterized by *X*-ray analysis for a substituted [8]CPP.[8] The same circumstance leads to a lower extinction coefficient for the substituted CPP **1**. This observation is in a good agreement to other functionalized CPPs.[8,19] The hypsochromic shift ($\Delta\lambda$) in case of the analogous substituted [8]CPP compared to the parent [8]CPP is slightly larger ($\Delta\lambda_{abs}$([8]CPP) = 28 nm) in respect to the here reported [10]CPP ($\Delta\lambda_{abs}$([10]CPP) = 14 nm).[8] CPP **1** has a larger ring size and lower degree of substitution with respect to the reported [8]CPP resulting in a less pronounced variation compared to the parent CPP. The fluorescence spectrum shows two emission maxima at 436 and 458 nm, respectively. The blue shifted maximum exhibits the highest intensity, which can only be observed as a shoulder in the unsubstituted case. According to Tretiak and coworkers these two maxima can be ascribed to vibronic features and accordingly decreased vibrational coupling.[28] Similar to the absorption, the fluorescence is shifted hypsochromically, compared to the unsubstituted case (474 nm). In comparison to the previously reported [8]CPP the aberration in [10]CPP **1** is much less distinct. While the substitution within the [8]CPP led to blue shift in the fluorescence of $\Delta\lambda_{em}$([8]CPP) = 87 nm,[8] it is only $\Delta\lambda_{em}$([10]CPP) = 16 nm in case of the [10]CPP.

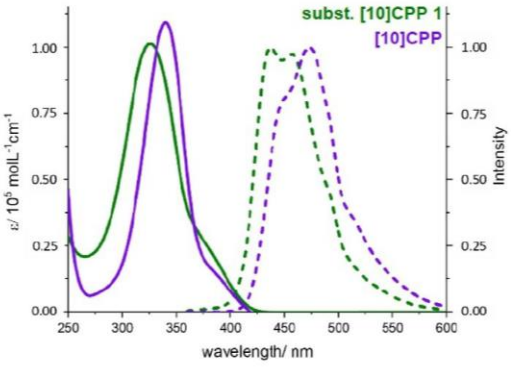

Figure 3. Absorption (solid lines, 10^{-5} M) and emission (dashed lines, 10^{-6} M) spectra of CPP **1** and [10]CPP measured in $CHCl_3$.

Conclusion

In conclusion, a synthesis for a substituted CPP was developed. The synthesis disclosed unexpected issues like a strongly hindered [2 + 2 + 2] cycloaddition of building block **6-Me**, as well as a remarkable stability of diol **3-TES-H** against deprotonation. In the end, all obstacles were overcome and the targeted substituted [10]CPP **1** was obtained in an overall yield of 8 %. In this context the extraordinary high yield of both, the macrocyclization and the aromatization has to be highlighted, which is in contrast to the previously reported synthesis of a diethylphthalane incorporated CPP and other syntheses of substituted nanohoops. With a hypsochromic shift in absorption and fluorescence, as well as a decrease in the extinction, the observed optoelectronic properties are in good agreement with other substituted cycloparaphenylenes.

Experimental Section

General Information

NMR spectroscopy: NMR spectra were measured on a Bruker Avance II 200 MHz, Avance II 400 MHz, Avance III 400 MHz HD or Avance III 600 MHz spectrometer at 25 °C if not otherwise noted. As the internal reference, the shifts of the solvent residual peaks were used.[29]

Mass spectrometry: ESI-MS spectra were measured on a Bruker Daltonics Micro TOF LC. The samples were dissolved in methanol. A positive voltage of 4500 V was applied to the capillary and −500 V to the End Plate Offset. The nebulizer was set to 0.4 bar. The dry heater was set to 180 °C and the flow of nitrogen as the dry gas to 4.0 l/min. For measurements in the negative ion mode, a negative voltage of 3000 V was applied, while the other parameters remained the same. For the MALDI-MS measurements a house made MALDI-source was used with 2,5-dihydroxybenzoic acid as the matrix. The mass spectrometer Q-Exactive™ by Thermo Fisher Scientific was connected to the MALDI-source.

Chemicals: The chemicals were purchased from Sigma-Aldrich, Acros Organics, Alfa Aesar, BLD-Pharm and TCI Europe. Anhydrous solvents were purchased from Acros Organics. Deuterated solvents were purchased from Euriso-Top GmbH. Technical grade solvents, used during work-up and purification, were distilled prior to use. Dry THF used for the aromatization step was distilled prior to use to remove the stabilizing agent. The unsubstituted diboronic ester **4** was synthesized according to a published synthesis.[23]

Column chromatography: Flash column chromatography was carried out with Silica 60 M (0.04–0.063 mm) from Macherey-Nagel GmbH & Co. KG. Thin layer chromatography was carried out on Polygram® SIL G/UV254 from Macherey-Nagel GmbH & Co. KG.

Melting point determination: Melting points were determined on a M5000 melting point meter from A. KRÜSS Optronic GmbH, Germany. A heating rate of 1 °C min^{-1} and a resolution of 0.1 °C were used, with an accuracy of ±0.3 °C (25–200 °C) and ±0.5 °C (200–400 °C).

EurJOC
European Journal of Organic Chemistry

Research Article
doi.org/10.1002/ejoc.202101357

Chemistry Europe
European Chemical Societies Publishing

Microwave reactions: Microwave reactions were performed in a Discoverer SP Activent® microwave reactor by CEM.

UV-Vis spectroscopy: Solvents for UV/Vis spectroscopy were purchased from Merck or Chemsolute (Uvasol® or HPLC quality). The measurements were carried out with a SPECORD® 200 PLUS spectrophotometer equipped with two automatic eight-fold cell changers and a Peltier element thermostat system (0.1 °C accuracy) by Analytik Jena.

Fluorescence spectroscopy: Solvents for UV/Vis spectroscopy were purchased from Merck or Chemsolute (Uvasol® or HPLC quality). The measurements were carried out with a FP-8300 fluorescence spectrometer from Jasco. The sample was irradiated with a Xe-lamp. Excitation and emission bandwidth were set to 2.5 nm.

Synthetic procedures

Synthesis of diketone 8: Propargyl ether **9** (84% in toluene, 3.49 g, 31.1 mmol, 1.00 eq.) and 200 ml dry THF were placed in a flame-dried flask and cooled to −78 °C. A solution of *n*-BuLi (1.6 M in hexanes, 46.0 ml, 73.6 mmol, 2.37 eq.) was added within 30 min and the resulting suspension was stirred for another 30 min. In a second flask, freshly recrystallized 1,4-benzoquinone (11.7 g, 109 mmol, 3.52 eq.) was dissolved in 150 ml dry THF. After cooling to −40 °C, the benzoquinone solution was transferred to the other flask *via* a transfer cannula. The residue was dissolved in 40 ml dry THF and again transferred to the reaction mixture, which was then stirred at −40 °C overnight. To quench the reaction, 80 ml saturated aq. NH_4Cl solution were added and the mixture was subsequently allowed to reach rt. The organic phase was extracted with ethyl acetate (3×150 ml) washed with brine (150 ml), dried over $MgSO_4$, filtered and concentrated under reduced pressure. The crude product was dissolved in ethyl acetate, filtered through Celite© and concentrated at reduced pressure. Afterwards, it was purified by flash silica column chromatography with ethyl acetate/cyclohexane as eluent (1:1 to 3:1) to obtain an off-white solid (5.14 g, 16.6 mmol, 53%). ^{1}H NMR (400 MHz, DMSO-d_6) δ 7.01–6.93 (m, 4H), 6.72 (s, 2H), 6.16–6.09 (m, 4H), 4.23 ppm (s, 4H). ^{13}C NMR (101 MHz, DMSO-d_6) δ 184.4 (2 C), 148.4 (4 C), 125.8 (4 C), 84.4 (2 C), 80.2 (2 C), 61.2 (2 C), 56.4 ppm (2 C). HRMS (ESI): calc. for $[C_{18}H_{14}NaO_5]^+$: $[M+Na]^+$ 333.0733, found 333.0731. MP > 115 °C (dec.).

Synthesis of dialkyne 6-Me: Diketone **8** (0.620 g, 2.00 mmol, 1.00 eq.) was placed in a flame-dried flask, dissolved in 40 ml dry THF and cooled to −70 °C. Sodium hydride (60% in mineral oil, 239 mg, 5.98 mmol, 2.99 eq.) was added and the mixture was stirred for 30 min. In a second flame-dried flask, 1,4-dibromobenzene (**10**) (1.94 g, 8.06 mmol, 4.03 eq.) was dissolved in 50 ml dry THF and subsequent cooled to −70 °C. *n*-BuLi (5.50 ml, 1.6 M in hexanes, 8.80 mmol, 4.40 eq.) was added and the resulting suspension was stirred for 30 min. Afterwards, the suspension containing lithiated bromobenzene was transferred to the diketone mixture *via* a transfer cannula within 10 min. The reaction mixture was stirred and allowed to reach rt overnight. The reaction mixture was cooled to −55 °C and 80 ml half-saturated aq. NH_4Cl solution were added to quench the reaction. After reaching rt, the organic phase was extracted with ethyl acetate (2×75 ml). The combined organic phases were washed with brine (75 ml), dried over $MgSO_4$, filtered and the volatiles were removed at reduced pressure. Cyclohexane (5 ml) was added to dissolve impurities, subsequently removed with a pipette and the solid was dried under vacuum. One third of the crude product was redissolved in 35 ml dry THF and cooled to −60 °C. Sodium hydride (105 mg, 60% in mineral oil, 2.65 mmol, 4.11 eq.) was added and the mixture was stirred for 30 min. Meanwhile, 15-crown-5 (0.55 ml, 2.75 mmol, 4.26 eq.) was dissolved in 5 ml dry THF and subsequently added to the reaction mixture at −55 °C. After stirring for 30 min, iodomethane (800 µl, 12.9 mmol, 19.9 eq.) was added at −50 °C. The reaction mixture was allowed to reach rt and was stirred overnight. Water (20 ml) was added to quench the reaction. The organic phase was extracted with ethyl acetate (2×20 ml) and the combined organic phases were washed with brine (20 ml), dried with $MgSO_4$, filtered and the volatiles were removed at reduced pressure. The product was purified twice by alumina oxide (neutral) column chromatography with cyclohexane/ethyl acetate/DCM (1st column: 10:1:1 to 8:1:1, 2nd column: 20:1:1 to 5:1:1) as eluent to obtain the product **6-Me** as a yellowish waxy solid (249 mg; 0.366 mmol, 56%). ^{1}H NMR (400 MHz, THF-d_8) δ 7.46–7.41 (m, 4H), 7.37–7.33 (m, 4H), 6.20–6.14 (m, 4H), 5.84–5.78 (m, 4H), 4.31 (s, 4H), 3.36 (s, 6H), 3.29 ppm (s, 6H). ^{13}C NMR (101 MHz, THF-d_8) δ 143.8 (2 C), 133.8 (4 C), 132.0 (4 C), 131.0 (4 C), 128.7 (4 C), 121.9 (2 C), 86.6 (2 C), 82.2 (2 C), 75.7 (2 C), 67.6 (2 C), 57.0 (2 C), 52.2 (2 C), 51.9 ppm (2 C). HRMS (ESI): calc. for $[C_{34}H_{32}Br_2O_5Na]^+$: $[M+Na]^+$ 701.0508, found 701.0506. MP Due to its texture, no melting point could be determined.

Synthesis of the TES-protected diketone 8-TES: Diketone **8** (318 mg, 1.02 mmol, 1.00 eq.) and imidazole (273 mg, 4.01 mmol, 3.91 eq.) were added to a flame-dried round bottom flask containing dry DMF (20 ml). The mixture was stirred until all solids were dissolved and subsequently TESCl (400 µl, 2.36 mmol, 2.30 eq.) was added dropwise to the stirring solution. After the complete addition, the resulting solution was stirred at rt overnight. Water (15 ml) was added to the crude reaction, which was then extracted with DCM (3×15 ml). The combined organic phases were washed with water (3×15 ml), brine (15 ml), dried over $MgSO_4$, filtered and concentrated at reduced pressure. The product was obtained as a yellow oil (527 mg, 0.980 mmol, 95%). ^{1}H NMR (400 MHz, DMSO-d_6) δ 7.00–6.95 (m, 4H), 6.19–6.14 (m, 4H), 4.27 (s, 5H), 0.92 (t, ^3J= 7.9 Hz, 18H), 0.65 ppm (q, ^3J=7.9 Hz, 12H). ^{13}C-NMR (101 MHz, DMSO-d_6) δ 184.2 (2 C), 147.8 (4 C), 126.1 (4 C), 83.8 (2 C), 81.8 (2 C), 63.4 (2 C), 56.5 (2 C), 6.8 (6 C), 5.7 ppm (6 C). HRMS (ESI): calc. for $[C_{30}H_{42}O_5Si_2Na]^+$: $[M+Na]^+$ 561.2463, found 561.2464.

Synthesis of 3-membered building block 5-TES through [2+2+2] cycloaddition: Dialkyne **8-TES** (527 mg, 0.978 mmol, 1.00 eq.), 3-hexyne (**7**) (2.25 ml, 19.6 mmol, 20.0 eq.), dry *i*-PrOH (35 ml) and dry THF (35 ml) were placed in a flame dried Schlenk tube under N_2. $[Rh(PPh_3)_3Cl]$ (67.8 mg, 73.3 µmol, 7.50 mol%) was added and the reaction mixture was heated to 50 °C overnight. Water (70 ml) was added and the aqueous phase was extracted with DCM (3×70 ml). The combined org. layers were washed with water (2×70 ml), brine (70 ml) and dried with $MgSO_4$. The solid was removed by filtration and the volatiles were evaporated at reduced pressure. The crude product was purified by flash silica chromatography with toluene/ethyl acetate/NEt_3 (10:1; 1% NEt_3) as eluent The product **5-TES** was obtained as a white crystalline solid (429 mg, 0.691 mmol, 71%). In case the column chromatography does not liberate the pure product, it can be further purified by recrystallization from *n*-pentane. ^{1}H NMR (400 MHz, $CDCl_3$) δ 7.02–6.96 (m, 4H), 6.31–6.26 (m, 4H), 5.21 (s, 4H), 2.61 (q, ^3J=8.0 Hz, 4H), 0.97–0.89 (m, 24H), 0.66 ppm (q, ^3J=8.6, 7.9 Hz, 12H). ^{13}C NMR (101 MHz, $CDCl_3$) δ 185.6 (2 C), 150.7 (4 C), 141.2 (2 C), 138.9 (2 C), 134.4 (2 C), 127.5 (4 C), 73.8 (2 C), 73.4 (2 C), 21.2 (2 C), 17.6 (2 C), 7.1 (6 C), 6.3 ppm (6 C). HRMS (ESI): calc. for $[C_{36}H_{52}O_5Si_2Na]^+$: $[M+Na]^+$ 643.3245, found 643.3247. MP 97–98 °C.

Synthesis of 5-membered building block 3-TES-H: 1,4-Dibromobenzene (**10**) (733 mg, 3.04 mmol, 3.79 eq.) was placed in a flame-dried Schlenk tube and subsequently dissolved in dry THF (30 ml). After cooling to −78 °C, *n*-BuLi (2.20 ml, 1.6 M in hexanes, 3.52 mmol, 4.37 eq.) was added. The suspension was stirred for 30 min while reaching −50 °C. At this temperature diketone **5-TES** (498 mg, 0.802 mmol, 1.00 eq.) was added and the reaction mixture was allowed to reach rt overnight. The reaction mixture was cooled

EurJOC
European Journal of Organic Chemistry

Research Article
doi.org/10.1002/ejoc.202101357

Chemistry Europe
European Chemical Societies Publishing

to −20 °C and half-saturated aq. NH_4Cl-solution (30 ml) was added. The mixture was allowed to reach rt and the organic phase was extracted with DCM (3×20 ml). The combined organic phases were washed with water (3×50 ml) and brine (50 ml). Subsequently, the organic phase was dried with $MgSO_4$, filtered and the volatiles were evaporated. A purification by flash silica chromatography with cyclohexane/DCM/ethyl acetate/ NEt_3 (20:1:1 to 10:1:1 with 1% NEt_3) as eluent afforded the product **3-TES-H** as a white crystalline solid (645 mg, 0.690 mmol, 86%). *Note gram scale:* On a 4.9 mmol scale, 2.9 g product were obtained (65%). ^{1}H NMR (400 MHz, DMSO-d_6) δ 7.55–7.48 (m, 4H), 7.38–7.33 (m, 4H), 6.13–6.05 (m, 8H), 5.83 (s, 2H), 4.80 (s, 4H), 2.48–2.36 (m, 4H), 0.90 (t, ^3J=7.8 Hz, 18H), 0.75–0.62 ppm (m, 18H). ^{13}C-NMR (101 MHz, DMSO-d_6) δ 145.0 (2 C), 140.8 (2 C), 137.5 (2 C), 136.8 (2 C), 131.4 (2 C), 130.8 (4 C), 130.5 (2 C), 128.3 (4 C), 120.4 (2 C), 72.6 (4 C), 66.8 (4 C), 26.3 (2 C), 20.8 (2 C), 17.3 (2 C), 7.0 (6 C), 5.6 ppm (6 C). HRMS (MALDI): calc. for $[C_{48}H_{62}Br_2O_5Si_2Na]^+$: $[M+Na]^+$ 955.2395, found 955.2404. MP 106–107 °C

Synthesis of OH-OTES-OMe-[10]macrocycle 2-TES-H: Tetra-substituted [5]building block **3-TES-H** (310 mg, 332 µmol, 1.00 eq.) and unsubstituted [5]building block **4** (251 mg, 319 µmol, 1.00 eq.) were dissolved in 80 ml DMF and 10 ml H_2O and subsequently degassed with N_2 (15 min). $Pd_2(dba)_3$ (31 mg, 33 µmol, 10 mol%), SPhos (28 mg, 67 µmol, 20 mol%) and $K_3PO_4\times H_2O$ (310 mg, 1.28 mmol, 3.85 eq.) were added and the reaction mixture was heated to 100 °C overnight. The reaction mixture was filtered through a plug of Celite® and water (100 ml) was added. The organic phase was extracted with DCM (3×100 ml), washed with water (6×100 ml), dried with $MgSO_4$, filtered and concentrated at reduced pressure. The crude product was purified by silica column chromatography with cyclohexane/DCM/EtOAc (10:1:1 to 5:1:1) and toluene:DCM:EtOAc (5:1:1 to 4:1:1) as eluent to afford a white solid (130 mg, 102 µmol, 31%). ^{1}H NMR (400 MHz, C_6D_6): δ 7.82 (s, 4H), 7.60–7.57 (m, 4H), 7.46–7.42 (m, 4H), 7.41–7.36 (m, 8H), 6.13–6.08 (m, 4H), 6.02–5.97 (m, 4H), 5.97–5.93 (m, 4H), 5.92–5.87 (m, 4H), 5.66 (s, 4H), 3.33 (s, 6H), 3.28 (s, 6H), 2.69–2.53 (m, 4H), 1.01 (t, ^3J=7.8 Hz, 18H), 0.88–0.72 ppm (m, 18H). ^{13}C NMR (101 MHz, C_6D_6) δ 144.2 (2 C), 143.8 (2 C), 142.8 (2 C), 141.4 (2 C), 140.8 (2 C), 140.1 (2 C), 139.1 (2 C), 137.9 (2 C), 133.5 (2 C), 133.5 (2 C), 133.4 (2 C), 130.2 (2 C), 127.6 (4 C), 127.2 (4 C), 127.2 (4 C), 127.0 (4 C), 126.8 (4 C), 74.5 (2 C), 74.4 (4 C), 74.3 (4 C), 73.7 (4 C), 68.5 (4 C), 51.8 (4 C, overlaying signals), 22.1 (2 C), 18.0 (2 C), 7.4 (6 C), 6.8 ppm (6 C). HRMS(ESI): calc. for $[C_{82}H_{94}O_9Si_2Na]^+$: $[M+Na]^+$ 1301.6328, found 1301.6329. MP >160 °C (dec.)

Synthesis of all-OMe-5-membered building block 3-Me: Building block **3-TES-H** (1.00 g, 1.07 mmol, 1.00 eq.) was dissolved in 20 ml THF and TBAF (2.60 ml, 1.0 M in THF, 2.60 mmol, 2.43 eq.) was added. The mixture was allowed to stir for 2 h at rt before water (20 ml) was added. The THF was evaporated whereat a white solid was formed, which was filtered off and washed with water and *n*-pentane to give the tetraalcohol as a white solid. The crude tetraalcohol was redissolved in dry THF (55 ml) and cooled to −60 °C. NaH (186 mg; 60% in mineral oil, 4.64 mmol, 4.80 eq.) was added and the reaction mixture was stirred for 30 min. MeI (0.61 ml, 9.67 mmol, 10.0 eq.) was added and the reaction was allowed to reach rt overnight. The reaction was quenched by adding water (50 ml). The organic phase was extracted with DCM (3×50 ml), washed with water (3×100 ml), brine (50 ml), dried with $MgSO_4$, filtrated and the volatiles were removed at reduced pressure. Crude product was washed with *n*-pentane to give the product as a white solid (670 mg, 0.879 mmol, 82%). ^{1}H NMR (400 MHz, $CDCl_3$) δ 7.52–7.45 (m, 4H), 7.35–7.28 (m, 4H), 6.30–6.19 (m, 4H), 6.16–6.07 (m, 4H), 5.04 (s, 4H), 3.29 (s, 6H), 3.24 (s, 6H), 2.58–2.45 (m, 4H), 0.79 ppm (t, ^3J=7.2 Hz, 6H). ^{13}C NMR (101 MHz, $CDCl_3$) δ 141.6 (2 C), 141.4 (2 C), 138.4 (2 C), 136.4 (2 C), 132.8 (4 C), 131.7 (4 C), 131.6 (4 C), 128.5 (4 C), 122.2 (2 C), 75.4 (2 C), 73.7 (2 C), 73.3 (2 C), 51.8 (2 C), 49.8 (2 C) 21.7 (2 C), 17.5 ppm (2 C). HRMS (ESI): calc. for $[C_{40}H_{42}Br_2O_5Na]^+$: $[M+Na]^+$ 783.1291, found 783.1294. MP 142–144 °C

Synthesis of all-OMe-[10]macrocycle 2-Me: Tetrasubstituted [5]building block **3-Me** (254 mg, 333 µmol, 1.00 eq.) and unsubstituted building block **4** (252 mg, 332 µmol, 1.00 eq.) were dissolved in 80 ml DMF and 10 ml H_2O and subsequently degassed with N_2 (15 min). $Pd_2(dba)_3$ (31.5 mg, 33.4 µmol, 10 mol%), SPhos (28.0 mg, 66.6 µmol, 20.0 mol%) and $K_3PO_4\times H_2O$ (323 mg, 1.33 mmol, 4.00 eq.) were added and the reaction mixture was heated to 100 °C overnight. The reaction mixture was filtered through a plug of Celite® and water (100 ml) was added. The organic phase was extracted with DCM (3×100 ml), washed with water (6×100 ml), dried with $MgSO_4$, filtered and concentrated at reduced pressure. The crude product was purified by silica column chromatography with cyclohexane/DCM/EtOAc (10:5:3) as eluent. Washing with *n*-pentane afforded the product as a white solid (169 mg, 153 µmol, 46%). ^{1}H NMR (400 MHz, CD_2Cl_2) δ 7.57–7.51 (m, 8H), 7.50–7.43 (m, 8H), 7.42 (s, 4H), 6.34–6.28 (m, 4H), 6.13–6.03 (m, 12H), 5.07 (s, 4H), 3.42–3.38 (m, 2 overlaying singlets, 12H), 3.35 (s, 6H), 3.27 (s, 6H), 2.36–2.21 (m, 4H), 0.56 ppm (*t*, ^3J=7.2 Hz, 4H). ^{13}C NMR (101 MHz, CD_2Cl_2) δ 143.3 (2 C), 143.3 (2 C), 141.5 (2 C), 140.8 (2 C), 140.0 (2 C), 139.7 (2 C), 138.4 (2 C), 136.0 (2 C), 133.2 (2 C), 133.0 (2 C), 132.6 (2 C), 132.0 (2 C), 127.4 (4 C), 127.0 (4 C), 126.6 (4 C), 126.5 (4 C), 126.0 (4 C), 75.9 (4 C), 74.0 (4 C), 74.0 (4 C), 73.7 (4 C), 73.6 (2 C), 51.7 (4 C, 2 overlaying signals), 51.6 (2 C), 49.4 (2 C), 21.7 (2 C), 17.3 ppm (2 C). HRMS (APCI): calc. for $[C_{74}H_{75}O_9]^+$: $[M+H]^+$ 1107.5406, found 1107.5405. MP >190 °C (dec.)

Sodium naphthalenide: Naphthalene (1.92 g, 15.0 mmol, 1.00 eq.) was placed in a flame died Schlenk tube and dry stabilizer-free THF (50 ml) was added. Sodium metal (517 mg, 22.5 mmol, 1.50 eq.) was added in small portions resulting in a deep green suspension, which was stirred at rt overnight. The metal residues were removed by filtration through a glass fiber pad and the sodium naphthalenide concentration of the obtained solution was determined by threefold titration of menthol.

Synthesis of substituted [10]CPP 1: Macrocycle **2-Me** (70.0 mg, 63.2 µmol, 1.00 eq.) and dry stabilizer-free THF (30 ml) were placed in a nitrogen filled flame dried Schlenk tube and cooled to −78 °C. Freshly prepared sodium naphthalenide (2.62 ml, 0.290 M in THF, 0.760 mmol, 12.0 eq.) was added and the reaction mixture was stirred for 2 h at that temperature. Then, I_2 (15 ml, 1 M in THF, 15 mmol) was added and the reaction was allowed to reach rt. Saturated aq. sodium thiosulfate solution was added to remove the excess of I_2. Water (60 ml) was added and the organic phase was extracted with DCM (3×60 ml). The combined organic layer was washed with brine (60 ml) and dried over $MgSO_4$, filtrated and the volatiles were removed under reduced pressure. The crude product was loaded on a pad of alumina oxide (neutral), whereat remaining naphthalene was removed with cyclohexane:DCM 1:1. The product was subsequently eluted with DCM and obtained as a yellow fluorescent solid (38.0 mg, 44.2 µmol, 70%). ^{1}H NMR (400 MHz, CD_2Cl_2): δ 7.64–7.54 (m, 26H), 7.54–7.50 (m, 4H), 7.17–7.13 (m, 4H), 4.01 (s, 4H), 3.04 (q, ^3J=7.4 Hz, 4H), 1.24 ppm (t, ^3J=7.4 Hz, 6H). ^{13}C NMR (101 MHz, CD_2Cl_2): δ 140.1 (2 C), 139.4 (2 C), 139.3 (2 C), 139.2 (2 C), 138.8 (4 C), 138.7 (2 C), 138.6 (2 C), 138.6 (2 C), 138.5 (4 C, 2 overlaying signals), 135.9 (2 C), 130.6 (4 C), 128.0 (4 C), 127.9 (4 C), 127.83 (4 C), 127.76 (8 C, 2 overlaying signals), 127.72 (4 C), 127.66 (4 C), 127.4 (4 C, 74.6 (2 C), 23.9 (2 C), 17.0 ppm (2 C). Digits were added to show the difference in the chemical shift. HRMS (APCI): calc. for $[C_{66}H_{51}O]^+$: $[M+H]^+$ 859.3935, found 859.3933. MP >250 °C (dec.)

EurJOC
European Journal of Organic Chemistry

Research Article
doi.org/10.1002/ejoc.202101357

Chemistry Europe
European Chemical Societies Publishing

Acknowledgements

The authors thank Katharina Heinrich, Domenic Dreisbach and Prof. Bernhard Spengler for the MALDI-MS measurements, Dr. Heike Hausmann for NMR measurements and Dr. Jonathan Becker for X-ray diffraction measurements. Furthermore, the authors thank Jan H. Griwatz and Sebastian Beeck for inspiration and fruitful discussions. Open Access funding enabled and organized by Projekt DEAL.

Conflict of Interest

The authors declare no conflict of interest.

Data Availability Statement

The data that support the findings of this study are available in the supplementary material of this article.

Keywords: Cyclotrimerization · Fluorescence · Macrocycles · Nanostructures · Synthesis design

[1] a) S. E. Lewis, *Chem. Soc. Rev.* **2015**, *44*, 2221–2304; b) Y. Segawa, A. Yagi, K. Matsui, K. Itami, *Angew. Chem. Int. Ed.* **2016**, *55*, 5136–5158; *Angew. Chem.* **2016**, *128*, 5222–5245; c) A.-F. Tran-Van, H. A. Wegner, *Beilstein J. Nanotechnol.* **2014**, *5*, 1320–1333; d) Y. Xu, M. von Delius, *Angew. Chem. Int. Ed.* **2020**, *59*, 559–573; *Angew. Chem.* **2020**, *132*, 567–582.
[2] R. Jasti, J. Bhattacharjee, J. B. Neaton, C. R. Bertozzi, *J. Am. Chem. Soc.* **2008**, *130*, 17646–17647.
[3] a) M. Fujitsuka, D. W. Cho, T. Iwamoto, S. Yamago, T. Majima, *Phys. Chem. Chem. Phys.* **2012**, *14*, 14585–14588; b) E. R. Darzi, R. Jasti, *Chem. Soc. Rev.* **2015**, *44*, 6401–6410; c) T. Iwamoto, Y. Watanabe, H. Takaya, T. Haino, N. Yasuda, S. Yamago, *Chem. Eur. J.* **2013**, *19*, 14061–14068; d) Y. Nakanishi, H. Omachi, S. Matsuura, Y. Miyata, R. Kitaura, Y. Segawa, K. Itami, H. Shinohara, *Angew. Chem. Int. Ed.* **2014**, *53*, 3102–3106; *Angew. Chem.* **2014**, *126*, 3166–3170; e) N. Grabicki, K. T. D. Nguyen, S. Weidner, O. Dumele, *Angew. Chem. Int. Ed.* **2021**, *60*, 14909–14914.
[4] a) Omachi, Y. Yamamoto, J. Bouffard, K. Itami, *Angew. Chem. Int. Ed.* **2009**, *48*, 6112–6116; *Angew. Chem.* **2009**, *121*, 6228–6232; b) S. Yamago, Y. Watanabe, T. Iwamoto, *Angew. Chem. Int. Ed.* **2010**, *49*, 757–759; *Angew. Chem.* **2010**, *122*, 769–771.
[5] F. E. Golling, M. Quernheim, M. Wagner, T. Nishiuchi, K. Müllen, *Angew. Chem. Int. Ed.* **2014**, *126*, 1551–1554.
[6] S. Hashimoto, E. Kayahara, Y. Mizuhata, N. Tokitoh, K. Takeuchi, F. Ozawa, S. Yamago, *Org. Lett.* **2018**, *20*, 5973–5976.
[7] Y. Miyauchi, K. Johmoto, N. Yasuda, H. Uekusa, S. Fujii, M. Kiguchi, H. Ito, K. Itami, K. Tanaka, *Chem. Eur. J.* **2015**, *21*, 18900–18904.
[8] A.-F. Tran-Van, E. Huxol, J. M. Basler, M. Neuburger, J.-J. Adjizian, C. P. Ewels, H. A. Wegner, *Org. Lett.* **2014**, *16*, 1594–1597.
[9] E. Kayahara, M. Nakano, L. Sun, K. Ishida, S. Yamago, *Chem. Asian J.* **2020**, *15*, 2451–2455.
[10] E. Kayahara, V. K. Patel, A. Mercier, E. P. Kündig, S. Yamago, *Angew. Chem. Int. Ed.* **2016**, *128*, 310–314.
[11] E. Kayahara, R. Qu, S. Yamago, *Angew. Chem. Int. Ed.* **2017**, *56*, 10428–10432; *Angew. Chem.* **2017**, *129*, 10564–10568.
[12] N. Kubota, Y. Segawa, K. Itami, *J. Am. Chem. Soc.* **2015**, *137*, 1356–1361.
[13] E. Kayahara, L. Sun, H. Onishi, K. Suzuki, T. Fukushima, A. Sawada, H. Kaji, S. Yamago, *J. Am. Chem. Soc.* **2017**, *139*, 18480–18483.
[14] E. J. Leonhardt, J. M. van Raden, D. Miller, L. N. Zakharov, B. Alemán, R. Jasti, *Nano Lett.* **2018**, *18*, 7991–7997.
[15] B. M. White, Y. Zhao, T. E. Kawashima, B. P. Branchaud, M. D. Pluth, R. Jasti, *ACS Cent. Sci.* **2018**, *4*, 1173–1178.
[16] a) K. Ypsilantis, T. Tsolis, A. Garoufis, *Inorg. Chem. Commun.* **2021**, *134*, 108992; b) F. E. Golling, S. Osella, M. Quernheim, M. Wagner, D. Beljonne, K. Müllen, *Chem. Sci.* **2015**, *6*, 7072–7078; c) P. Della Sala, C. Talotta, M. de Rosa, A. Soriente, S. Geremia, N. Hickey, P. Neri, C. Gaeta, *J. Org. Chem.* **2019**, *84*, 9489–9496; d) D. Lu, G. Zhuang, H. Jia, J. Wang, Q. Huang, S. Cui, P. Du, *Org. Chem. Front.* **2018**, *5*, 1446–1451; e) S. Cui, G. Zhuang, J. Wang, Q. Huang, S. Wang, P. Du, *Org. Chem. Front.* **2019**, *6*, 1885–1890; f) Y. Xu, B. Wang, R. Kaur, M. B. Minameyer, M. Bothe, T. Drewello, D. M. Guldi, M. von Delius, *Angew. Chem. Int. Ed.* **2018**, *57*, 11549–11553; *Angew. Chem.* **2018**, *130*, 11723–11727; g) Y. Kuroda, Y. Sakamoto, T. Suzuki, E. Kayahara, S. Yamago, *J. Org. Chem.* **2016**, *81*, 3356–3363; h) E. Kayahara, X. Zhai, S. Yamago, *Can. J. Chem.* **2017**, *95*, 351–356; i) K. Itami, H. Shudo, M. Kuwayama, M. Shimasaki, T. Nishihara, Y. Takeda, T. Kuwabara, A. Yagi, Y. Segawa, **2021**, ChemRxiv preprint DOI: 10.33774/chemrxiv-2021-7kd63; j) T. C. Lovell, Z. R. Garrison, R. Jasti, *Angew. Chem. Int. Ed.* **2020**, *59*, 14363–14367; *Angew. Chem.* **2020**, *132*, 14469–14473.
[17] J. Xia, M. R. Golder, M. E. Foster, B. M. Wong, R. Jasti, *J. Am. Chem. Soc.* **2012**, *134*, 19709–19715.
[18] N. Hayase, Y. Miyauchi, Y. Aida, H. Sugiyama, H. Uekusa, Y. Shibata, K. Tanaka, *Org. Lett.* **2017**, *19*, 2993–2996.
[19] N. Hayase, H. Sugiyama, H. Uekusa, Y. Shibata, K. Tanaka, *Org. Lett.* **2019**, *21*, 3895–3899.
[20] C. Huang, Y. Huang, N. G. Akhmedov, B. V. Popp, J. L. Petersen, K. K. Wang, *Org. Lett.* **2014**, *16*, 2672–2675.
[21] a) G. Domínguez, J. Pérez-Castells, *Chem. Soc. Rev.* **2011**, *40*, 3430–3444; b) G. Nishida, N. Suzuki, K. Noguchi, K. Tanaka, *Org. Lett.* **2006**, *8*, 3489–3492.
[22] S. Nishigaki, Y. Shibata, A. Nakajima, H. Okajima, Y. Masumoto, T. Osawa, A. Muranaka, H. Sugiyama, A. Horikawa, H. Uekusa, H. Koshino, M. Uchiyama, A. Sakamoto, K. Tanaka, *J. Am. Chem. Soc.* **2019**, *141*, 14955–14960.
[23] J. Xia, J. W. Bacon, R. Jasti, *Chem. Sci.* **2012**, *3*, 3018–3021.
[24] T. J. Sisto, M. R. Golder, E. S. Hirst, R. Jasti, *J. Am. Chem. Soc.* **2011**, *133*, 15800–15802.
[25] M. Wächter, *Tabellenbuch der Chemie. Daten zur Analytik, Laborpraxis und Theorie*, Wiley-VCH, Weinheim, **2012**.
[26] a) V. K. Patel, E. Kayahara, S. Yamago, *Eur. J. Org. Chem.* **2015**, *21*, 5742–5749; b) Y. Yang, O. Blacque, S. Sato, M. Juríček, *Angew. Chem. Int. Ed.* **2021**, *133*, 13641–13647.
[27] E. R. Darzi, T. J. Sisto, R. Jasti, *J. Org. Chem.* **2012**, *77*, 6624–6628.
[28] L. Adamska, I. Nayyar, H. Chen, A. K. Swan, N. Oldani, S. Fernandez-Alberti, M. R. Golder, R. Jasti, S. K. Doorn, S. Tretiak, *Nano Lett.* **2014**, *14*, 6539–6546.
[29] G. R. Fulmer, A. J. M. Miller, N. H. Sherden, H. E. Gottlieb, A. Nudelman, B. M. Stoltz, J. E. Bercaw, K. I. Goldberg, *Organometallics* **2010**, *29*, 2176–2179.

Manuscript received: November 8, 2021
Revised manuscript received: December 10, 2021
Accepted manuscript online: December 15, 2021

4.2 Balancing Attraction and Repulsion: The Influence of London Dispersion in [10]Cycloparaphenylene-Fullerene Complexes

Reference: J. Volkmann[+], D. Kohrs[+], H. A. Wegner, *Chem. Eur. J.* **2023**, *29*, e202300268.

DOI: 10.1002/chem.202300268

[+]These authors contributed equally.

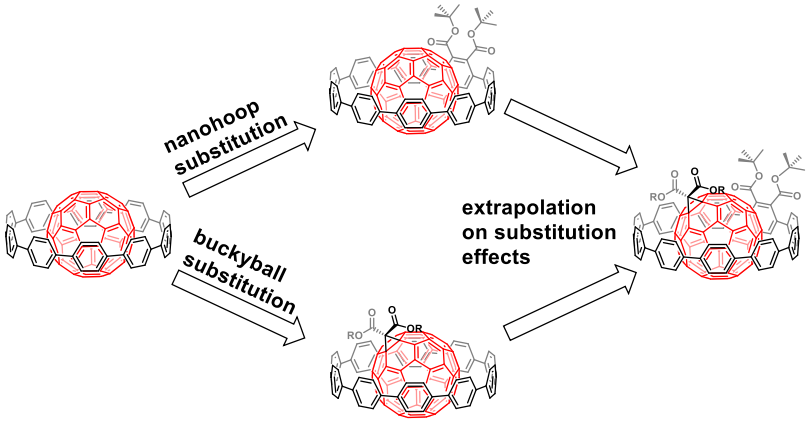

"The supramolecular assembly between substituted [10]cycloparaphenylene (s[10]CPP) and fullerenes was studied to investigate the subtle interplay of steric repulsion, conformation and attractive London dispersion interactions. For this, [10]CPP and a *tert*-butyl ester-substituted analogue were employed as host molecules whose fluorescence is quenched upon addition of C_{60} as well as alkyl malonyl ester-substituted fullerenes."

Cover Feature: Balancing Attraction and Repulsion: The Influence of London Dispersion in [10]Cycloparaphenylene-Fullerene Complexes (Chem. Eur. J. 20/2023)

Reference: J. Volkmann[+], D. Kohrs[+], H. A. Wegner, *Chem. Eur. J.* **2023**, *29*, e202300737.

DOI: 10.1002/chem.202300737

[+]These authors contributed equally.

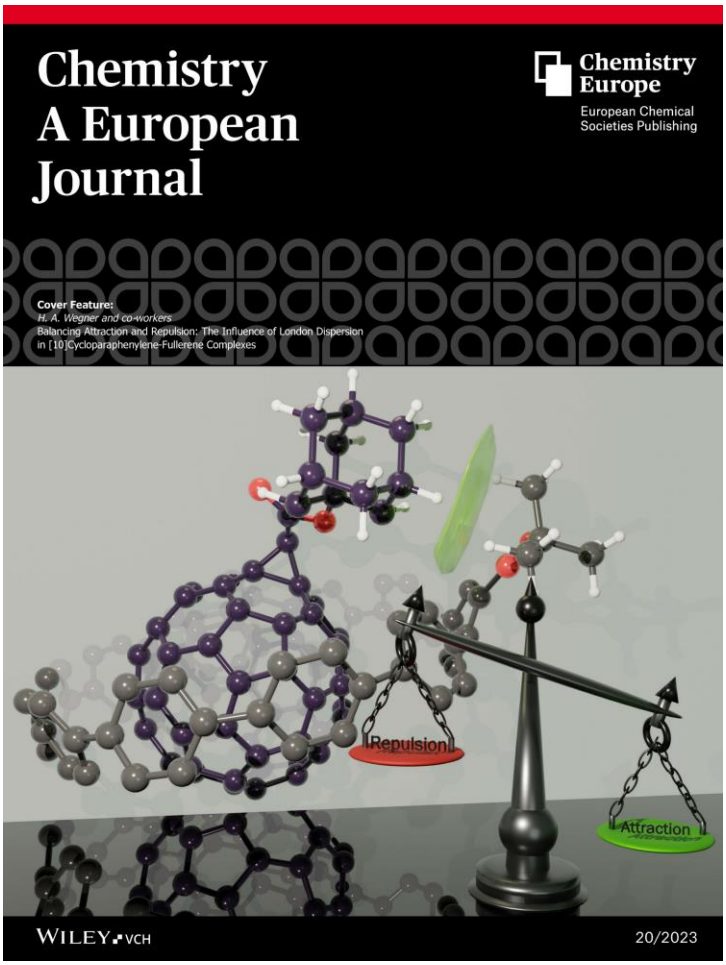

"**Molecular interactions** are a combination of different attractive and repulsive forces. We have studied the delicate balance within a supramolecular [10]cycloparaphenylene–fullerene complex—both functionalized with alkyl esters—to evaluate the attractive and repulsive interplay between the substituents on the components."

eck for updates

Chemistry–A European Journal | Research Article
doi.org/10.1002/chem.202300268

Chemistry Europe
European Chemical Societies Publishing

www.chemeurj.org

Balancing Attraction and Repulsion: The Influence of London Dispersion in [10]Cycloparaphenylene-Fullerene Complexes

Jannis Volkmann[+],[a, b] Daniel Kohrs[+],[a, b] and Hermann A. Wegner*[a, b]

Abstract: Herein we present a systematic study of the influence of different alkyl chains in malonyl ester fullerene adducts with [10]cycloparaphenylene ([10]CPP]) and a *tert*-butyl (*t*Bu) ester-substituted [10]CPP analogue. The association constants between the nanoring hosts and the fullerene guests were determined by fluorescence quenching experiments. The trends in association were rationalized by an interplay of repulsion arising from an extended volume and London dispersion as an attractive counterpart.

Introduction

On a basic level, every noncovalent interaction between two molecular species can be regarded as supramolecular chemistry. One prominent example of molecular structures exploited in supramolecular assemblies, especially in the field of carbon nanomaterials, are fullerenes. Their spheric structure makes them ideal candidates especially for curved host molecules. Cycloparaphenylenes ([*n*]CPP), strained carbon nanohoops,[1] are a prime example of such a molecular motif in this regard. The complex between C_{60} and [10]CPP represents the perfect fit regarding the size of guest and host.[2] Here, mainly π–π interactions between the concave side of the CPP and the convex fullerene surface are the driving force within this process. The high association is rationalized by ideal distance between the aromatic entities, making this peapod a curved analogue of two graphene layers. Generally, the association can be tuned by the complementarity in size, shape and interactions. For instance, changing the size of the CPP from [10] to [8], [9] or [11] decreases the association by more than one order of magnitude (K_{SV}).[2] In methylene bridged macrocycles, such as cyclotriveratrylenes and calixarenes, the increased flexibility increases the complementarity in size, while it decreases in shape.[3,4] Additionally, the extension of such systems, such as the substitution on cyclotriveratrylenes with additional phenyl groups, drastically increases the association.[3] A similar behavior was observed for the π-extension in hexa-*peri*-hexabenzocoronene embedded [12]CPP. While the diameter is too large for an efficient complexation of C_{70}, the extended π-interactions lead to a remarkable high association constant.[5] The conceptual binding motif between fullerene and CPP was used to study a Russian doll-type complex between [15]CPP, [10]CPP and C_{60},[6] as well as the differences to the fullerene derivative C_{70}.[7] The strong interaction between the entities was further used in a π–π templating strategy to build a rotaxane based on fullerenes and one [10]CPP unit.[8] In addition to these all-carbon buckyballs, endohedral fullerenes were studied in this manner as well. Here, the interaction is additionally based on charge transfer.[9] This driving force has also been assigned in the complex between [6,6]-phenyl-C_{61}-butyric acid methyl ester (PCBM), an electron acceptor material in organic solar cells, and a porphyrin unit connect to a [10]CPP unit.[10] Our group exploited this binding motif in order to study the stabilizing effect of the nanoring on a fullerenyl radical,[11] as well as the electronic communication between two CPP units through a dumbbell shaped fullerene dimer.[12] We found that the binding is influenced by London dispersion forces which stabilize the 2:1 complex and thus contribute to a positive cooperativity.

Even though this is an illustrative example of weak forces controlling supramolecular complexes no in-depth study has been done to elucidate the different forces operating. Molecular balances offer an experimental tool to quantify these often neglected weak forces.[13] Crucial for these balances is a high sensitivity for energy changes, as these forces are weak for small molecules, but can reach large values for extended systems, though. Cockroft and co-workers adapted a system originally designed by the group of Wilcox to study alkyl-alkyl interactions.[14] In this system two main conformers, the dispersion promoting folded and the dispersion prohibiting unfolded conformer, could be distinguished and quantified by ^{1}H NMR spectroscopy.[15] An additional example of a balance system relying on the interconversion of two different con-

[a] J. Volkmann,[+] D. Kohrs,[+] Prof. Dr. H. A. Wegner
Institute of Organic Chemistry
Justus Liebig University Giessen
Heinrich-Buff-Ring 17, 35392 Giessen (Germany)
E-mail: Hermann.A.Wegner@org.chemie.uni-giessen.de

[b] J. Volkmann,[+] D. Kohrs,[+] Prof. Dr. H. A. Wegner
Center for Materials research (ZfM/LaMa)
Justus Liebig University Giessen
Heinrich-Buff-Ring 16, 35392 Giessen (Germany)

[+] These authors contributed equally to this work.

Supporting information for this article is available on the WWW under https://doi.org/10.1002/chem.202300268

Chemistry–A European Journal | Research Article doi.org/10.1002/chem.202300268 | Chemistry Europe European Chemical Societies Publishing

formers is realized in a thiobarbiturate system, in which the *anti* and *syn* relationship between two *tert*-butyl (*t*Bu) groups is analyzed.[16] Furthermore, the bond isomerism in cyclooctatetraene was used for the purpose of investigating London dispersion, as the substituents are only in close proximity in one diastereomer.[17] A balance system consisting of an intermolecular system was presented by Chen and co-workers and is based on N-heterocycles which form a proton-bound dimer.[18] The change of dissociation energy was investigated in solution and in the gas phase as well as computationally.

This approach allows an estimation of dispersive interactions between the substrates by comparing the obtained data in the different states. A further example consisting of two entities is the dimerization of a titanium triscatecholate helicate, in which different ester moieties were investigated on their ability to stabilize the dimers by noncovalent interactions.[19] The symmetry of this system increases its accuracy as the signals obtained are threefold amplified. Our group contributed with the use of azobenzene photoswitches with which we could investigate London dispersion as well as solvent effects.[20,21]

In this study we aim to apply the ability of the [10]CPP-C_{60} host-guest system to enforce close proximity of two molecular entities in order to study the influence of substitution of the buckyball on the binding behavior with [10]CPP and a substituted CPP derivative. For this purpose we employed a bis-*tert*-butyl ester-substituted CPP (s[10]CPP) which we reported earlier.[22] As guest molecules we synthesized and employed malonyl ester-substituted fullerene derivatives. To evaluate the interactions between substituents, the effects of the different substitution on the fullerene or the CPP have to be outlined (Figure 1). The backbone motif consists of [10]CPP and C_{60} whose association is mainly driven by π-π interactions (ΔG_1). The introduction of substituents on the fullerene adds an entropic penalty of reduced rotation in the complex, as well as interactions between the substituents on the fullerene and the unsubstituted [10]CPP (ΔG_2). Attachment of *t*Bu ester on the CPP provides the substituted analogue s[10]CPP, which adds strain energy to the equation which is built by dihedral interactions between the substituted phenyl ring and the neighboring ones as well as interaction energies between the substituents and C_{60} (ΔG_3). The association between substituted fullerenes and s[10]CPP can thus be divided into the measurable energies ΔG_1, ΔG_2, ΔG_3, including the unknown interaction energies as well as the substituent-substituent interaction energy [$\Delta G_{Interactions}(S_F-S_C)$], which is then the only unknown variable in this equation.

Results and Discussion

Synthesis of materials

Employing the Bingel-Hirsch reaction to a mixture of C_{60} and symmetric malonyl esters gave access to a library of substituted fullerene derivatives.[23] The employed malonyl esters for this cyclopropanation reaction were formed applying nucleophilic catalysis under Steglich conditions. In this manner, the targeted fullerene derivatives carrying linear as well as branched alkyl chains could be effectively synthesized in two steps from commercially available starting materials (Scheme 1). Besides the linear C_1–C_4 substituents [methyl (Me), ethyl (Et), *n*-propyl (*n*Pr), *n*-butyl (*n*Bu)] different branched substituents [*i*-propyl (*i*Pr), *tert*-butyl (*t*Bu) and 1-adamantyl (Ad)] were incorporated. The unsubstituted nanoring [10]CPP was synthesized following a procedure published by Jasti and co-workers,[24] and *t*Bu ester-substituted [10]CPP was prepared as recently described by us,[22] which follows a "class III" strategy for substituted CPPs,

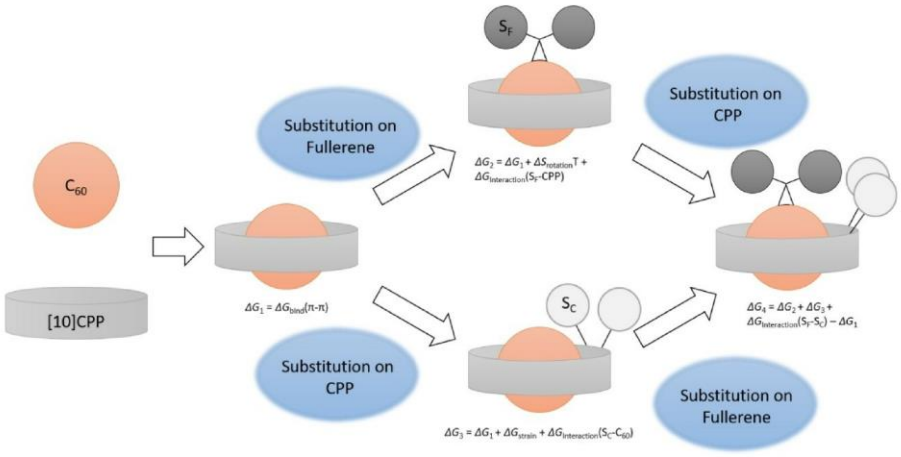

Figure 1. Schematic visualization of the methodological approach for evaluating the noncovalent interactions (S_F = substituents on fullerene, S_C = substituents on s[10]CPP).

Chemistry–A European Journal | Research Article doi.org/10.1002/chem.202300268 | Chemistry Europe European Chemical Societies Publishing

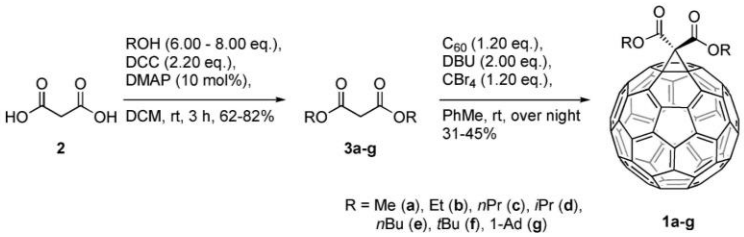

Scheme 1. Synthesis of malonyl ester-substituted fullerenes **1 a–g**.

using a [2+2+2] cycloaddition before macrocyclization through cross coupling allowing an efficient build-up.[25]

In principle the association between the two entities can have two different binding states (*syn* andor *anti*) (Scheme 2) which both contribute to the overall association as they quench the fluorescence of the CPP. The contribution of the substituent-substituent interactions within the assembly can still be estimated as this is the only additional force in the case of both substituted entities. To prove the existence of this alignment we conducted a HH NOESY experiment for the complex of s[10]CPP and **1 g** which revealed an noncovalent interaction between the *t*Bu groups and the adamantly groups which can only exist in the *syn* alignment (Figure S3 in the Supporting Information).

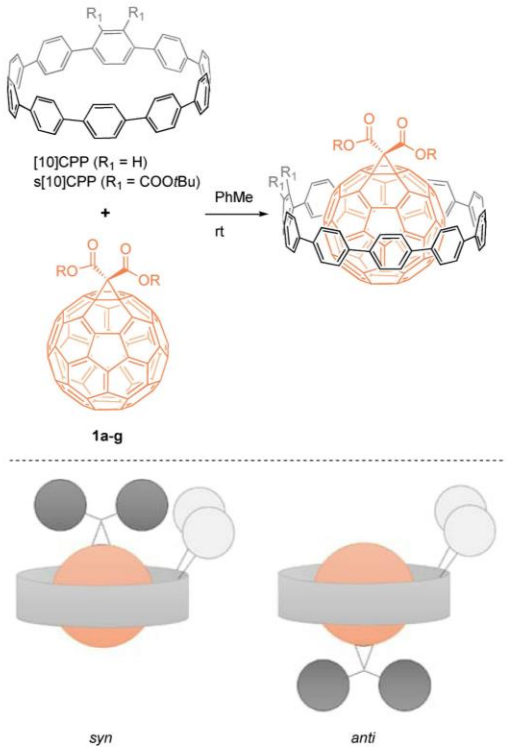

Scheme 2. Top: Representative procedure for the complex formation. Bottom: Schematic visualization of the two binding modes in the case of the s[10]CPP.

The association constants between the substituted fullerenes **1 a–g** and [10]CPP as well as s[10]CPP were determined by fluorescence quenching. Following the decreasing fluorescence intensity of the nanoring upon addition of the fullerene guest allowed operation at low concentrations; this is beneficial for complexes for which large association constants are expected.[26] A triple determination was executed to prove the reliability and test the accuracy of the results. Two emission wavelengths of the s[10]CPP were analyzed which further improved the accuracy of the measurements.

Discussion of association constants

For an easier insight into the interactions between the substituents we considered the associations found in relation to the corresponding complex with bare C_{60}. Thus, we could cancel out additional effects like an increased strain in the nanohoop upon substitution which is built by enforcing a small dihedral angle in the complex or simple substituent-buckyball (S_F-CPP) or substituent-nanohoop (S_C-C_{60}) interactions (Figure 1).

Now we could directly evaluate the impact of a substituent on the binding behavior in the final complex. For a consistent and reliable data set, the association constant of [10]CPP and C_{60} was determined in the first step to gain the necessary ΔG_1, being in good agreement with the values determined by the group of Hirsch,[27] which differ from the original values reported by the group of Yamago.[2] By substitution of the fullerene the association to the nanohoops is decreased which can be rationalized by the locked rotation and, hence, entropic penalty as well as substituent-fullerene interactions (Scheme 1, ΔG_2). Starting with the association of parent [10]CPP with substituted fullerenes we found a maximum for the Me/Et derivatives. The binding constant is in comparison to the value of C_{60} ~80% lower. For longer and more branched alkyl groups it is further decreased (by 80–82%; Figure 2, Table 1). The adamantyl fullerene derivative **1 g** deviates in this context,

Chemistry–A European Journal | Research Article doi.org/10.1002/chem.202300268 | Chemistry Europe European Chemical Societies Publishing

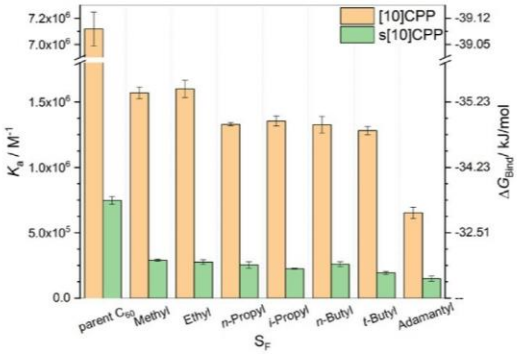

Figure 2. Summary of association constants K_a and binding energies ΔG_{bind} for the fullerene complexes of the parent and *t*Bu ester-substituted [10]CPP.

Table 1. Summary of the determined association energies ΔG_{bind} of the fullerenes C_{60}, and **1a–g** with s[10]CPP and [10]CPP, respectively.

Guest	Energy [kJ mol^{-1}] $\Delta G_{bind,s[10]CPP}$	$\Delta G_{bind,[10]CPP}$
C_{60}	−33.5 ± 0.1	−39.09 ± 0.05
1a	−31.17 ± 0.07	−35.35 ± 0.07
1b	−31.0 ± 0.2	−35.4 ± 0.1
1c	−30.8 ± 0.2	−35.1 ± 0.3
1d	−30.54 ± 0.05	−34.98 ± 0.07
1e	−30.9 ± 0.2	−34.9 ± 0.1
1f	−30.2 ± 0.2	−34.84 ± 0.06
1g	−29.5 ± 0.4	−33.2 ± 0.2

having an association of roughly one order of magnitude lower relative to C_{60}. This finding can be explained by the increased steric demand of this bulky substituent.

Next, we investigated the association behavior between the s[10]CPP and the substituted fullerene derivatives to achieve ΔG_3 and ΔG_4. On a first glance, the association with bare C_{60} is one order of magnitude smaller than for unsubstituted [10]CPP. This corresponds to ~5.5 kJ mol^{-1} and can be attributed to dihedral strain which increases due to planarization in order to achieve efficient complexation. The association constants of s[10]CPP with the linear alkyl substituted fullerene derivatives **1a–c**, **e** are around $^2/_3$ lower relative to the value for C_{60}. The decrease in binding strength is thus lower compared to the case of unsubstituted [10]CPP. In contrast to the complexation of unsubstituted [10]CPP with fullerene derivatives **1a–g**, branching reduced the association in a linear trend with the Ad derivative **1g** bearing the smallest association constant for the complexation with s[10]CPP. Even though the steric interactions between nanoring and fullerene should be more pronounced in the case of the s[10]CPP, the relative change in association for longer alkyl chains is less distinct than in the unsubstituted case with [10]CPP.

To get a better insight into the effect of substitution on the association (energies), the energies were subtracted from the values for C_{60}, thus directly providing the energetic penalties of substitution ($\Delta G_2 - \Delta G_1$ for [10]CPP and $\Delta G_4 - \Delta G_3$ for s[10]CPP).

Figure 3 shows that all substituted derivatives are more endergonic than the complex with C_{60} whereby the complexes with substituted [10]CPP (green bars) pay a smaller penalty than for [10]CPP (orange bars). To envision the differences between the substituted fullerenes, the differences in energy penalties were subtracted and depicted in purple bars. The obtained values are equal to the interaction energies $\Delta G_{Interaction}(S_F - S_C)$. All these values are negative, meaning stabilization occurs for s[10]CPP in contrast to parent [10]CPP (Table 2). Within the fullerene derivatives two strategies were followed: On the one hand increasing the alkyl chain length (Me, Et, *n*Pr, *n*Bu) and on the other increasing branched alkyl substituents (Me, Et, *i*Pr, *t*Bu, Ad) to follow the trend of increasing bulk. Within the set of linear alkyl groups it is surprising that the Me fullerene derivative **1a** is already with 1.4 kJ mol^{-1} stabilized. A further increase in alkyl chain length at the fullerene adduct towards Et fullerene derivative **1b** (1.2 kJ mol^{-1}) and *n*Pr derivative **1c** (1.3 kJ mol^{-1}) does not continue this effect. Only the *n*Bu fullerene derivative **1e** has a higher value in this regard (1.6 kJ mol^{-1}). This is in agreement with an earlier study of our group in which *n*Bu groups had the strongest stabilizing effect on the *Z* isomer of azobenzene.[21] For branched substituents this trend is more obvious: exchanging one H with a methyl group in Et fullerene derivative **1b** does not influence the stabilization (1.2 kJ mol^{-1} for *i*Pr fullerene derivative **1d**) while it is reduced to 0.9 kJ mol^{-1} for the *t*Bu fullerene derivative **1f**. This trend is inverted in the case of the Ad fullerene derivative **1g**. Here the substituents have the strongest stabilizing effect in the set of investigated substituents with 1.9 kJ mol^{-1}. This relation between *t*Bu and the larger Ad group can also be found, for example, in a recent study on the equilibrium in alkyl substituted bifluorenylidenes.[28]

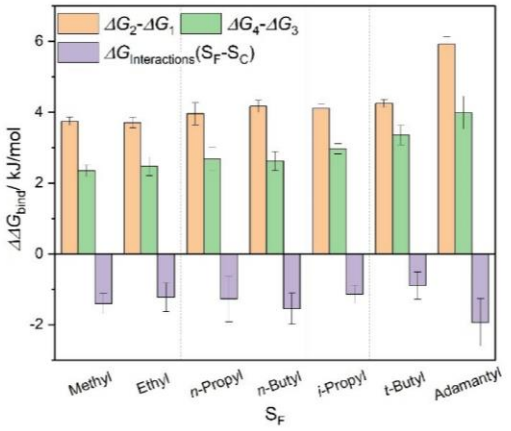

Figure 3. Energy differences relative to the complex with C_{60} for [10]CPP ($\Delta G_2 - \Delta G_1$, orange bars), s[10]CPP ($\Delta G_4 - \Delta G_3$, green bars) and the differences between them ($\Delta G_{Interactions}(S_F - S_C)$, purple bars).

Chemistry–A European Journal | Research Article doi.org/10.1002/chem.202300268 | Chemistry Europe European Chemical Societies Publishing

Table 2. Energy differences $\Delta G_2-\Delta G_1$, $\Delta G_4-\Delta G_3$ and $\Delta G_{interaction}(S_F-S_C)$ calculated with equations EQS2 and EQS3 (Supporting Information).

Guest	Energy difference [kJ mol^{-1}] $\Delta G_2-\Delta G_1$	$\Delta G_4-\Delta G_3$	$\Delta G_{interaction}(S_F-S_C)$
1a	3.75±0.12	2.34±0.16	−1.40±0.28
1b	3.70±0.15	2.47±0.26	−1.23±0.40
1c	3.95±0.32	2.68±0.33	−1.28±0.65
1d	4.11±0.11	2.97±0.14	−1.15±0.26
1e	4.16±0.17	2.62±0.27	−1.55±0.44
1f	4.25±0.11	3.35±0.28	−0.90±0.39
1g	5.92±0.21	3.98±0.46	−1.94±0.67

Conclusion

In conclusion, we have presented a systematic supramolecular study of fullerene Bingel adducts bearing alkyl groups with different chain lengths with [10]CPP and the substituted [10]CPP derivative. We investigated the steric-repulsion versus London dispersion effects between *t*Bu ester and branched, and elongated alkyl chains. Interestingly, we found different trends for the investigated CPP derivatives. In absolute numbers, all cases led to an increased repulsion while adding the substituents to the buckyball. In order to evaluate the influence of substituents, the total interactions were dissected in individual contributions with reference systems that should cancel out additional, undesired interactions, allowing the substituent–substituent interactions to be quantified. These interactions were expected to be small in energy. Hence, the fluorescence quenching method was applied for these supramolecular complexes, as small energy changes can be reliably determined.

Increasing the chain length of the linear alkyl substituents did not have a large effect on the overall binding, whereby the *n*Bu fullerene derivative **1e** showed the strongest stabilization (1.6 kJ mol^{-1}) of the complex with s[10]CPP. Overall, branched alkyl groups (*i*Pr **1d**, *t*Bu **1f**, 1-Ad **1g**) showed a stronger effect, and both s[10]CPP and unsubstituted [10]CPP were more endothermic for larger substituents. However, the effect was more pronounced for [10]CPP, leading to a net stabilization for the Ad-substituted fullerene derivative **1g**.

The presented system allowed low-energy interactions to be quantified efficiently and with high accuracy. Due to the complexity of interactions, only a qualitative rational of the operating effects can be formulated, though. Nevertheless, this proof-of-principle study shows potential for addressing multiple interactions in complex systems. Additionally, it provides guidelines for the design of carbon-based supramolecular functional systems in the future.

Experimental Section

Experimental details are described in the Supporting Information.

Acknowledgements

The authors are grateful for the financial support provided by the Justus Liebig university and the DFG (SPP 1807). The authors are grateful to Dr. Heike Hausmann for NMR measurements. Open Access funding enabled and organized by Projekt DEAL.

Conflict of Interest

The authors declare no conflict of interest.

Data Availability Statement

The data that support the findings of this study are available in the supplementary material of this article.

Keywords: cyclophanes · fullerenes · host-guest systems · pi interactions · supramolecular chemistry

[1] Y. Xu, M. von Delius, *Angew. Chem. Int. Ed.* **2020**, *59*, 559–573; *Angew. Chem.* **2019**, *132*, 567–582.
[2] T. Iwamoto, Y. Watanabe, T. Sadahiro, T. Haino, S. Yamago, *Angew. Chem. Int. Ed.* **2011**, *50*, 8342–8344.
[3] H. Matsubara, A. Hasegawa, K. Shiwaku, K. Asano, M. Uno, S. Takahashi, K. Yamamoto, *Chem. Lett.* **1998**, *27*, 923.
[4] T. Haino, M. Yanase, Y. Fukazawa, *Angew. Chem. Int. Ed.* **1997**, *36*, 259–260; *Angew. Chem.* **1997**, *109*, 288–290.
[5] D. Lu, G. Zhuang, H. Wu, S. Wang, S. Yang, P. Du, *Angew. Chem. Int. Ed.* **2017**, *56*, 158–162; *Angew. Chem.* **2017**, *129*, 164–168.
[6] S. Hashimoto, T. Iwamoto, D. Kurachi, E. Kayahara, S. Yamago, *ChemPlusChem* **2017**, *82*, 1015–1020.
[7] T. Iwamoto, Y. Watanabe, H. Takaya, T. Haino, N. Yasuda, S. Yamago, *Chem. Eur. J.* **2013**, *19*, 14061–14068.
[8] Y. Xu, R. Kaur, B. Wang, M. B. Minameyer, S. Gsänger, B. Meyer, T. Drewello, D. M. Guldi, M. von Delius, *J. Am. Chem. Soc.* **2018**, *140*, 13413–13420.
[9] a) T. Iwamoto, Z. Slanina, N. Mizorogi, J. Guo, T. Akasaka, S. Nagase, H. Takaya, N. Yasuda, T. Kato, S. Yamago, *Chem. Eur. J.* **2014**, *20*, 14403–14409; b) Y. Nakanishi, H. Omachi, S. Matsuura, Y. Miyata, R. Kitaura, Y. Segawa, K. Itami, H. Shinohara, *Angew. Chem. Int. Ed.* **2014**, *53*, 3102–3106; c) H. Ueno, T. Nishihara, Y. Segawa, K. Itami, *Angew. Chem. Int. Ed.* **2015**, *54*, 3707–3711.
[10] Y. Xu, B. Wang, R. Kaur, M. B. Minameyer, M. Bothe, T. Drewello, D. M. Guldi, M. von Delius, *Angew. Chem. Int. Ed.* **2018**, *57*, 11549–11553; *Angew. Chem.* **2018**, *130*, 11723–11727.
[11] a) A. Stergiou, J. Rio, J. H. Griwatz, D. Arčon, H. A. Wegner, C. P. Ewels, N. Tagmatarchis, *Angew. Chem. Int. Ed.* **2019**, *58*, 17745–17750; *Angew. Chem.* **2019**, *131*, 17909–17914; b) Y. Tanuma, A. Stergiou, A. Bužan Bob-

Chemistry–A European Journal | Research Article doi.org/10.1002/chem.202300268 | Chemistry Europe European Chemical Societies Publishing

nar, M. Gaboardi, J. Rio, J. Volkmann, H. A. Wegner, N. Tagmatarchis, C. P. Ewels, D. Arčon, *Nanoscale* **2021**, *13*, 19946–19955.
[12] J. Rio, S. Beeck, G. Rotas, S. Ahles, D. Jacquemin, N. Tagmatarchis, C. Ewels, H. A. Wegner, *Angew. Chem. Int. Ed.* **2018**, *57*, 6930–6934; *Angew. Chem.* **2018**, *130*, 7046–7050.
[13] a) A. Elmi, S. L. Cockroft, *Acc. Chem. Res.* **2021**, *54*, 92–103; b) M. Giese, M. Albrecht, *ChemPlusChem* **2020**, *85*, 715–724; c) F. Holtrop, K. W. Visscher, A. R. Jupp, J. C. Slootweg in *Adv. Phys. Org. Chem.*, Elsevier, **2020**, pp. 119–141; d) D. J. Liptrot, P. P. Power, *Nat. Chem. Rev.* **2017**, *1*, 4; e) M. A. Strauss, H. A. Wegner, *Eur. J. Org. Chem.* **2019**, *2019*, 295–302; f) J. P. Wagner, P. R. Schreiner, *Angew. Chem. Int. Ed.* **2015**, *54*, 12274–12296; *Angew. Chem.* **2015**, *127*, 12446–12471.
[14] S. Paliwal, S. Geib, C. S. Wilcox, *J. Am. Chem. Soc.* **1994**, *116*, 4497–4498.
[15] L. Yang, C. Adam, G. S. Nichol, S. L. Cockroft, *Nat. Chem.* **2013**, *5*, 1006.
[16] U. Berg, I. Pettersson, *J. Org. Chem.* **1987**, 5177–5184.
[17] M. H. Lyttle, A. Streitwieser, Jr., R. Q. Kluttz, *J. Am. Chem. Soc.* **1981**, *103*, 3232–3233.
[18] R. Pollice, M. Bot, I. J. Kobylianskii, I. Shenderovich, P. Chen, *J. Am. Chem. Soc.* **2017**, *139*, 13126–13140.
[19] D. van Craen, W. H. Rath, M. Huth, L. Kemp, C. Räuber, J. M. Wollschläger, C. A. Schalley, A. Valkonen, K. Rissanen, M. Albrecht, *J. Am. Chem. Soc.* **2017**, *139*, 16959–16966.
[20] a) L. Schweighauser, M. A. Strauss, S. Bellotto, H. A. Wegner, *Angew. Chem. Int. Ed.* **2015**, *54*, 13436–13439; *Angew. Chem.* **2015**, *127*, 13636–13639; b) M. A. Strauss, H. A. Wegner, *Angew. Chem. Int. Ed.* **2019**, *58*, 18552–18556; *Angew. Chem.* **2019**, *131*, 18724–18729; c) M. A. Strauss, H. A. Wegner, *Angew. Chem. Int. Ed.* **2021**, *60*, 779–786; *Angew. Chem.* **2021**, *133*, 792–799.
[21] M. A. Strauss, H. A. Wegner, *ChemPhotoChem* **2019**, *3*, 392–395.
[22] D. Kohrs, J. Becker, H. A. Wegner, *Chem. Eur. J.* **2022**, *28*, e202104239.
[23] a) C. Bingel, *Chem. Ber.* **1993**, *126*, 1957–1959; b) X. Camps, A. Hirsch, *J. Chem. Soc. Perkin Trans. 1* **1997**, 1595–1596.
[24] E. R. Darzi, T. J. Sisto, R. Jasti, *J. Org. Chem.* **2012**, *77*, 6624–6628.
[25] D. Kohrs, J. Volkmann, H. A. Wegner, *Chem. Commun.* **2022**, *58*, 7483–7494.
[26] P. Thordarson, *Chem. Soc. Rev.* **2011**, *40*, 1305–1323.
[27] I. Solymosi, J. Sabin, H. Maid, L. Friedrich, E. Nuin, M. E. Pérez-Ojeda, A. Hirsch, *Org. Mater.* **2022**, *4*, 73–85.
[28] F. M. Wilming, B. Marazzi, P. P. Debes, J. Becker, P. R. Schreiner, *J. Org. Chem.* **2022**, *88*, 1024–1035.

Manuscript received: January 26, 2023
Accepted manuscript online: February 14, 2023
Version of record online: March 3, 2023

4.3 Influence of Substitution on the Supramolecular Chemistry of Cycloparaphenylene-Fullerene Complexes

Reference: D. Kohrs[+], J. Volkmann[+], H. A. Wegner, *Eur. J. Org. Chem.* **2023**, e202300575.

DOI: 10.1002/ejoc.202300575

[+]These authors contributed equally.

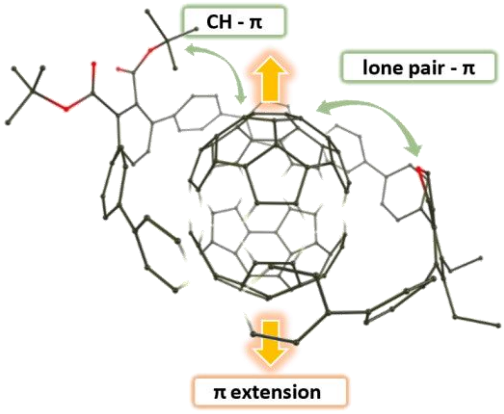

"Herein a detailed host-guest study of [10]cycloparaphenylene and three substituted analogues with the fullerenes C_{60} and C_{70} is presented. Fluorescence quenching experiments as well as computational chemistry were employed in order to shine light on the influence of substitution on the association behavior. An increased steric demand was facing additional attractive interactions between substituents and the fullerene itself."

ck for updates

EurJOC
European Journal of Organic Chemistry

Research Article
doi.org/10.1002/ejoc.202300575

Chemistry Europe
European Chemical Societies Publishing

www.eurjoc.org

Influence of Substitution on the Supramolecular Chemistry of Cycloparaphenylene-Fullerene Complexes

Daniel Kohrs[+],[a, b] Jannis Volkmann[+],[a, b] and Hermann A. Wegner*[a, b]

We present a comprehensive host-guest study of four substituted and unsubstituted [10]cycloparaphenylenes with the fullerenes C_{60} and C_{70}. Within this study, the influence on the complexation behavior was investigated experimentally and computationally. Due to the increased steric demand the substitution on the nanohoop results in an energetic penalty, which could be partially compensated by additional substituent-fullerene interactions. These attractive interactions are intensified in the C_{70} complexes and with an increased degree of substitution. For the computational investigation conformer ensembles were taken into account, providing reliable structures with Boltzmann weighted energies. An analysis of the noncovalent interactions elucidated the origin of the enhanced substituent-C_{70} interaction. The ellipsoid fullerene C_{70} can be considered as a π-extended version of C_{60}, which is able to increase the attractive van der Waals interactions within these supramolecular complexes.

Introduction

Interactions between not covalently bound molecules are omnipresent, reaching from solvation to protein folding and beyond. In the field of π-conjugated (nano)carbons, π-π interactions play a crucial role between the nanocarbons, as well as in their solvation. The term π-π interaction joins a library of interactions consisting of quadrupole interactions,[1] electrostatic interactions as well as London dispersion among others.[2]

A prime example among these interactions is the π-stacking of two graphene layers within graphite. Here, the lattices stack in a displaced manner with an interlayer distance of 3.40 Å.[3] Wrapped-up graphene sheets, carbon nanotubes (CNT), have an increased and decreased electron density on the concave and convex site, respectively, which makes them suitable candidates to host fullerenes in their electron-rich cavity. The shortest repeatable cut-out of an armchair CNT is a [*n*]cycloparaphenylene ([*n*]CPP) which can thus be seen as the perfect model substrate for single-walled CNTs. After years of throwbacks on the synthetic odyssey towards these strained polyaromatic hydrocarbons,[4] three main strategies were developed to form this class of curved compounds.[5] Having these strategies established, it was possible to investigate a variety of different sized CPPs for which [10]CPP revealed superior supramolecular properties regarding complexation with fullerenes. The [10]CPP@C_{60} complex, for instance, has an exceptional association constant of around 10^7 M^{-1} in toluene.[6] In this complex the distance between the nanohoop and the fullerene coincides with the interlayer distance in graphite. A similar strategy was applied by our group for the stabilization of the azafullerenyl radical $C_{59}N^{\bullet}$,[7] as well as by others for the synthesis of a rotaxane[8] or the complexation of charge-delocalized endofullerenes.[9] In case of bisazafullerene $(C_{59}N)_2$, the fullerene dimer can be encapsulated by two [10]CPPs, whereat the first complexation promotes the second by additional London dispersion forces.[10]

While a substituted *para*-phenylene unit within a CPP influences the association constant due to a decreased diameter and conjugation originating from the larger dihedral angle of the substituted core unit with the adjacent phenylenes, additional interactions – such as London dispersion – can positively contribute to the association (Figure 1). Recently, we investigated these additional interactions in complexes consisting of a di *tert*-butyl ester functionalized [10]CPP as a host unit encapsulating different methanofullerenes, functionalized with branched as well as linear alkyl chains.[11] In all cases, the

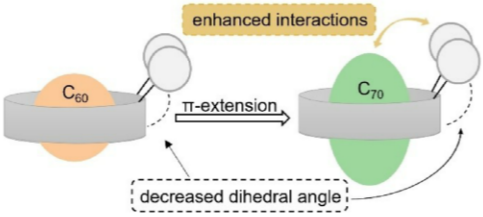

Figure 1. Schematic representation of the proposed enhanced interaction between the π-extended fullerene C_{70} and the substituents on the CPP.

[a] D. Kohrs,[+] J. Volkmann,[+] Prof. Dr. H. A. Wegner
Institute of Organic Chemistry
Justus Liebig University Giessen
Heinrich-Buff-Ring 17, 35392 Giessen (Germany)
E-mail: Hermann.A.Wegner@org.chemie.uni-giessen.de
[b] D. Kohrs,[+] J. Volkmann,[+] Prof. Dr. H. A. Wegner
Center for Materials research (ZfM/LaMa)
Justus Liebig University Giessen
Heinrich-Buff-Ring 16, 35392 Giessen (Germany)
[+] These authors contributed equally to this work.

Supporting information for this article is available on the WWW under https://doi.org/10.1002/ejoc.202300575

EurJOC
European Journal of Organic Chemistry

Research Article
doi.org/10.1002/ejoc.202300575

Chemistry Europe
European Chemical Societies Publishing

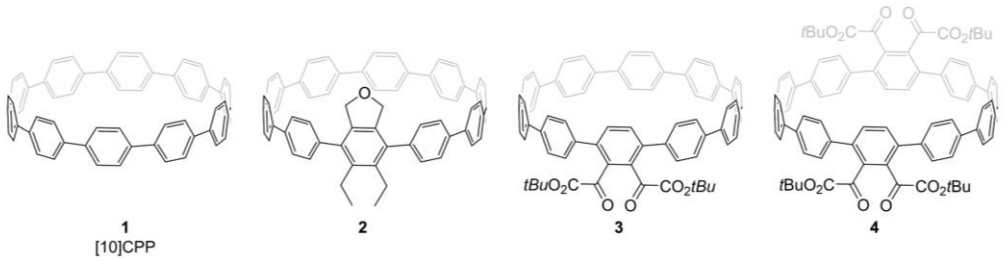

Figure 2. CPPs applied within this study.

attractive interactions dominated, with the dispersion donors *n*-butyl and 1-adamantyl showing the strongest effect. To get an in-depth understanding of the substitution effects in CPP-fullerene complexes, we have herein conducted fluorescence quenching experiments with the previously reported di- and tetra-*tert*-butyl ester functionalized [10]CPPs **3** and **4**, as well as the diethyl phthalane incorporated [10]CPP **2**, in comparison to the parent [10]CPP **1** (Figure 2). The fullerenes C_{60} and C_{70} were employed as guest molecules and the impact of the different shapes of the fullerenes on the association behavior with the substituted nanohoops were investigated experimentally as well as by theoretical calculations.

Results and Discussion

Experimental details

The substituted CPPs – di- and tetra-*tert*-butyl ester functionalized [10]CPPs **3** and **4**, as well as diethyl phthalane incorporated [10]CPP **2** – were synthesized according to previously published syntheses,[12,13] following a similar strategy relying on a combination of a [2+2+2] cycloaddition for the introduction of substituents and a cross-coupling reaction for the selective formation of the 10-membered ring.[14] The unsubstituted [10]CPP **1** was synthesized following a synthesis reported by Jasti and coworkers.[15]

For the determination of the association constants, trifold fluorescence quenching experiments were conducted in toluene and the thus obtained standard deviation was employed for the errors. While the concentration of the emitting host (CPP) was kept constant, the guest concentration was varied, and the quenching of the fluorescence was followed. The data were evaluated by non-linear regression utilizing the online tool "bindfit" by Thordarson.[16] For the determination of the stoichiometry, association mode and association constant the corresponding recommendations by Thordarson were followed. Even though the association constant of parent [10]CPP with C_{70} is literature known, we repeated the experiments to rule out systematic deviations originating from different experimental setups.

Association Constants

The association constants and energies of the different C_{60} and C_{70}/CPP-complexes are summarized in Table 1 and Figure 3. In general, the association drops upon substitution of the nanohoop which is in accordance with our earlier results for methanofullerenes.[11] This trend can be rationalized by the increased dihedral angle between the substituted aromatic ring and the adjacent ones which effectively reduces the inner diameter and thus the cavity available for the fullerene (Figure 1). The dihedral angle has to be reduced upon complex-

Table 1. Summary of the binding energies used for Figure 1 as well as the corresponding association energies for the investigated complexes with the standard deviations after trifold determination. The values **1**@C_{60} and **3**@C_{60} are taken from ref. [11].

Host	Guest	K_{bind}/M^{-1}	$\Delta G_{bind,measure}$/kJ/mol
1	C_{60}	$7.1 \pm 0.1 \cdot 10^6$	-39.09 ± 0.05
	C_{70}	$4.7 \pm 0.2 \cdot 10^5$	-32.4 ± 0.1
2	C_{60}	$1.15 \pm 0.08 \cdot 10^5$	-28.9 ± 0.2
	C_{70}	$3.75 \pm 0.08 \cdot 10^4$	-26.10 ± 0.06
3	C_{60}	$7.5 \pm 0.3 \cdot 10^5$	-33.5 ± 0.1
	C_{70}	$7.7 \pm 0.3 \cdot 10^4$	-27.88 ± 0.08
4	C_{60}	$1.0 \pm 0.1 \cdot 10^5$	-28.6 ± 0.3
	C_{70}	$4.1 \pm 0.7 \cdot 10^4$	-26.3 ± 0.5

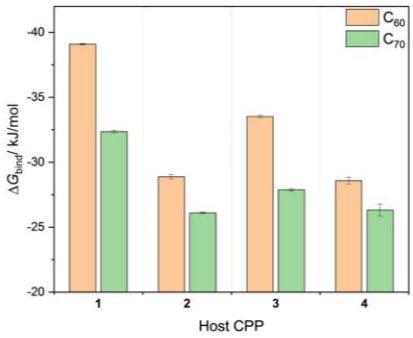

Figure 3. Association energies of the investigated nanohoop molecules with C_{60} as well as C_{70}.

EurJOC
European Journal of Organic Chemistry

Research Article
doi.org/10.1002/ejoc.202300575

Chemistry Europe
European Chemical Societies Publishing

ation – a penalty which has to be paid with association energy. Additionally, this trend amplifies with an increasing degree of substitution and contributes to both, the association with C_{60} and C_{70}. For the two fourfold-substituted derivatives **2** and **4** the values are very similar, indicating a weak influence of the nature of the substituents in the investigated cases.

To analyze the interactions, the binding energies were normalized to the energies of the parent complexes **1**@C_{60} and **1**@C_{70}, respectively (Figure 4, orange and green bars). Thus, the sum of energetic penalty arising from a decreased effective inner diameter and attractive non-covalent interactions can be rationalized. In all cases the association energy is reduced by 10%–30%, correlating to a reduction of the association constant by about one order of magnitude, given the exponential relation between association constant and its energy (Supporting Information, EQ S1). However, it is clearly visible that the relative drop in the association energy is stronger for C_{60} among all substituted CPPs. This fact is supported by the $\Delta\Delta G_{bind,rel}$ values calculated with Equation (1). This value emphasizes the differences between the C_{60} and C_{70} complexes. A value of 100% indicates no influence of the nature of fullerene, while a value $<100\%$ indicates a stabilization of C_{70} over C_{60}, and *vice versa*. In all three cases $\Delta\Delta G_{bind,rel}$ is $<100\%$, showing the stabilizing effect of C_{70} over C_{60} (Figure 4, purple bar).

$$\Delta\Delta G_{bind,rel} = \frac{\Delta G_{bind,rel}(C_{60})}{\Delta G_{bind,rel}(C_{70})} \quad (1)$$

While the lower sphericity of C_{70} leads to a weaker interaction with the nanoring, even in the parent complexes, it bears an additional surface for further interactions in the substituted cases which is the main reason for the smaller penalty paid upon substitution.

C_{70} can be seen as an π-extended C_{60}. The attractive CH-π and lone pair-π interactions of the CPP substituents with the convex surface of the fullerene improve the association and lead to a smaller decrease in association compared to C_{60}. This assumption is supported by the fact that this trend is enhanced upon a higher degree of substitution, possessing thus more interacting entities.

For the twofold substituted CPP **3** the value is very close to 100% and hence, there is only a marginal difference between the fullerenes, which indicates interactions with C_{60} and C_{70} to have a similar quantity. On the other hand, the fourfold substituted CPPs **2** and **4** exhibit a value of around 90%, which could be explained by a similar contact surface between substituents and curved fullerene surface.

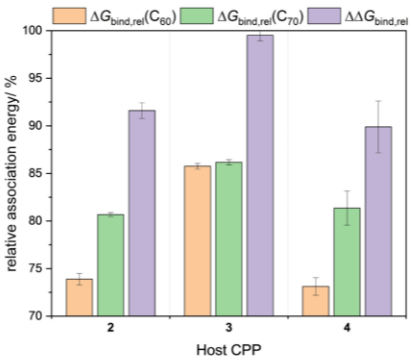

Figure 4. Relative association energies normalized on the association energy of the parent complex with [10]CPP.

Theoretical Investigation

Computational details

The computational details are briefly described in the following while a more exhaustive description can be found in the supplementary information. All density functional theory (DFT) calculations were executed with the software package orca (version 5.0.4).[17] The RIJCOSX approximations,[18–21] utilizing the auxiliary basis set def2-J were used as default. To get reliable geometries and energies, the hosts, as well as the complexes were subjected to the conformer-rotamer ensemble sampling tool (CREST) by Grimme.[22] The obtained ensemble was submitted to the command line energetic sorting of conformer rotamer ensembles (CENSO) workflow,[23] obtaining a narrowed ensemble with geometries and energies on a DFT level. The geometries were obtained by the r2SCAN-3c/mDZ method,[24] accompanied with the solvation model based on molecular electron density (SMD[25]) energy and the modified rigid rotator harmonic oscillator (mRRHO[26]) approach with Grimme's extended tight binding method (xTB-gfn2)[27] based thermodynamic correction. The single point energies were obtained with the hybrid DFT method PBE0 with D4 dispersion correction,[19,20][18,28] combined with the triple-ζ def2-TZVP basis set,[19] in conjuction with the SMD solvent model and the mRRHO(gfn2) approximation for the thermodynamic contribution. The final ensemble represents 99% of the Boltzmann distribution among all observed conformers. Utilizing the Boltzmann weighted energies for the CPPs and complexes, the energy contributions of the present conformers were taken into account. The non-covalent interaction (NCI) in the supramolecular complexes were calculated with the NCIPLOT 4.0 software.[29] Additionally, the data were visualized with vmd,[30] using a color code based on $\mathrm{sign}(\lambda_2)\cdot\rho$ [−1.5 (blue), 0 (green), +1.5 (red)]. The required wavefunctions were obtained with PBE0/def2-TZVP.

Theoretical Evaluation of the Binding Constants

The above-described workflow allows to obtain the structures and energies of a small representative of the most likely ensemble of both, the hosts and the complexes. By that the possible error of taking the less probable (not lowest lying) conformer(s) into account is reduced. Additionally, by utilizing

EurJOC
European Journal of Organic Chemistry

Research Article
doi.org/10.1002/ejoc.202300575

Chemistry Europe
European Chemical Societies Publishing

the Boltzmann weighted energies of the lowest lying conformers, representing 99% of the total energy, mimic the conformational reality of the system even further. In Table 2 and Figure S18 (Supporting Information) the thus obtained calculated association energies are displayed. These energies were determined by the Gibbs free energy of the complex, subtracted with the Gibbs free energies of the host and the guest. In general, the binding is slightly overestimated, which is known for such complexes.[6,31,32]

The non-corrected basis set superposition error (BSSE) can be taken into account as an additional factor. For all investigated CPPs, the overbinding is stronger for the C_{70} complex than the C_{60} ones. This circumstance originates from the calculated binding energy, which is in three of four cases higher for C_{70} than for the corresponding C_{60} complex.

Theoretical Evaluation of the Geometries and Non-covalent Interactions

For the discussion of the non-covalent interactions occurring within the investigated supramolecular complexes, the most abundant conformer (MAC) was utilized for the visualization of intermolecular forces. Within the ensemble of the diethyl phthalane CPP **2**, only conformers with the ether moiety facing inside the cavity were observed. This is in agreement with the crystal structure of the diethyl phthalane incorporated [8]CPP reported earlier by our group.[33] The fact that the ether moiety is facing inside – in both cases, the CPP and its complexes – is further supported by ^{1}H-NMR spectroscopy of the **2**@C_{60} complex (Supporting Information, Figure S13). The optimized geometries of **3** and **4** show that the substituents tend to face out of the nanohoop, minimizing the repulsive interactions which is in agreement with the solid state structure of CPP **3** which we presented earlier.[12]

The NCI plots of the MAC of the four investigated CPPs with the fullerenes are displayed in Figure 5. The parent [10]CPP complexes, show the π-π interactions which are expected to be present in the backbone of the substituted nanohoop as well. In both complexes a large interaction surface can be observed between the nanohoop and the fullerene. As indicated by the green color the interactions are of a weak nature, displaying π-π van der Waals forces. The shape of the NCI plot is similar in both, the C_{60} and the C_{70} complex.

Table 2. Summary of the calculated binding free energies.

Host	Guest	$\Delta G_{bind,calc}$	$\Delta G_{bind,measure}$ kJ/mol	abs. deviation
1	C_{60}	−49.18	−39.09	10.10
	C_{70}	−50.82	−32.35	18.47
2	C_{60}	−35.75	−28.88	6.87
	C_{70}	−33.30	−26.10	7.20
3	C_{60}	−51.32	−33.52	17.80
	C_{70}	−52.22	−27.88	24.34
4	C_{60}	−48.13	−28.58	19.54
	C_{70}	−48.18	−26.28	21.90

For a better understanding of the interactions, NCI scatter-plots of the complexes were depicted. The corresponding graphs for [10]CPP complexes with C_{60} and C_{70} are displayed in Figure 4b. In these 2D plots, the reduced density gradient (RDG) is plotted against the density multiplied by the sign of the second hessian eigenvalue (sign(λ_2)·ρ). Thus, spikes close to sign(λ_2)·ρ = 0 display weak interactions. Both NCI scatter-plots of **1**@C_{60} and **1**@C_{70} have sharp spikes close to sign(λ_2)·ρ = 0, originating from the π-π interactions, which qualitatively appear similar, while being slightly more expressed in the C_{70} complex (green circle) which resembles the more rough interactions in the NCI plot.

Additional interactions can be observed for the complexes of CPP **2**. As the lone pair of the oxygen is facing to the π-surface of the fullerene, strong attractive interactions can be observed, which are indicated by the blue color in the NCI plot. These additional interactions are similar for both complexes (C_{60} and C_{70}). The scatter-plots of both reveal weak interactions close to sign(λ_2)·ρ = 0. Comparing the data of the C_{60} and the C_{70} complex of CPP **2** a stronger interaction can be observed for the C_{70} complex recognizable by the more intense spikes in the scatter plot (green bar). The C_{60} and C_{70} complexes of the CPPs **3** and **4** with their *tert*-butyl esters can form CH-π van der Waals interactions between the *tert*-butyl groups and the guests. In the C_{60} complexes of CPPs **3** and **4**, only the belt-like NCI surface can be observed between the host and the guest which are the result of the concave-convex π-π interaction. Other attractive interactions between the substituents on the nanohoop and the fullerene guest cannot be observed. However, extending the π-surface of the fullerene – by changing from C_{60} to C_{70} – a new NCI surface emerges between the *tert*-butyl substituents of the nanohoop **3** and the egg-shaped fullerene. With a $H_{substituent}$—C_{C70} distance of ~3.8 Å these interactions are in the range of London dispersion forces. The increased number of weak interactions is also represented in the corresponding scatter-plots. Two new spikes appear at very low ρ values (green bar), while the blurry spike at −0.01 is approaching the RDG = 0 line (green circle). This finding supports our interpretation of C_{70} behaving like a π-extended C_{60} in these supramolecular complexes. Interestingly, in none of the observed conformer of **3**@C_{70} both *tert*-butyl groups are facing toward the fullerene core, indicating that sterics and/or dipole moment outnumbers the potential additional London dispersion forces. In case of the more substituted CPP **4** the complexation of C_{70} also induces an additional non-covalent interaction between the *tert*-butyl substituents and the fullerene compared to C_{60}, represented by a light green NCI surface. Surprisingly, only one out of four substituents interacts with the encapsulated fullerene in the MAC.

The insight obtained from the NCI plots and their scatter-plots support our assumptions originating from the experimental data: In all substituted cases the weak interactions are more pronounced for the C_{70} complexes in comparison to the corresponding C_{60} complex visualized by the scatter-plots. This effect appears to be stronger for the substituted nanohoops than for the parent [10]CPP, explaining the stronger beneficial substitution effect for the substituted nanohoops, described by

EurJOC
European Journal of Organic Chemistry

Research Article
doi.org/10.1002/ejoc.202300575

Chemistry Europe
European Chemical Societies Publishing

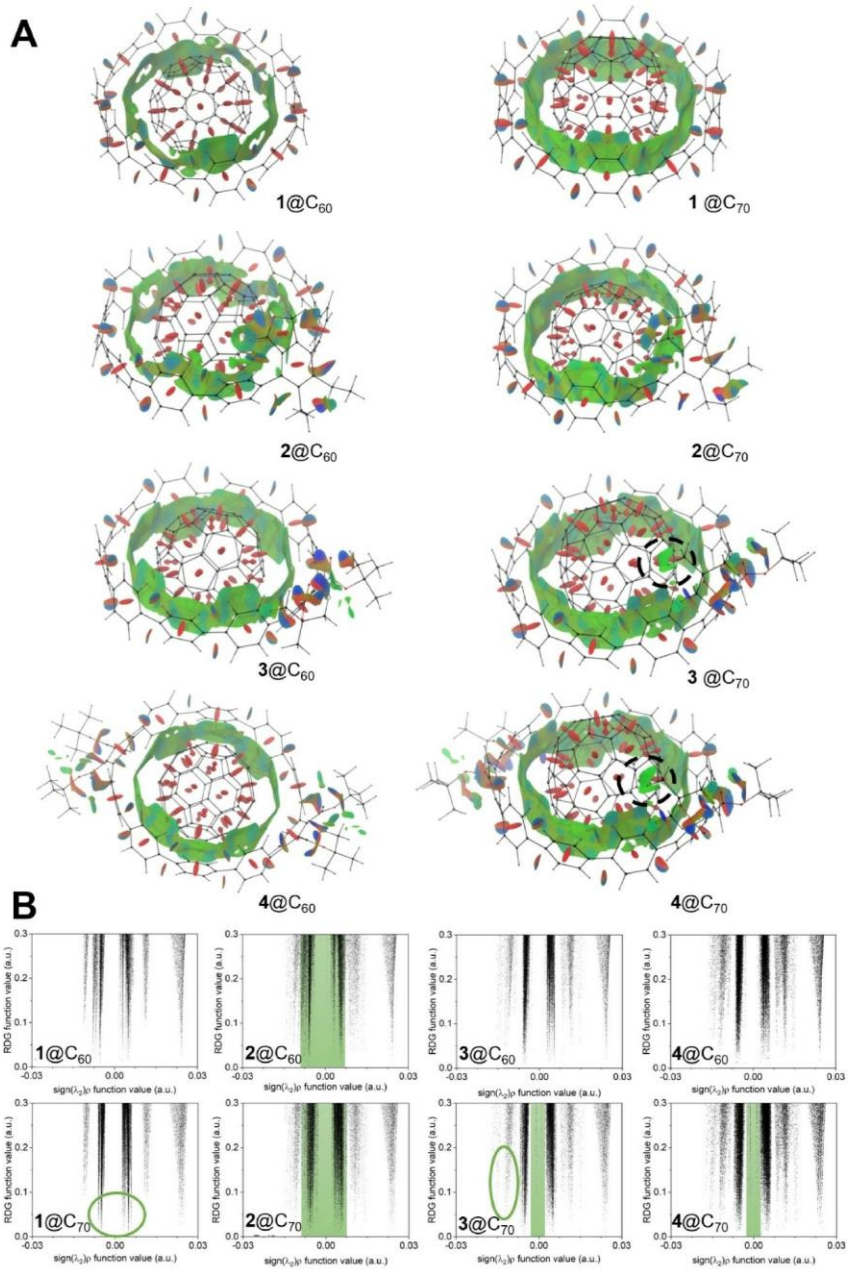

Figure 5. Calculated structures of the MAC of each complex with the isosurface displaying noncovalent interactions (A). Scatter plot (RDG function value vs. sign(λ_2)ρ function value) of the noncovalent interactions of each in A shown complex (B).

the lower relative association energy (Figure 4, purple bar). In the visualized NCI plots the additional interactions with C_{70} are visible for the *tert*-butyl ester functionalized CPPs **3** and **4** while they are not as obvious in case of CPP **2** as in the C_{60} complex

EurJOC
European Journal of Organic Chemistry

Research Article
doi.org/10.1002/ejoc.202300575

Chemistry Europe
European Chemical Societies Publishing

already attractive substituent fullerene interactions can be observed.

Conclusions

In summary, we presented a comprehensive host-guest study of substituted [10]CPPs with the fullerenes C_{60} and C_{70} investigating the association and interactions experimentally, as well as theoretically. With the method of fluorescence quenching the association energies of the complexes could be determined even though the differences are small. The observed trend shows an attractive substituent-fullerene interaction with regard to the ellipsoid fullerene C_{70}, which bears additional π-surface for attractive van der Waals forces. Additionally, the experimental data reveal, that the nature of the substituent has a comparable low impact, in contrast to the degree of substitution. The theoretical investigation was based on the whole ensemble of conformers utilizing the tools CREST and CENSO to obtain reliable structures and energies. Even though, the calculated energies overestimate the binding, these values perform well with respect to the literature cases of [10] and [11]CPP, which report an overbinding of one order of magnitude.[6,31] Visualization and analysis of the noncovalent interactions support the assumptions based on the observed trends by qualitative comparison of the NCI plots. Interactions of the substituents with the encapsulated fullerene – especially in case of C_{70} – reveal the attractive nature of these additional stabilizing effects. The presented results contribute to the understanding of non-covalent interactions within supramolecular complexes and provide quantitative data to design supramolecular carbon structures utilizing non-covalent interactions.

Experimental Section

Materials: Fullerenes C_{60} and C_{70} were purchased from TCI. The four substituted and unsubstituted cycloparaphenylenes were previously synthesized and used without further treatment.[11–13]

C_{60}: ^{13}C NMR (151 MHz, C_6D_6) δ 143.3.

C_{70}: ^{13}C NMR (151 MHz, $CDCl_3$) δ 150.7, 148.2, 147.4, 145.4, 130.9.

[10]CPP **1**: ^{1}H NMR (400 MHz, $CDCl_3$) δ 7.56 (s, 40H), ^{13}C NMR (101 MHz, $CDCl_3$) δ 138.3, 127.5.

Substituted CPP **2**: ^{1}H NMR (400 MHz, CD_2Cl_2): δ 7.64–7.54 (m, 26H), 7.54–7.50 (m, 4H), 7.17–7.13 (m, 4H), 4.01 (s, 4H), 3.04 (q, ^{3}J = 7.4 Hz, 4H), 1.24 (t, ^{3}J = 7.4 Hz, 6H); ^{13}C NMR (101 MHz, CD_2Cl_2): δ 140.1, 139.4, 139.3, 139.2, 138.8, 138.7, 138.6, 138.6, 138.5, 135.9, 130.6, 128.0, 127.9, 127.83, 127.76, 127.72, 127.66, 127.4, 74.6, 23.9, 17.0. Digits were added to show the difference in the chemical shift. HRMS (APCI): calc. for $[C_{66}H_{51}O]^+$: $[M+H]^+$ 859.3935, found 859.3933.

Substituted CPP **3**: ^{1}H NMR (400 MHz, $CDCl_3$): δ 7.60–7.51 (m, 32H), 7.46–7.40 (m, 4H), 6.75 (s, 2H), 1.46 (s, 18H); ^{13}C NMR (101 MHz, $CDCl_3$): δ 167.0, 139.6, 139.4, 138.9, 138.47, 138.45, 138.43, 138.31, 138.28, 134.44, 131.42, 130.12, 127.56, 127.53, 127.51, 126.8, 82.5, 28.02. Digits were added to show the difference in the chemical shift. HRMS (ESI): calc. for $[C_{70}H_{56}O_4+Na]^+$: $[M+Na]^+$ 983.4071, found 983.4072.

Substituted CPP **4**: ^{1}H NMR (600 MHz, CD_2Cl_2): δ 7.61 (s, 16H), 7.59–7.55 (m, 8H), 7.47–7.43 (m, 8H), 6.84 (s, 4H), 1.45 (s, 36H); ^{13}C NMR (151 MHz, CD_2Cl_2): δ 167.5, 140.3, 140.0, 139.7, 139.14, 139.09, 135.1, 132.1, 130.8, 128.23, 128.17, 127.6, 83.1, 28.4. Digits were added to show the difference in the chemical shift. HRMS (ESI): calc. for $[C_{80}H_{72}O_8+2Na]^+$: $[M+2Na]^{2+}$ 603.2505, found 603.2504.

Fluorescence Quenching Experiments: The fluorescence quenching experiments were performed with a FP-8300 fluorescence spectrometer from Jasco. Solvents for spectroscopy were purchased from Merck or Chemsolute (Uvasol® or HPLC quality). The samples were irradiated with a Xe-lamp. Excitation and emission bandwidth were set to 2.5 nm. The fluorescence was measured between 400 nm and 600 nm with a scan speed of 200 nm/min and a data interval of 0.2 nm. The response time was set to 0.5 sec. The titrations with parent [10]CPP were irradiated at 340 nm, with di- and tetra-*tert*-butyl ester substituted [10]CPP at 338 nm and with diethyl phthalane incorporated [10]CPP at 326 nm.

The association constants were determined by threefold titrations. For each titration a 10^{-6} M to 10^{-7} M solution of the CPP was prepared in toluene. These solutions were used as solvent for a 10^{-4} M to 10^{-6} M solution of the different fullerene guests. Starting with 1800 µl of CPP solution the fullerene (in CPP) solution was added in portions of 15–100 µl. After each step of addition, the solution was mixed thoroughly, and a fluorescence spectrum was measured.

For the determination of the association constant the fluorescence (in a.u.) at the maxima (one maximum in case of parent [10]CPP and two maxima in case of the substituted [10]CPPs) were used. The data were plotted with non-linear regression utilizing the online tool "Bindfit" by P. Thordarson.[16] As error of the mean values the standard deviation was used.

Supporting Information

The authors have cited additional references within the Supporting Information.[34]

Acknowledgements

The authors are grateful to Dennis Gerbig for computational support and the Justus Liebig University for financial support. Open Access funding enabled and organized by Projekt DEAL.

Conflict of Interests

The authors declare no conflict of interest.

Data Availability Statement

The data that support the findings of this study are available in the supplementary material of this article.

EurJOC
European Journal of Organic Chemistry

Research Article
doi.org/10.1002/ejoc.202300575

Chemistry Europe
European Chemical Societies Publishing

Keywords: host-guest systems · macrocycles · computational chemistry · substituent effects · noncovalent interactions

[1] C. A. Hunter, J. K. M. Sanders, *J. Am. Chem. Soc.* **1990**, *112*, 5525–5534.
[2] S. E. Wheeler, J. W. G. Bloom, *J. Phys. Chem. A* **2014**, *118*, 6133–6147.
[3] E. Riedel, C. Janiak, *Anorganische Chemie*, De Gruyter, Berlin, **2022**, pp. 554–561.
[4] S. E. Lewis, *Chem. Soc. Rev.* **2015**, *44*, 2221–2304.
[5] a) R. Jasti, J. Bhattacharjee, J. B. Neaton, C. R. Bertozzi, *J. Am. Chem. Soc.* **2008**, *130*, 17646–17647; b) H. Takaba, H. Omachi, Y. Yamamoto, J. Bouffard, K. Itami, *Angew. Chem. Int. Ed.* **2009**, *48*, 6112–6116; c) S. Yamago, Y. Watanabe, T. Iwamoto, *Angew. Chem. Int. Ed.* **2010**, *122*, 769–771.
[6] T. Iwamoto, Y. Watanabe, T. Sadahiro, T. Haino, S. Yamago, *Angew. Chem. Int. Ed.* **2011**, *50*, 8342–8344.
[7] A. Stergiou, J. Rio, J. H. Griwatz, D. Arčon, H. A. Wegner, C. P. Ewels, N. Tagmatarchis, *Angew. Chem. Int. Ed.* **2019**, *58*, 17745–17750.
[8] Y. Xu, R. Kaur, B. Wang, M. B. Minameyer, S. Gsänger, B. Meyer, T. Drewello, D. M. Guldi, M. von Delius, *J. Am. Chem. Soc.* **2018**, *140*, 13413–13420.
[9] H. Ueno, T. Nishihara, Y. Segawa, K. Itami, *Angew. Chem. Int. Ed.* **2015**, *54*, 3707–3711.
[10] J. Rio, S. Beeck, G. Rotas, S. Ahles, D. Jacquemin, N. Tagmatarchis, C. Ewels, H. A. Wegner, *Angew. Chem. Int. Ed.* **2018**, *57*, 6930–6934.
[11] J. Volkmann, D. Kohrs, H. A. Wegner, *Chem. Eur. J.* **2023**, *29*, e202300268.
[12] D. Kohrs, J. Becker, H. A. Wegner, *Chem. Eur. J.* **2022**, *28*, e202104239.
[13] J. Volkmann, D. Kohrs, F. Bernt, H. A. Wegner, *Eur. J. Org. Chem.* **2022**, *2022*, e202101357.
[14] D. Kohrs, J. Volkmann, H. A. Wegner, *Chem. Commun.* **2022**, *58*, 7483–7494.
[15] E. R. Darzi, T. J. Sisto, R. Jasti, *J. Org. Chem.* **2012**, *77*, 6624–6628.
[16] a) http://supramolecular.org; b) D. Brynn Hibbert, P. Thordarson, *Chem. Commun.* **2016**, *52*, 12792–12805; c) P. Thordarson, *Chem. Soc. Rev.* **2011**, *40*, 1305–1323.
[17] a) F. Neese, *WIREs Comput. Mol. Sci.* **2012**, *2*, 73–78; b) F. Neese, *WIREs Comput. Mol. Sci.* **2022**, *12*, e1606.
[18] C. Adamo, V. Barone, *J. Chem. Phys.* **1999**, *110*, 6158–6170.
[19] F. Weigend, R. Ahlrichs, *Phys. Chem. Chem. Phys.* **2005**, *7*, 3297–3305.
[20] B. Helmich-Paris, B. de Souza, F. Neese, R. Izsák, *J. Chem. Phys.* **2021**, *155*, 104109.
[21] F. Weigend, *Phys. Chem. Chem. Phys.* **2006**, *8*, 1057–1065.
[22] P. Pracht, F. Bohle, S. Grimme, *Phys. Chem. Chem. Phys.* **2020**, *22*, 7169–7192.
[23] S. Grimme, F. Bohle, A. Hansen, P. Pracht, S. Spicher, M. Stahn, *J. Phys. Chem. A* **2021**, *125*, 4039–4054.
[24] a) S. Grimme, A. Hansen, S. Ehlert, J.-M. Mewes, *J. Chem. Phys.* **2021**, *154*, 64103; b) J. W. Furness, A. D. Kaplan, J. Ning, J. P. Perdew, J. Sun, *J. Chem. Phys. Lett.* **2020**, *11*, 8208–8215.
[25] A. V. Marenich, C. J. Cramer, D. G. Truhlar, *J. Phys. Chem. B* **2009**, *113*, 6378–6396.
[26] S. Spicher, S. Grimme, *J. Chem. Theory Comput.* **2021**, *17*, 1701–1714.
[27] C. Bannwarth, E. Caldeweyher, S. Ehlert, A. Hansen, P. Pracht, J. Seibert, S. Spicher, S. Grimme, *WIREs Comput. Mol. Sci.* **2021**, *11*, e1493.
[28] E. Caldeweyher, S. Ehlert, A. Hansen, H. Neugebauer, S. Spicher, C. Bannwarth, S. Grimme, *J. Chem. Phys.* **2019**, *150*, 154122.
[29] E. R. Johnson, S. Keinan, P. Mori-Sánchez, J. Contreras-García, A. J. Cohen, W. Yang, *J. Am. Chem. Soc.* **2010**, *132*, 6498–6506.
[30] W. Humphrey, A. Dalke, K. Schulten, *J. Mol. Graphics* **1996**, *14*, 33–38.
[31] T. Iwamoto, Y. Watanabe, H. Takaya, T. Haino, N. Yasuda, S. Yamago, *Chem. Eur. J.* **2013**, *19*, 14061–14068.
[32] J. Antony, R. Sure, S. Grimme, *Chem. Commun.* **2015**, *51*, 1764–1774.
[33] A.-F. Tran-Van, H. A. Wegner, *Beilstein J. Nanotechnol.* **2014**, *5*, 1320–1333.
[34] a) J. G. Brandenburg, C. Bannwarth, A. Hansen, S. Grimme, *J. Chem. Phys.* **2018**, *148*, 64104; b) S. Ehlert, M. Stahn, S. Spicher, S. Grimme, *J. Chem. Theory Comput.* **2021**, *17*, 4250–4261; c) M. Bursch, J.-M. Mewes, A. Hansen, S. Grimme, *Angew. Chem. Int. Ed.* **2022**, *61*, e202205735.

Manuscript received: June 14, 2023
Revised manuscript received: June 20, 2023
Accepted manuscript online: June 21, 2023

5 Additional Contributions to Literature

5.1 Cycloparaphenylenes *via* [2+2+2] Cycloaddition

Reference: D. Kohrs[+], J. Volkmann[+], H. A. Wegner, *Chem. Commun.* **2022**, *58*, 7483–7494.

DOI: 10.1039/D2CC02289C

[+]These authors contributed equally.

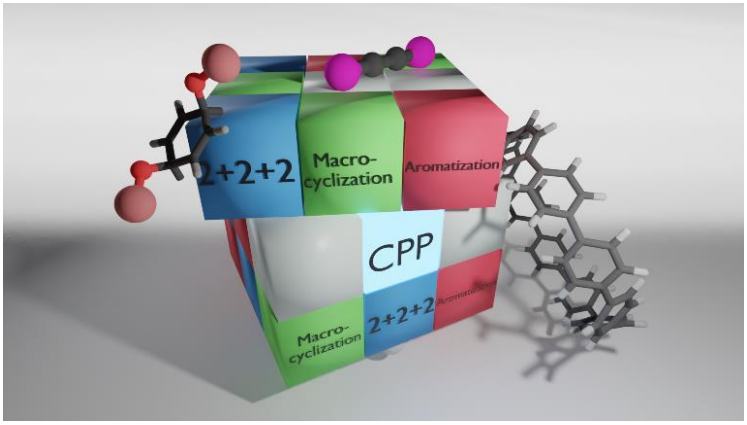

“The [2+2+2] cycloaddition (CA) offers great potential as an atom economic method for the formation of substituted aromatic rings. In this article, we highlight the application of this versatile method in synthetic approaches towards substituted cycloparaphenylenes (CPPs). The [2+2+2] CA can take over different tasks within the synthesis depending on the targeted CPP. These approaches were divided into three key steps: aromatization (which finalizes the CPP), macrocyclization (the formation of a strain-reduced macrocycle) and the [2+2+2] CA. Based on this analysis the strategies were categorized into four classes based on which task the [2+2+2] CA fulfills. We point out the benefits and drawbacks of each synthetic strategy and summarize our findings to provide the reader with an easy insight into this research field.”

5.2 Robust coherent spin centers from stable azafullerene radicals entrapped in cycloparaphenylene rings

Reference: Y. Tanuma, A. Stergiou, A. Bužan Bobnar, M. Gaboardi, J. Rio, J. Volkmann, H. A. Wegner, N. Tagmatarchis, C. P. Ewels, D. Arčon, *Nanoscale* **2021**, *13*, 19946–19955.

DOI: 10.1039/D1NR06393F

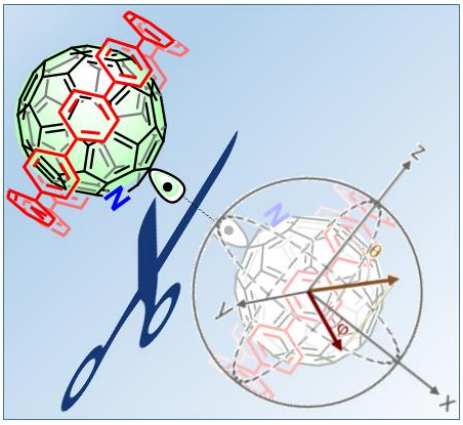

"Molecular entities with robust spin-1/2 are natural two-level quantum systems for realizing qubits and are key ingredients of emerging quantum technologies such as quantum computing. Here we show that robust and abundant spin-1/2 species can be created *in situ* in the solid state from spin-active azafullerene $C_{59}N$ cages supramolecularly hosted in crystals of [10]cycloparaphenylene ([10]CPP) nanohoops. This is achieved *via* a two-stage thermally-assisted homolysis of the parent diamagnetic [10]CPP⊃$(C_{59}N)_2$⊂[10]CPP supramolecular complex. Upon cooling, the otherwise unstable $C_{59}N^{\bullet}$ radical is remarkably persistent with a measured radical lifetime of several years. Additionally, pulsed electron paramagnetic resonance measurements show long coherence times, fulfilling a basic condition for any qubit manipulation, and observed Rabi oscillations demonstrate single qubit operation. These findings together with rapid recent advances on the synthesis of carbon nanohoops offer the potential to fabricate tailored cycloparaphenylene networks hosting $C_{59}N^{\bullet}$ centers, providing a promising platform for building complex qubit circuits."

5.3 Long Spin Coherence Times on $C_{59}N$-C_{60} Heterodimer Radicals Entrapped in Cycloparaphenylene Rings

Reference: Y. Tanuma, T. Knaflič, B. Anézo, C. Stangel, J. Volkmann, N. Tagmatarchis, H. A. Wegner, D. Arčon, C. P. Ewels, *J. Phys. Chem. C* **2023**, *127*, 6552–6561.

DOI: 10.1021/acs.jpcc.2c09049

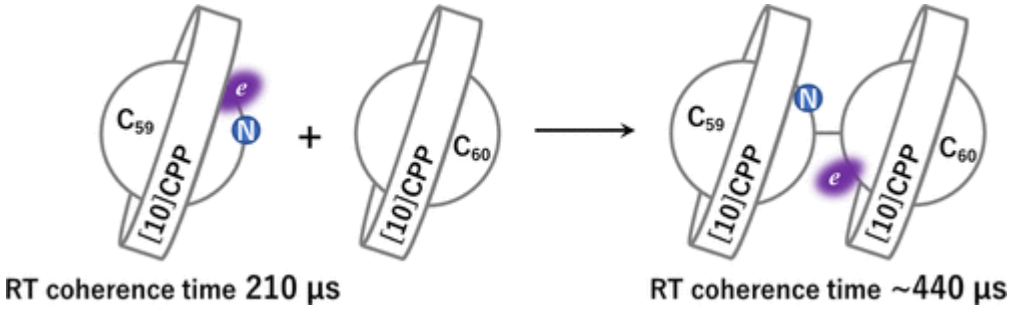

"We investigate the effect of introducing C_{60} to $(C_{59}N)_2$ and the molecular ring, [10]cycloparaphenylene ([10]CPP), using electron paramagnetic resonance (EPR) measurements supported by density functional theory (DFT) calculations. Incorporating C_{60} into the system results in the formation of novel stable [10]CPP⊃C_{59}N-$C_{60}^{\bullet}$⊂[10]CPP encapsulated heterodimer radicals whose spin is localized on C_{60} and manifests in EPR measurements as a signal at g = 2.0022 without any discernable hyperfine structure. This signal has an exceptionally long spin coherence lifetime of 440 µs at room temperature, far longer than any of the radical fullerene species reported in the literature and over twice that of the $C_{59}N^{\bullet}$⊂[10]CPP radical. The radicals are long-lived, with EPR signal still strong over a year after thermal activation. The [10]CPP⊃C_{59}N-$C_{60}^{\bullet}$⊂[10]CPP oligomer is more stable than $C_{59}N^{\bullet}$⊂[10]CPP radicals and becomes the predominant species at room temperature after annealing. Its formation is thermally activated with an experimental activation energy of only 0.189 eV, as compared to 0.485 eV for the pure azafullerene-[10]CPP case. The [10]CPP⊃C_{59}N-$C_{60}^{\bullet}$⊂[10]CPP radicals discovered here could be used to bridge $C_{59}N^{\bullet}$⊂[10]CPPs acting as qubits, providing effective coupling between them."

6 DANKSAGUNG

Zu Beginn möchte ich mich bei meinem Doktorvater Prof. Dr. Hermann A. Wegner bedanken für die Möglichkeit, meine Doktorarbeit in seiner Arbeitsgruppe anzufertigen. Ich bin dankbar für die vertrauensvolle Unterstützung und Hilfe bei der Bearbeitung dieser interessanten und anspruchsvollen Forschung, zu deren Erfolg er mit seinen hilfreichen und kreativen Ideen maßgeblich beigetragen hat.

Des Weiteren möchte ich mich herzlich bei Prof. Dr. Peter R. Schreiner, PhD für das Anfertigen des Zweitgutachtens bedanken.

Meiner Freundin Fabienne möchte ich besonders danken. Mit ihrer Geduld und ihrem Verständnis, auch in den stressigen und frustrationsreichen Zeiten, hat sie mich immer wieder aufgebaut und mir Kraft gegeben. Das finale Üben meiner Präsentationen mit dir als Publikum hat mir immer sehr geholfen.

Aufrichtiger Dank gilt meinen Eltern und meiner gesamten Familie. Durch ihre beständige Unterstützung haben sie mir das Studium und Promotion erst ermöglicht und ich konnte mich zu jeder Zeit auf ihre Hilfe und Unterstützung verlassen. Hierfür bin ich auch Stefan und Isolde dankbar.

Ein besonderes Dankeschön geht an meine Freunde, auf die ich mich immer verlassen und bei denen ich den Stress der Promotion schnell vergessen konnte. Mit ihnen habe ich auf Festivals neue Kraft tanken können, um anschließend im Labor wieder durchzustarten. Ohne euch hätte ich es niemals geschafft.

Ich danke von Herzen der gesamten Arbeitsgruppe Wegner. Besonders bedanken möchte ich mich bei den „Nanocarbons“ Daniel Kohrs, Jan Griwatz, Felix Bernt und Nathaniel Ukah, ebenso wie Sebastian Beeck, der mir in meiner Anfangszeit zur Seite stand. Eure Hilfe in Theorie und Praxis, eure guten Ideen und eure kritischen Nachfragen haben mir sehr geholfen und dadurch zum Erfolg dieser Arbeit beigetragen. Für die großartige Zeit, die entspannte, freundschaftliche Atmosphäre im Labor und in der Arbeitsgruppe, ebenso wie die schönen Kaffeepausen, Feierabendbiere und Bouldersessions, danke ich den ehemaligen und aktuellen Mitgliedern der Arbeitsgruppe Dr. Andreas Heindl, Dr. Sebastian Ahles, Dr. Long-Chen Hong, Dr. Anne Kunz, Dr. Julia Ruhl, Dr. Marcel Strauss, Dr. Atanu Patra, Dr. Jan Geldsetzer, Mari Janse van Rensburg, Katinka Grimmeisen, Finn Schneider, Giovanni Parolin, Chiara di Berardino, Dominik Schatz, Conrad Averdunk, Christopher Leonhardt, Michel Große und Kai Hanke. Weiterer Dank gilt meinen ehemaligen Student:innen Pia

Mader, Elisa Badin, Antonio Carnevali und Mika Keßler, von und mit denen ich immer wieder neues lernen konnte.

Unseren Kooperationspartnern bin ich für die konstruktive und freundschaftliche Zusammenarbeit dankbar. Besonderer Dank gilt hierbei Prof. Denis Arčon und Dr. Nikos Tagmatarchis, ebenso wie ihren Mitarbeitern für die herzliche Aufnahme in ihren Arbeitsgruppen.

Ich möchte auch den anderen Arbeitsgruppen des Instituts, der AG Schreiner, der AG Gellrich sowie der AG Göttlich für die gute Zusammenarbeit, Hilfsbereitschaft und freundschaftliche Atmosphäre danken.

Des Weiteren gilt ein großer Dank allen Mitarbeiter:innen des organischen Instituts der JLU, die mir mit technischer und administrativer Hilfe zur Seite standen und die diese Arbeit mit ihrer Hilfe und ihren Messungen erst möglich gemacht haben. Dabei danke ich Dr. Heike Hausmann, Anika Bernhardt, Anja Platt und Inna Klein für die Messung aller NMR-Spektren, auch wenn die Proben oft tückisch waren, oder es schnell gehen musste. Außerdem danke ich Dr. Raffael Wende, Stefan Bernhardt, Steffen Wagner, Brigitte Weinl-Boulakhrouf und Edgar Reitz. Des Weiteren danke ich dem Team der Chemikalienausgabe: Eike Santowski und Mario Dauber, sowie dem Team der Materialienausgabe und Glasbläserei: Anja Beneckenstein, Dr. Wolfgang Herrendorf, Hans-Jürgen Wolf, Michaela Jäkel und Petra Grundmann für die Bereitstellung und Bestellungen von Chemikalien und Laborausstattung. Vielen Dank auch an Dr. Jörg Neudert, der bei der allgemeinen Organisation des Instituts sowie der OC-Praktika immer zuvorkommend und unterstützend handelte, ebenso wie Dr. Kai Maaß, für die Unterstützung und schöne Zeit im Nebenfachpraktikum.

Zuletzt geht ein großer Dank an Anika Jäger, Michaela Richter und Maurice Monnard, die mir bei organisatorischen und verwaltungstechnischen Fragen und Abläufen immer helfend zur Seite standen.

7 ABBREVIATIONS

OAc	Acetate
Ar	Aryl
Bu	Butyl
Bn	Benzyl
biph	Biphenyl
CNT	Carbon nanotube
cat.	Catalytic amount
C_{60}	(C_{60}-*I*$_h$)[5,6]fullerene
C_{70}	(C_{70}-*D*$_{5h}$)[5,6]fullerene
δ	Chemical Shift
CPDMS	(3-Cyanopropyl)dimethylsilyl
cod	Cyclooctadiene
CPP	Cycloparaphenylene
CPPAs	Cycloparaphenyleneacetylene
DFT	Density functional theory
DCM	Dichloromethane
SPhos	Dicyclohexyl(2',6'-dimethoxy[1,1'-biphenyl]-2-yl)phosphane
Hünig's Base	Di*iso*propylethylamine
DMSO	Dimethylsulfoxide
engl.	In Englisch
EQ	Equation
Et	Ethyl
e.g.	*Exempli gratia*, for example
HOMO	Highest occupied molecular orbital
:B	Lewis base
LD	London dispersion
LUMO	Lowest unoccupied molecular orbital
MOM	Methoxymethyl
Me	Methyl
MW	Microwave irradiation
MWCNT	Multi walled carbon nanotube
µm	Micrometer
nm	Nanometer
NP	Naphthalenide
n-BuLi	*n*-Butyllithium
DMF	*N,N*-Dimethylformamide
NCI	Non-covalent interactions
NMR	Nuclear magnetic resonance
OPP	Oligoparaphenylene
o-DCB	ortho-Dichlorobenzene
ppm	Parts per million
Ph	Phenyl
PCBM	[6,6]-Phenyl-C_{61}-butyric acid methyl ester
Bpin	Pinacolborane
PG	Protection group

quant.	Quantitatively
H_8-binap	*R*-(+)-2,2′-Bis-(diphenylphospino)-5,5′,6,6′,7,7′,8,8′-octahydro-1,1′-binaphthyl, [(1*R*)-5,5′,6,6′,7,7′,8,8′-octahydro-[1,1′-binaphthalin]-2,2′-diyl]-bis-[diphenylphosphin]
rt	Room temperature
P_4-*t*-Bu	Schwesinger P_4-Base; N‴-(1,1-Dimethylethyl)-N,N′,N″-tris[tris(dimethylamino)phosphoranylidene]phosphorimidic triamide
SWCNT	Single walled carbon nanotube
TBAF	Tetrabutylammonium fluoride
THF	Tetrahydrofuran
TD-DFT	Time-dependent density functional theory
TEA	Triethylamine
TMS	Trimetylsilyl